Investigating the mechanism of ARPC5/L driven Lymph node retention of malignant B cells in Mantle Cell Lymphoma

Thesis submitted in accordance with the requirements of the University of Liverpool for the degree of Doctor in Philosophy

By

Mariah Nawwab Abdullah

February 2023

I dedicate my humble work to my biggest supporter,

my family

Abstract

Investigating the mechanism of ARPC5/L driven Lymph node retention of malignant B cells in Chronic Lymphocytic Leukemia and Mantle Cell Lymphoma

Mariah Nawwab Abdullah

The immune system is a complex network that can roughly be divided into innate and adaptive immunity. This system consists of blood cells (hematopoietic) which are able to sense the presence of pathogenic particles and cooperate to eliminate these agents. Innate immunity provides the first-line defense and is essential for infection control. However, it is not always sufficient to eliminate infectious pathogens. Adaptive immunity has evolved to provide a second line of defense which increases the protection mechanism against infectious organisms. It consists predominantly of subtypes of T- and B- cells. Antigen recognition activates B cells by triggering a series of events that activate several pathways by initiating kinase phosphorylation cascades and, eventually, gene expression. More recently, these pathways are being investigated as a central pathological mechanism in B cell malignancies. Clinically, a variety of BCR-related signaling pathways promote malignancy progression in Chronic Lymphocytic Leukemia (CLL) and Mantle Cell Lymphoma (MCL) by accumulating those malignant B cells in survival areas for proliferation.

In our lab, a previous phosphoproteomic study has shown that the Arp2/3 complex member ARPC5L showed a selective enrichment over its isoform ARPC5 after BCR stimulation. From this finding, we predicted that ARPC5 paralogues may regulate actin organisation after BCR activation. These isoforms may influence BCR signaling and control the migration/adhesion of malignant CLL and MCL cells. Characterizing ARPC5/L in MCL cell lines may indicate their selective role in BCR signaling. Their functionality may provide evidence of ARPC5/L influencing actin dynamics in BCR signalling.

In MAVER-1 cells, BCR signalling seems to manipulate ARPC5/L expression and protein distribution. Although ARPC5/L functionality is not essential for BCR signaling, a noticeable slowness in cell migration indicates to isoform requirement for malignant cell mobility. These findings provide a foundation for further exploration of ARPC5/L role in controlling cytoskeletal events in B cells to give further information on the pathophysiology of MCL cells.

Acknowledgment

Firstly, I would like to thank my supervisors Dr, Tobias Zech and Prof, Joseph Slupsky for providing me with great guidance and creating a supportive environment to conduct this project.

Great appreciation to all of Zech and Slupsky lab members for their friendship and support over the past years, especially, Dr, Lorna Young, Dr, Thomas Waring, Dr, Kathy Till, Dr, Andrew Duckworth, and Alzahra Alshayeb.

I also would like to thank those whose work involved to the success of this thesis. Dr, Anne Reversat for her invaluable help in providing ARPC5/L overexpression cells and preparing the tool for migration assay. Dr, Adam Linley for his support in conducting the BCR internalisation assay, and Mohmmed Jawad for his support in conducting Mass Cytometry related experiment.

Finally, I would like to thank Northern Border University specifically and the Saudi government generally for the fund they provided to achieve my PhD study.

Covid-19 Pandemic and Research restriction

The period where the lockdown had started greatly affected my experimental progress and the outcome of my project aims since I could not attend the lab. Working from home (writing thesis) was challengeable since I have two children who needed support with homeschooling. Moreover, my husband had the same issue since he has been doing a PhD as well in the same field. My supervisors were supporting me at that time in term in guiding me toward writing my thesis but again it was not an easy time at all. According to Saudi government recommendation, I went back home in beginning of June 2020. Attending to the lab was partially allowed at the end of July 2020 but I could not really come back immediately since the flights were off in Saudi and so that delayed my experimental work even more. Thus, I was able to restart my work in the mid of September 2020. The second school lockdown in January 2021 for three months again prevented me to attend the lab in regular basis since the school refused the letter from University of Liverpool for us being classified as critical worker. Unfortunately, a request for more extension was rejected from my sponsor which limited my work time.

Accordingly, after the discussion with my supervisors, I tried to slightly reduce the aims of my thesis with excluding working with primary CLL cells and attempted hardly working even during the weekends trying to catch up and finishing my experimental work on the time frame provided.

Content

List of Figures

List of Tables

Abbreviations

ABC-DLBCL Activated B cell-like diffuse large B cell lymphoma

ADP Adenosine diphosphate

APRIL A proliferation inducing legend

ARP2/3 Actin related protien2/3

ATP Adenosine triphosphate

BAFF B cell activator factor

B-ALL B-acute Lymphocytic Lukemia

BCMA B-cell maturation antigen

BCR B cell receptor

BL Birkett Lymphoma

CCLE Cancer cell line encyclopaedia

CLL Chronic Lymphocytic Lukemia

CSR Class Switch Recombination

DAG Diacylglycerol

ERK Extracellular signal-regulated kinase

ERM Ezrin /Radixin/ Moesin

FDL Follicular dendritic cell

FL Follicular Lymphoma

Foxo Forkhead box class O

GBD GTPase binding domine

GRAIL Genes related to anergy in lymphocytes

HNSCC Head and neck squamous cell carcinoma

HS1 Haematopoietic lineage cell-specific protein 1

IKKS I-κB kinases

IP3 Inositol 1,4,5-trisphosphate diacylglycerol

IS Immunological synapse

ITAM Immune Tyrosine Activation Motif

MCL Mantle cell lymphoma

MHC Major histocompatibility

Mir-133a Micro-RNA133a

MM Multiple Myeloma

PI3K Phosphoinositide 3-kinase

PIP2 Phosphatidylinositol 4,5-bisphosphate

PIP3 Phosphatidyl-inositol 3,4,5-trisphosphate

PKB Protein Kinase B

PLCγ2 Phospholipase C-γ

RAG Recombination-Activating Gene

S1PR1 sphinosine-1 phosphate receptor

SH3 Src homology 3

SHM Somatic Hypermutation

SLP65 SH2 domine containing Leukocyte protein

Syk Spleen tyrosine kinase

TACI Transmembrane activator and calcium-modulator and cyclophilin ligand

TCR T cell Receptor

TNF Tumour necrosis Factor

VCA Verprolin/ cofilin/ acidic

VCAM-1 Vascular cell adhesion molecule 1

Chapter 1: Main introduction

1.1 B cell development:

The development of hematopoietic cells occurs through a process called Hematopoiesis in which hematopoietic pluripotent stem cells are differentiated and committed to a specific lineage [1], and give rise to different blood cells including B lymphocytes (Fig1-1). The maturation from stem cells to mature B lymphocytes is marked by specific expression of the genes coding for immunoglobulin heavy chain of the B cell receptor (BCR). The development process initiates in the bone marrow when hematopoietic stem cells differentiate into a common lymphoid progenitor which further differentiates to progenitor (pro-B cells) [2]. Igα *(*CD79a*)* and Igβ (CD79b), transmembrane proteins accompanying mature B cell receptors and required for their signaling, are expressed on the surface of the pro-B cells [3]. To give diversity of antigen recognition, the genes responsible for the antigen-recognition site of the BCR are rearranged. This process is catalysed by recombination-activating genes (RAG1 and RAG2), which then generates the rupture of double chains of DNA in specific recognition sites between the gene segments coding for variable (V), diversity (D), and joining (J) regions of the heavy chain (IgH). This process continues until a mature protein can be expressed, at which stage pro-B cells differentiate to late pro-B cells [4]. Differentiation to the pre-B cell stage is coupled with expression of a surrogate light chain that enables expression of the BCR on the cell surface, and V/J gene rearrangement of the Ig light chain, and ultimate formation of the intact BCR (Fig 2). At this stage constitutive

signaling throught the BCR encourages proliferation and pre-B cells significantly increase their number [5]. Of note, the double DNA breaks of the IgH and IgL diversity genes occurs randomly in order to enable the BCR repertoire to be highly diverse and recognise a variety of foreign antigens. This means BCR on each mature B cell recognises only one specific epitope sequence within the antigen [6].

With the expression of intact BCR on pre-B cell membranes, the cells then differentiate to immature B cells (Fig1-2) [5]. At the immature B cell stage, expressed BCR is tested for autoreactivity, and those cells found self-reactive are processed via three main mechanisms: receptor edition, apoptosis, and anergy. The strength of autoantigen-BCR interaction determines which mechanism is utilized. BCR which expresses high affinity to surrounding self-antigens in the bone marrow are subjected to receptor editing in which the IgL chain undergoes another round of rearrangement [7]. If immature B cells fail to achieve receptor editing, they go through clonal deletion (Apoptosis) [7, 8]. Weak interaction (low affinity) to autoantigens results in receptor anergy, a state in which the BCR fails to signal efficiently [9]. Anergic B-cells together with the clones of B cells that lack interaction with autoantigens (naive B cells) migrate to the periphery and become so-called differentiated transitional B cells [10].

Transitional B cells express BCR in the form of surface IgM and IgD [11], and give rise to different mature naive B cell subsets: marginal zone B cells, conventional B cells (B2) or, B1 B cells which differ in their location, cell

surface phenotype, and antigen specificity [12]. Anergic B cells die in the periphery because of the lack of appropriate survival signals [13]. On the other hand, naive B cells migrate to secondary lymphoid organs where they look for foreign antigen to bind.

If an antigen is recognised, mature activated cells differentiate into plasma cells or memory cells. During this differentiation in germinal centers of lymph node, cells are subjected to both Somatic Hypermutation (SHM) and class switch recombination (CSR) processes. In SHM, B cells experience mutation in both the heavy and light immunoglobulin variable region genes to increase receptor affinity to foreign antigen. The CSR process produces secretable antibody isoforms by removing a specific gene segment/s from the heavy chain immunoglobulin that can then optimally act to opsonise foreign antigens and/or make them for destruction by phagocytes [14, 15]. If B cells fail to find cognate antigen within approximately ~5-6 weeks, they die from neglect [16]. Defects in BCR formation and/or their signaling restrict normal B cell maturation which clearly emphasises the role of BCR components and their signaling in B cell development.

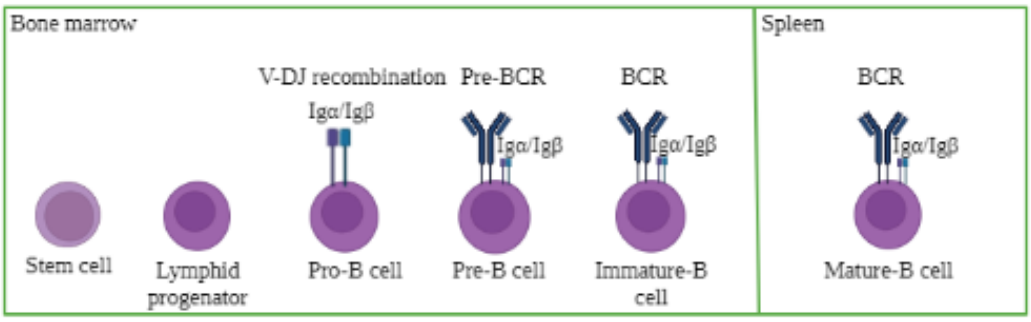

Figure 1-1: B cell development. Human B cells arise in primary lymphoid tissue (Bone marrow) and further develop in secondary lymphoid tissue (e.g. Human lymph nodes and spleen). The development starts when stem cell differentiates to lymphoid progenitor and ends when mature B cell is formed. Through the steps of development, the transmembrane Igα (CD79a) and Igβ (CD79b) and BCR maturation occur. Pro: Progenitor, Pre: precursor, BCR: B cell receptor. Adapted from [17].

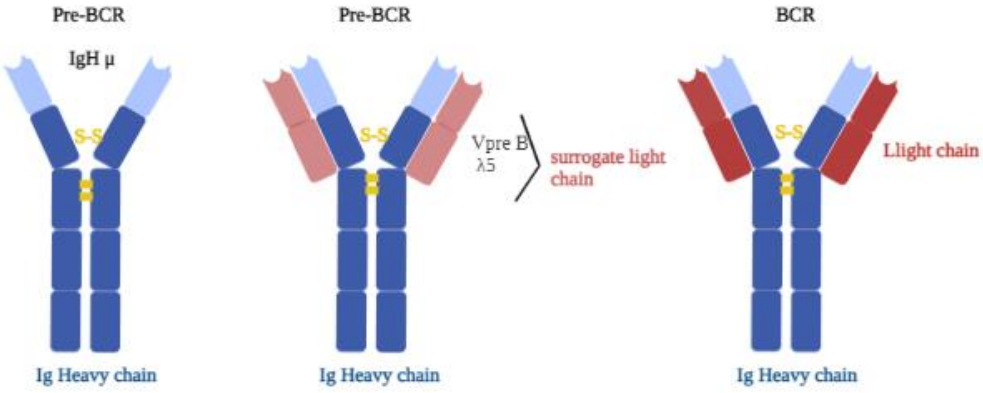

Figure 1-2: Pre-BCR and BCR structure. The Pre-BCR and BCR are disulfide-linked tetramers composed of two identical heavy and two identical light chains. In Pre-BCR, the IgH μ is formed followed by the formation of a surrogate light chain consisting of the non-covalently associated polypeptides VpreB and lambda5. The BCR in mature B cells comprises Ig heavy and Ig light chains (either VpreB or lambda5). S-S: disulfide bonds, Ig: Imunoglubuline, Pre: Precourser, BCR: B cell receptor. Adapted from [18]

1.2 BCR signaling in B cells:

BCR signaling plays an essential role in determining the fate of B cells. The complexity of the signal permits many distinct outcomes, including survival, tolerance, apoptosis, proliferation, and differentiation into either antibody-producing cells or memory B cells. The outcome of the response is determined by the maturation state of the cell, the nature of the antigen, the magnitude and duration of BCR signaling, and signals from other receptors such as CD40 [19].

The signalling components in mature B cells contribute to the phosphorylation of kinases in a cascade pattern, leading to BCR activation and final signalling results. Since the BCR consists of the two heavy and light chain immunoglobulins that do not have signaling sequences, they are accompanied by two transmembrane proteins Igα\Igβ (CD79A\CD79B) which transduce signals from surface BCR to inside the cells via immunoreceptor tyrosine activation motifs (ITAM) within their cytoplasmic tails (Fig1-3).

BCR engagement initiates three major signaling pathways: the phosphoinositide 3-kinase (PI3K) pathway, the phospholipase C-γ (PLCγ2) pathway, which causes calcium mobilization, and the Ras pathway which leads to extracellular signal-regulated kinase (ERK) activation [20]. Upon BCR ligation with antigens, BCR are aggregated into lipid microdomains to form microcluster shapes where the two tyrosine residues within the ITAM motif are phosphorylated [21]. ITAM phosphorylation is enabled by Lyn (

which gets activated by CD45 [22]) and Fyn, which reside within the lipid rafts [23, 24]. This binding process promotes the recruitment and phosphorylation of proteins such as spleen tyrosine kinase (Syk). Syk is predominantly responsible for BCR signaling propagation [25], and signalosome formation. Lyn also phosphorylates the co-receptors CD19/CD21 [26]. What follows is the recruitment of PI3Kdelta (PI3Kδ), which gets activated by CD19, and generates phosphatidylinositol 3,4,5 trisphosphate (PIP3) from phosphatidylinositol 4,5 bisphosphate (PIP2) [27, 28]. This allows formation of the signalosome consisting of scaffolding proteins, including B-cell linker protein (BLNK), and pleckstrin homology domain-containing proteins such as Bruton's tyrosine kinase (BTK) an PLCγ2 [29]. Recruited scaffolding proteins are, in turn, phosphorylated by the proximal kinases Lyn and Syk [30].

BTK becomes activated by association with the plasma membrane and BLNK, and phosphorylates PLCγ2, a step necessary for the latter's lipase activity [31]. Fully activated PLCγ2 hydrolyses PIP2 to generate the second messengers inositol 1,4,5-trisphosphate (IP3) and diacylglycerol (DAG). IP3 in turn binds to the IP3 receptor located on the endoplasmic reticulum and results in calcium release from internal stores [32]. Together, released calcium and DAG cause protein kinase C (PKC) isoform activation, essential for NF-κB pathway activation [33].

DAG also stimulates PKC to phosphorylate RasGRP3, a Ras guanine nucleotide exchange factor (RasGEF) [34]. RasGRP3 in combination with

Grb2-Sos, activated by BLNK, activates Ras [35, 36], which eventually stimulates the Raf/MEK/ERK signaling cascade [37].

Erk1/2 phosphorylation plays an important role in cell proliferation and the prevention of apoptosis through the regulation of several transcription factors [38, 39]. PIP3 generated by activated PI3Kδ recruits and activates AKT [40], crucial for cell growth and proliferation through the mTOR protein complex [41]. Ultimately transcription factors get activated to connect BCR signaling to gene transcription [42].

BCR engagement with antigen also results in actin cytoskeleton reorganization to induce immunological synapse (IS) formation and arrest of cell movement through VAV2. VAV2 stimulates formation of active Rho family GTPases (GTP-RAC and GTP-CDC42) to induce cytoskeleton rearrangement (see section1.7) [43, 44]. This has the effect of initiating BCR internalisation. Following receptor ligation, a small population of BCR are inductively phosphorylated and selectively retained at the cell surface where they serve as a foundation for the assembly of signaling molecules and contribute to endocytosis of a larger population of non-phosphorylated receptors [45, 46]. The endocytosis of this large population of BCR is required to present antigen peptides to T cells [47]. Since B cells are considered antigen-presenting cells, they internalise ligand-BCR complexes via clathrin-coated pits and present the ligand on their surface in conjunction with MHC class II proteins [48]. Of note, the ligand-BCR internalization is sensitive to inhibition of the Arp2/3 complex, indicating the necessity of this

complex for this process [49]. Internalisation of BCR is followed by its trafficking to lysosomes, degradation of the associated ligand to peptides, and loading of these peptides on to major histocompatibility complex class II (MHC II) proteins which are then expressed on the cell surface ready for interaction with T cells [49]. Presentation of peptides to cognate $CD4^+$ T helper cells allows the recruitment of these helper cells to facilitate complete B cell activation through the interaction of CD40 on B cell surface and CD40L on T cells surface [50, 51].

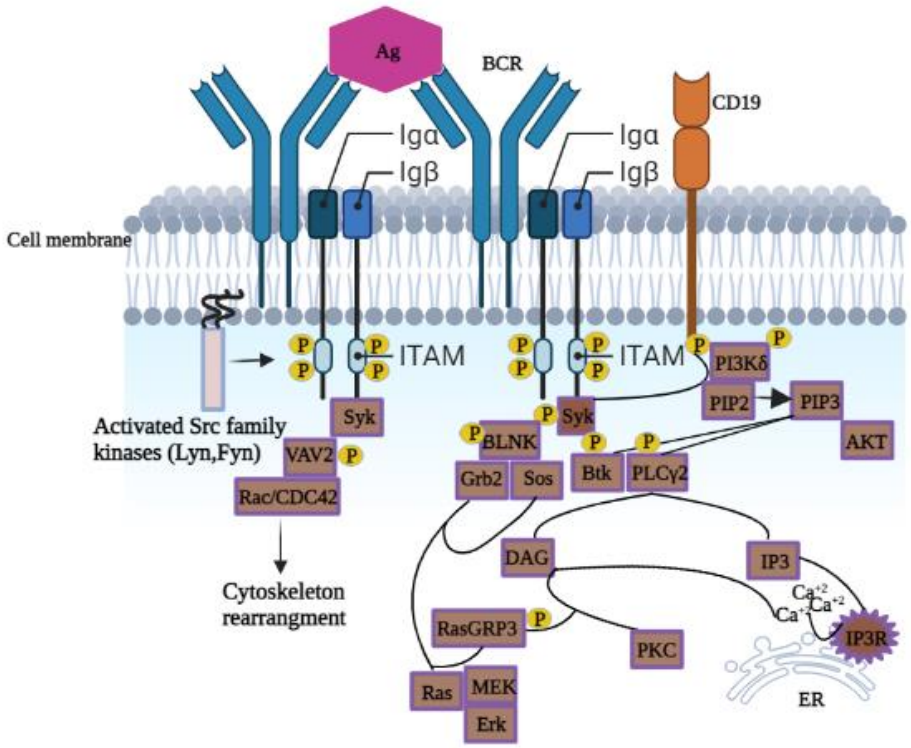

Figure 1-3: B cell receptor pathway. The BCR is composed of an immunoglobulin M molecule linked to an Igα/Igβ heterodimer. BCR signaling is triggered upon antigen engagement, and signal initiation occurs when the tyrosine residues in the cytoplasmic ITAM portion of Igα/Igβ are phosphorylated by kinases Lyn. This event results in the formation of a signalosome, composed of kinases and adaptor proteins, such as Syk, Btk, BLNK, Grb2, and Sos. Downstream signal propagation advances through activation of various pathways: Specifically, Syk phosphorylates the adaptor protein BLNK which allows BLNK to assemble Btk, PLCγ2, and Grb2. When these molecules are recruited, Syk can phosphorylate Btk to activate PLCγ2. Following its activation PLCγ2 generates IP3, which induces calcium influx from the intracellular stores in the ER. DAG in combination with released calcium activates PKC and Ras and eventually MEK/ERK. In addition, phosphorylation of the CD19 co-receptor by Lyn causes PI3Kδ activation which phosphorylates PIP2 to generate PIP3 to activate AKT. Syk also phosphorylates VAV2 to stimulate the bond change within Rho family GTPases (RAC and CDC42) and induce cytoskeleton rearrangement. Ag: Antigen, BCR: B cell receptor, ER: Endoplasmic reticulum, ITAM: Immunoreceptor tyrosine-based activation motif.

1.3 Actin cytoskeleton reorganisation:

The cytoskeleton refers to a system of filaments in eukaryotic cells which exists to serve a variety of functions including the ability to change cell shape and facilitate cell movement. The cytoskeleton is broadly divided into three main filaments: Actin filaments, Microtubules, and intermediate filaments. The Actin filaments are composed of a network of actin filaments (F actin) that are polymerised from actin monomers, or globular actin (G actin) [52].

Actin filaments have two ends, a barbed end, and a pointed end. The polymerisation process develops when G-actin monomers added on to the barbed ends of existing F-actin. These monomers are all added to the filament in the same orientation. G-actin monomers are also added in the other direction (to the pointed ends of F-actin) but the rate of growth is slower and is not stable, which allows the overall growth of actin filaments towards the barbed end [53]. The difference in actin filament growth rate in both directions mainly relies on ATP-actin and ADP-actin activity. ADP-actin is associated with pointed ends of F-actin, and more readily dissociates from this end of the actin filament compared to ATP-actin that is associated with barbed ends. The balance between ADP-actin and ATP-actin is important because it also governs, respectively, net loss of actin monomers from the pointed end and net addition of monomers at the barbed end [54].

1.4 Actin polymerisation factors:

Actin filament polymerisation and depolymerisation are controlled by many accessory proteins termed Actin Binding Proteins (ABPs) which regulate the growth of actin filaments in space and time. These ABPs are classified into a number of families according to their primary functions such as filament nucleation proteins, severing, capping, and crosslinking proteins [55]. Formins are a class of actin nucleators that mediate the formation of the linear actin bundle. Formins are activated by Rho family GTPases to derive actin polymerisation at the barbed end [56]. In B cells, when the antigen receptor is activated, uptake of the antigen needs the activity of formins that are present near receptor foci that then produce the linear filaments required for internalisation [49]. Another actin nucleator is the Arp2/3 complex, which will be described in detail later in this chapter.

A variety of stimuli lead to reorganisation of actin filaments, and this includes BCR stimulation [57]. This remodelling of actin provides a force that is needed for proper B cell activation [58].

1.5 Actin cytoskeleton controls BCR signaling:

The actin cytoskeleton plays a role in regulating BCR signaling and B cell activation. Evidence has shown that perturbation of the actin cytoskeleton by cytochalasin D (an inhibitor of actin polymerisation), induces a rapid and sustained elevation of intracellular calcium flux [59]. Moreover, follow up studies report that disruption of the actin cytoskeleton after BCR stimulation leads to prolonged activation of the MAP kinase pathway, elevates

sustained Ca^{2+} signaling, and enhances activation of the transcription factors NF-κB and NFAT [60].

Prior to antigen engagement of the BCR, actin filaments contribute to the prevention of spontaneous stimulation. Association of the BCR with cortical actin maintains its steady state in resting B cells. This cortical actin network consists of branched actin filaments that are held together by ABPs and tethered to the plasma membrane through the interaction with ezrin /radixin/ moesin [ERM] proteins [61]. ERM proteins bind this network to lipid rafts located within the plasma membrane [62]. A role of ezrin in this regard is to establish a barrier to BCR diffusion, particularly within actin-rich areas of the cell membrane because BCR located in actin-rich regions is observed to exhibit slower diffusion than those located actin-poor regions of B cell membranes [63]. Any signaling in this environment by BCR is likely to be tonic in nature, and not lead to activation of the cell.

Disruption of the ezrin-defined actin network, by antigen engagement of the BCR, removes constraints to BCR diffusion and leads to initiation of intracellular signaling, possibly as a result of microcluster formations of multiple BCRs [64] [63, 65]. Under these conditions, ezrin undergoes transient dephosphorylation associated with rapid actin depolymerisation and detachment of cortical actin networks from the plasma membrane [66]. This disassembly frees BCR from the barriers, permitting them to collide and interact with each other and form microclusters [64] that ultimately amplify BCR signaling [67]. Disassembly of cortical actin networks is

followed by actin reassembly [68] at the outer edge of the membrane allowing the B cell to increase the contact zone with antigen. This expansion of the B cell contact surface also enables an increase in the number of antigen-engaged BCR [69], which eventually leads to contraction of the cell. In this latter process, BCR microclusters coalesce with each other, resulting in the formation of a central cluster to bring BCR–antigen complexes inwards and facilitate antigen internalisation [48, 70] (Fig 1-4).

Thus, the transition in the function of actin remodelling from controlling BCR diffusion, to driving B-cell spreading and contraction, and finally facilitating BCR microcluster formation ultimately leads to initiation of BCR downstream signaling.

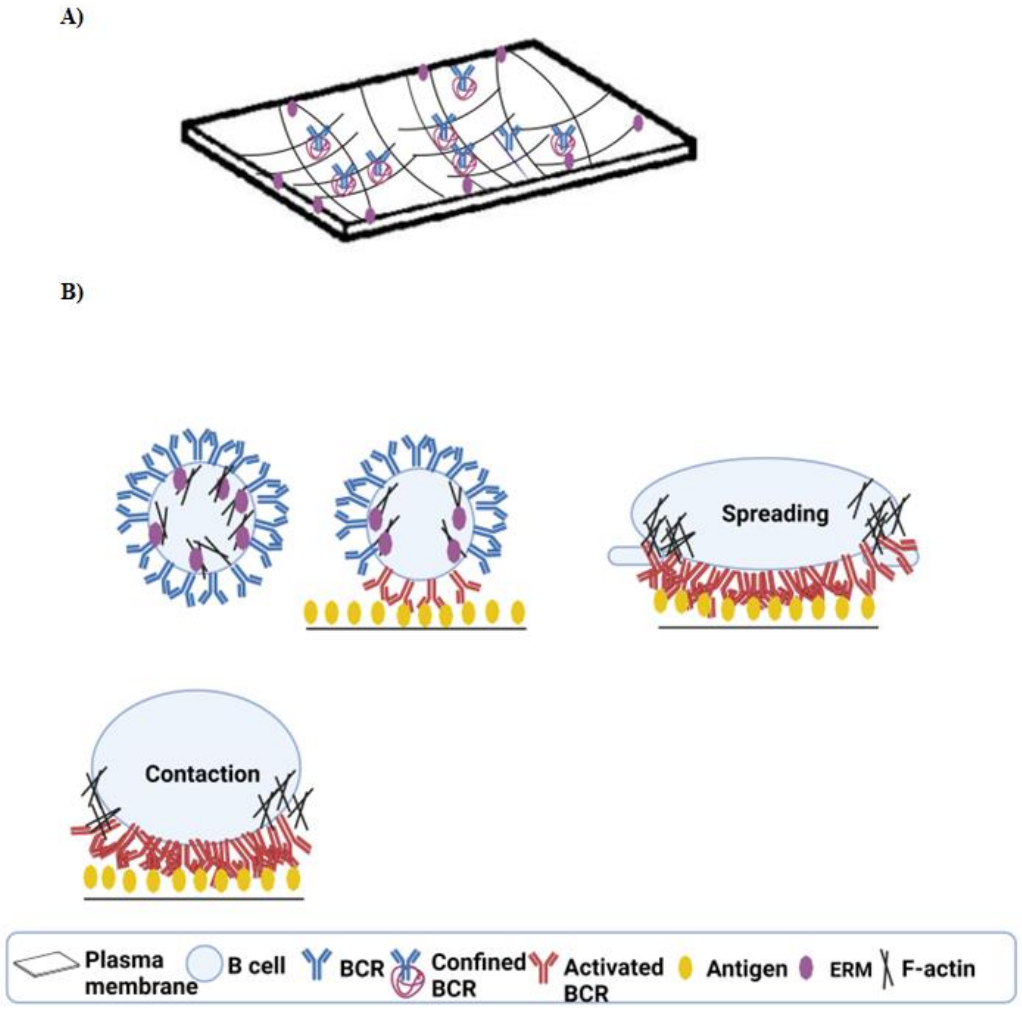

Figure 1-4: Actin cytoskeleton role in preventing spontaneous BCR stimulation and facilitating their antigen-based stimulation. A- ERM proteins hold the cortical actin to the plasma membrane to reduce the BCR diffusion and prevent their clustering. B- upon antigen ligation, ERM deactivated associated with cortical actin depolymerisation and detachment from the plasma membrane allowing BCR interaction, clustering, and B cell spreading to gather more antigen. De novo actin repolymerised after BCR clustering to reduce the B cell size(contraction) facilitating BCR-antigen internalisation. BCR: B cell receptor, ERM: ezrin /radixin/ moesin. Adapted from [71, 72].

1.6 Arp2/3 complex identification and characterisation:

The Arp2/3 complex is a ubiquitous and key component of the actin cytoskeleton in cells. The Arp2/3 complex is a 220 kD seven-protein complex. It contains two actin-related proteins, five other protein subunits, and is an important regulator of cellular motility by giving rise to actin polymerisation of new filaments [73]. The complex was first discovered in the protozoon Acanthamoeba, followed by a finding that determined the predicted amino acid sequence of all seven subunits referred to as Arp2, Arp3, p41-Arc, p34-Arc, p21-Arc, p20-Arc, and p16-Arc (ARPC1-5). Each of these subunits has homology in diverse eukaryotes, implying that the structure and function of the complex has been conserved through evolution [74] (Fig 1-5).

Two types of actin nucleation factors are functioning to generate new actin filaments in cells, formins and the Arp2/3 complex. Both nucleation factors cooperate to form the cortical cytoskeleton at the plasma membrane of a cell [75]. Formins nucleate actin filament directly from actin monomers and produce unbranched filaments. However, Arp2/3 nucleates new actin filaments from the sides of pre-existing filaments (mother filament) at a 70° angle (called the Y-branching nucleator) and produce branched network and lamellipodial cell protrusions. The pointed end of the new branch is capped by the Arp2/3 complex, and growth of the actin filament will be from its barbed end [76].

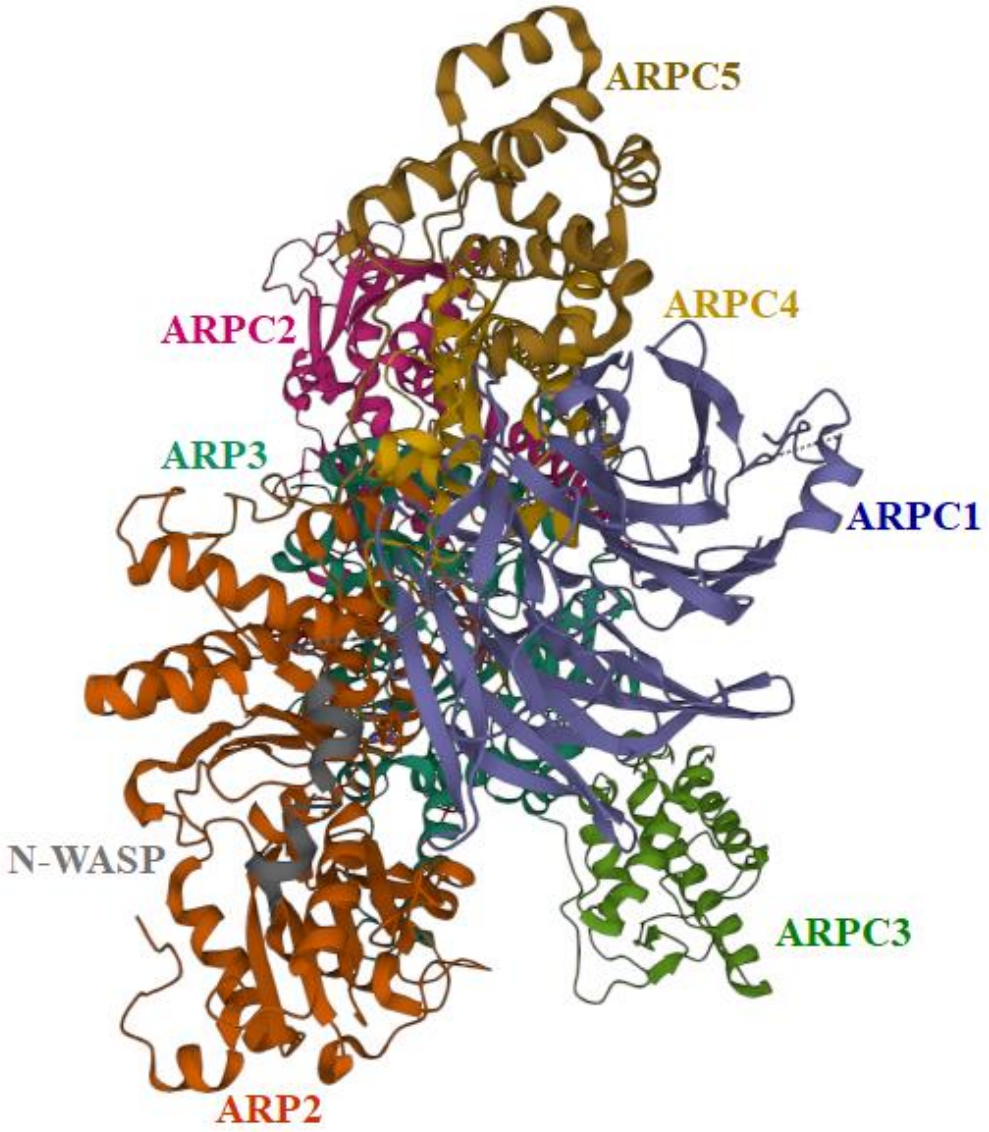

Figure 1-5: Cryo-electron microscopy (CryoEM) structure of human Arp2/3 complex with bound NPFs. Arp2/3 complex contains two actin-related proteins and five other protein subunits. Arp2, Arp3, and (ARPC1-5). Taken from Protein data bank with accession number 6UHC.

1.7 BCR signalling induces Arp2/3 complex activation:

The Arp2/3 complex is considered the essential molecular machine for nucleating actin filament assembly. It is a central player in regulating both the initiation of actin polymerisation and promoting the formation of branched F-actin filaments. The complex is activated by conformational change within the Arp2 and Arp3 subunits [77]. These changes stimulate weak spontaneous filament nucleation activity, but in order for efficient actin assembly in the cell to occur other factors are needed.

VAV2, a guanine exchange factor, is phosphorylated by Syk when it is located at the plasma membrane [78]. VAV2 stimulates exchange of GDP to GTP within Rho family GTPases (Rac and CDC42) [79]. These small GTPases bind nucleation-promoting factors (NPFs) via Rac binding domains, and facilitate phosphorylation of these factors by Lyn and Btk [80], possibly by recruiting NPFs to the plasma membrane [80] where Lyn and Btk are present.

Type I NPFs (WASp, N-WASp, WAVE, WASH, WHAMM, and JMY), when phosphorylated, bind directly to the Arp2/3 complex to induce conformational change that facilitates efficient actin assembly [77, 81], which eventually enhances IS formation [82, 83]. These proteins bring individual actin molecules together with the Arp2/3 complex via a conserved carboxy-terminal Verprolin and Cofilin**,** Acidic (VCA) domain [84]. The juxtaposition of the Arp2/3 complex with monomeric actin stimulates dissociation of the NPF, and this allows elongation of the actin filament.

Induction of actin polymerisation by BCR signaling is mainly achieved by WASp family and WAVE proteins [85]. WASp and its paralogue N-WASp are expressed in blood cells. WASp and N-WASp exhibit ~50% homology but have distinct functions. WASp deficiency causes Wiskott-Aldrich syndrome, an immune deficiency condition resulting from B cells that are unable to perform their normal function. This indicates that despite the structural and functional homology that exists between WASp and N-WASp, the latter is not able to perform all the functions performed by WASp [86]. Both NPFs are important for B cells where they act to connect BCR signaling to the actin cytoskeleton.

Actin polymerisation in response to BCR activation is facilitated by WASp through phosphorylation by Btk. This occurs at the plasma membrane in conjunction with Vav, and is dependent on the presence of PIP2 [80]. The critical role of Btk is demonstrated by experiments where B cells are treated with a Btk inhibitor to inhibit the rate of BCR internalisation, BCR trafficking to the late endosome, and efficiency of BCR-mediated antigen presentation [87].

WASp and N-WASp exist in autoinhibited forms. The two regions, GTPase binding domain (GBD) and VCA interact with each other to keep the inactive auto-inhibitory conformation [88]. When BCR engages with antigen, the interaction of CDC42 with WASp occurs through the GTPase binding domain (GBD) that leads to a conformational change of WASp. PIP2 cooperates with CDC42 and facilities WASp and N-WASp activation,

possibly by enhancing their recruitment to the plasma membrane [89]. When WASp and N-WASp reach the cell membrane, they become phosphorylated by Lyn and Btk on tyrosine residues [80]. However, further investigation is needed to fully clarify the mechanism of WASp and N-WASp activation. WAVE is comprised of five subunits in B cells. This complex undergoes changes from an inactive to active state when BCR is engaged. GTP-Rac generated from such engagement binds to WAVE to permit it's access to the Arp2/3 complex and catalyze actin polymerisation. The WAVE complex contributes to the formation of membrane protrusions during B cell mobility [90].

In contrast to type I NPFs, type II NPFs. such as cortactin and HS1, are weaker activators of the Arp2/3 complex. This is because these proteins fail to promote conformational change in the Arp2/3 complex [77]. Nevertheless, cortactin does promote the association of the Arp2/3 complex with F-actin, and this results in partial activation of the complex [91]. Cortactin binds to the Arp2/3 complex via a motif located near to its N terminus, and to actin filaments via a region of central repeat domains that help target Arp2/3 complexes to branch points [92]. Cortactin binds to filamentous actin instead of actin monomers, and, in contrast to WASp and NWASp, creates *de novo* branches within filaments [77, 93]. Importantly, Cortactin and N-WASp are able to bind simultaneously to the Arp2/3 complex where N-WASp is released after nucleating an actin filament and cortactin remains associated with the complex at the branch point [94], to stabilise and protect the filament from disassembly from coronin 1B

associated actin disassembly [95, 96]. Interestingly, the ability of cortactin to stabilise actin filaments is dependent on the presence / absence of particular paralogues (namely ARPC5, ARPC5L, ARPC1A and ARPC1B) within the Arp2/3 complex (see section 1.12) [97]. In B cells, the activation of the Arp2/3 complex occurs through interaction with nucleation-promoting factors such as WASP, N-WASP, and cortactin, all of which can bind the complex directly [98-100].

In addition to WASp and cortactin, another important actin remodeling regulator in B cells is Haematopoietic lineage cell-specific protein 1 (HS1). HS1 is a paralogue of cortactin, and functions as an actin-binding protein [101, 102]. HS1 is exclusively expressed in hematopoietic cells and, like cortactin, it promotes actin polymerisation. It is a Lyn kinase substrate that, when overexpressed and highly phosphorylated in CLL cells, is associated with poor prognosis [103]. HS1 can also bind the Arp2/3 complex in a similar way as cortactin, but may not have the same capability to facilitate the formation of branched actin filaments due to weaker actin binding affinity [104]. Both WASp and HS1 are known to interact with actin filaments and stimulate their assembly, pointing at a potential relationship between BCR signaling and actin cytoskeleton dynamic.

HS1 is connected to B cell signaling via a C-terminal Src homology 3 (SH3) domain [105]. As mentioned previously (in section 1.6), in B cells and after BCR crosslinking, HS1 phosphorylation by Lyn promotes Arp2/3 complex-mediated actin polymerisation. Unlike cortactin, HS1 does not require the

central repeat domains that mediate F-actin binding. When these domains are deleted in HS1, this protein maintains a significant F-actin binding activity but fails to bind the Arp2/3 complex. On the other hand, the deletion of the coiled-coil region of HS1 abolishes F-actin binding ability and significantly reduces the ability to activate the Arp2/3 complex for actin nucleation and actin branching. These observations indicate that both repeat domains and the coiled-coil region act synergistically in the modulation of the Arp2/3 complex-mediated actin polymerization [106] (Fig1-6).

Thus, type I NPFs function as primary activators of the Arp2/3 complex through their ability to recruit G-actin to the proximity of the Arp2/3 complex. In constrast, the more crucial role of class II NPFs is to stabilise nascent filamentous actin (F-actin), and subsequently both types of NPFs contribute actively in the organisation of the actin networks that are generated by the now active Arp2/3 complex.

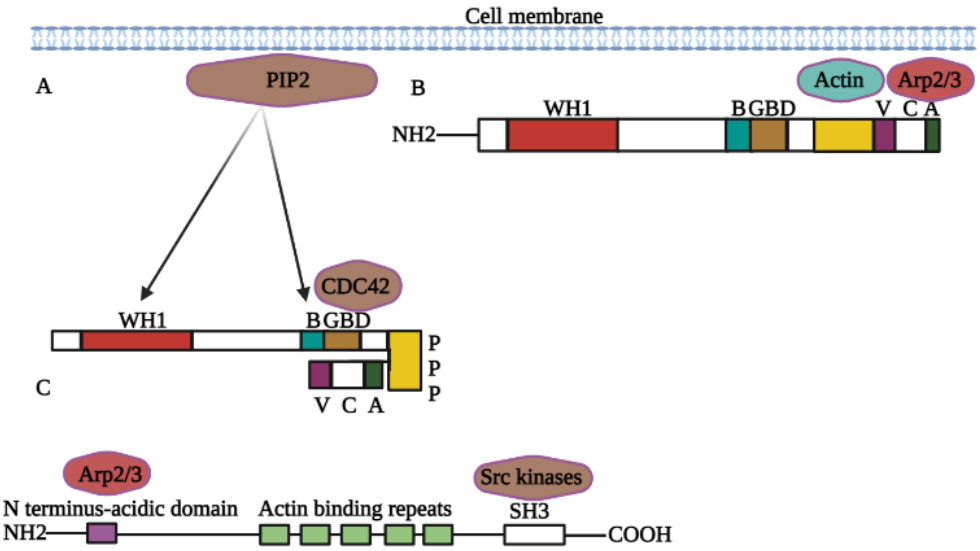

Figure 1-6: Arp2/3 complex activation by type I NPFs and type II NPFs. Multiple domains exist in type I NPFs and type II NPFs. A) Type I NPFs including WASp exist in an autoinhibited form by the interaction of GBD domine with VCA domine. During the B cell activation process, PIP2 binds to B rejoin and/or WH1 and CDC42 binds to the GBD domain causing the requirement of WASp to the cell membrane and its activation. of the WASp. B) In the activated WASp, the V domine binds to actin monomers, and C, A rejoins bind to the Arp2/3 complex leading to their activation. C) Type II NPFs (Cortactin) activated by Src kinases binds to filamentous actin by actin-binding repeats and Arp2/3 complex through the N terminus acidic domain. NPF: Nucleation-promoting factors, GBD: GTPase-binding domain, V: Verpolin, C: Central, A Acidic. Adapted from [107, 108].

1.8 Arp2/3 complex function in BCR singling:

In human B cell lines, during stimulation and after initial cell spreading, F-actin in immunological synapses forms a highly dynamic pattern composed of actin foci interspersed with linear filaments. The foci are generated by Arp2/3-produced branched-actin filaments and stochastically associated with antigen clusters to mediate antigen-BCR internalisation. Moreover, for B cell signaling propagation, BCR microcluster centralisation is essential and a study has shown that using the Arp2/3 complex activity inhibitor CK-666, the centralisation of BCR micro clusters is abolished pointing at the requirement of Arp2/3 complex for centralisation of BCR-Ag microclusters**.** Interestingly, B cells treated with the Arp2/3 complex inhibitor, CK-689 exhibited significantly lower phospho-CD79 levels suggesting that the Arp2/3 complex also contributes to amplifying proximal BCR signaling [82]. Inhibition of Arp2/3 complex activity impaired the ability of primary B cells to increase their cell surface levels of CD69 after BCR stimulation [82], indicating the role of the Arp2/3 complex in modulating the activation state of B cell.

Thus, these findings emphasize the indispensable role of Arp2/3 complex-dependent actin remodeling in B cell responses including initiation and amplification of BCR signaling.

1.9 Arp2/3 complex subunits:

As mentioned previously, Arp2/3 is a seven-protein complex. The protein subunits contribute differentially within the Arp2/3 complex leading to the

maintenance of Arp2/3 structural integrity and actin nucleation activity. Within the complex, Arp2 and Arp3 are critical for actin assembly since they bind to ATP for actin nucleation [109] and mimic the actin monomers to initiate actin filament formation [84]. WASp stabilises ARPC2/p34-dependent closure of the complex, keeping Arp2 and Arp3 close to each other which results in a conformational change within the complex for its activation [110]. Depletion of ARPC2/p34 leads to loss of all Arp2/3 complex subunits [97]. ARPC2/p34 and ARPC4/p20 subunits interact tightly with each other making substantial contact with the mother filament. They are necessary for the assembly of the complex since they hold the structural integrity of the complex while the remaining subunits are located more peripherally within the complex [111, 112]. Interestingly, when the BCR engages with antigen, ARPC2 is localised to the IS and is essential for the production of actin foci in these synapses [49]. ARPC3/p21 forms a bridge between the mother filament and Arp3 [113] and increases the efficiency of the filament nucleation. ARPC3/p21 and ARPC1/p41 coupled Arp3 and Arp2 respectively, likely represent the two VCA-binding sites on the Arp2/3 complex [101]. Moreover, ARPC1/p41 has another paralogue ARPC1B and actin assembly and disassembly are greatly affected by the composition of the complex with either paralogue [97]. For example, Arp2/3 complexes containing ARPC1B are better at promoting actin assembly than complexes with ARPC1. ARPC1B is also required for T cell activity. One study has shown that cytotoxic T lymphocyte function is impaired by the depletion of ARPC1B in terms of cell migration and actin reorganisation across the

immune synapse. Moreover, the presence of ARPC1B is crucial for T cell receptors (TCR) at the cell surface where they are required for signaling and proliferation upon engagement [114].

In the complex, ARPC5/p16 has shown interaction with Arp2, ARPC4, and ARPC1. Depletion of ARPC5 leaves only traces of ARPC1 in Arp2/3 complex, emphasising the importance of ARPC5 for either ARPC1 association/ expression within the Arp2/3 complex, or for maintaining its stability within this complex [115]. While ARPC1 and ARPC5 are dispensable for branch formation by the Arp2/3 complex, they are important for filament nucleation since it has been reported that the Arp2/3 complex with the ARPC1 and ARPC5 deletion shows 85-fold less Arp2/3 nucleation activity than the intact complex. This evidence indicates the requirement for ARPC1 and ARPC5 by the Arp2/3 complex for actin nucleation activity [115].

Taken together, these findings suggest that individual Arp2/3 complex subunits perform separable functions in actin filament formation and organisation and may be differentially regulated in cells.

1.10 ARPC5 paralogue:

The molecular mechanism underlying the roles of Arp2/3 complex subunits regulating the function of the complex is incomplete. For the purpose of this thesis, I will focus on the roles of ARPC5 and its paralogue ARPC5L.

ARPC5 and ARPC5L can be incorporated into the Arp2/3 complex, in a either/or configuration. These proteins are encoded by different genes that share a ~ 67% sequence identity [116]. In terms of tissue distribution, the two paralogues show differences. ARPC5 was found to be highly enriched in the spleen and thymus, while ARPC5L shows a ubiquitous expression with more abundance in the brain [116]. Within cells, both paralogues have been found in lamellipodia and cytosolic puncta in conjunction with the Arp2/3 complex [74]. The sequence differences between the two paralogues are spread throughout their length, and many are surface-exposed [112]. This raises the hypothesis that these differences between ARPC5 and ARPC5L function to alter the properties of the Arp2/3 complexes these paralogues find themselves within (Table1.1).

As indicated above, actin nucleation by the Arp2/3 complex differs depending on which ARPC5 paralogue is present. In 2017, a study has shown that these paralogue diversities determine the actin filament dynamics within cells [97]. Cells depleted with either paralogue and infected with vaccinia virus show different actin properties. When ARPC5 is missing in cells the movement of vaccinia virus is faster than it is in cells missing ARPC5L. Furthermore, Arp2/3 complexes containing ARPC5L are more efficient at stimulating actin polymerisation when activated by the VCA domain of N-WASp compared to complexes containing ARPC5. Interestingly, actin branches assembled by Arp2/3 complexes containing ARPC5 are more susceptible to coronin mediated disassembly than those complexes induced by ARPC5L, and this function relies on cortactin since

cortactin preferentially stabilies ARPC5L containing complexes in actin filaments to protects them from coronin-mediated disassembly [97].

These findings suggest that the Arp2/3 complex in higher eukaryotes is a family of complexes with different properties. Understanding how ARPC5 paralogues affect Arp2/3 complex behaviour in BCR signaling and ultimately regulate B cell function is still unclear.

	ARPC5	ARPC5L
Genetic locus	1q25	9q33
Protein length	151 amino acids	153 amino acids
Localisation	Lamellipodia	Lamellipodia
Tissue distribution	Spleen, thymus	Brain
Molecular weight	16kDa	17kDa

Table 1-1: Characterisation of ARPC5 paralogues. Upon their discovery, ARPC5 paralogues were characterised structurally and in terms of tissue distribution.

1.11 CLL and MCL pathophysiology:

CLL and MCL are classically considered indolent and aggressive neoplasms, respectively. They are mainly identified by the uncontrollable accumulation and proliferation of mature B cells that may involve the bone marrow, blood, lymphoid tissues, and extranodal sites. The clinical evolution of both malignancies is very heterogeneous, with subsets of patients having stable disease for long periods, while others require immediate intervention. These two tumors differ in their genomic alterations, molecular pathways, and clinical behavior. However, the pathogenesis of the two entities integrates the relevant influence of BCR signaling, tumor cell microenvironment interactions, and some genomic alterations that configure the evolution of the tumors and offer new possibilities for therapeutic intervention [117].

The malignant cells of CLL are likely derived from normal $CD5^+$ B cells. [118]. This is supported by a recent study comparing gene expression in CLL cells with that in normal $CD5^+$ B cells where they found high similarity between the two [119]. Additionally, all CLL is derived from monoclonal B lymphocytosis, a pre-cursor condition where clonal expansion of $CD5^+$ B cells is observed. In contrast, the cell of origin in MCL is different, arising from follicular mantle B cells which are able to express CD5 on their cell surface. A defining feature of MCL cells is presence of the t(11;14) (q13; q32) chromosomal translocation which leads to overexpression of cyclin D1 and unregulated proliferation of the malignant cells [118].

Importantly, BCR is an important driver of malignant cell survival and proliferation in both CLL and MCL. With respect to CLL, analysis of IgHV gene sequences lead to the discovery of common BCR structures between patients, and that changes in the level of mutation (defined as mutated when greater than 2% from germline sequence, and unmutated when less than 2% from germline sequence) configured reactivity of the expressed BCR. CLL cells with unmutated IGHV were more polyreactive than CLL cells with mutated IGHV. Unmutated CLL is associated with progressive disease and B cells that have not undergone the germinal centre reaction. On the other hand, cases of mutated CLL bear mutation of IgHV genes that have been subjected to SHM as part of the germinal centre reaction. Patients with mutated CLL generally have disease with behaves in an indolent fashion [120]. This distinction of GC naïve versus experienced cells is supported by studies showing that unmutated CLL is derived from $CD5^+$ $CD27^-$ B cells while mutated CLL is derived from $CD5^+$ $CD27^+$ B cells [119]. CD27 expression is upregulated on memory, or GC-experienced, B cells.

With respect to MCL cells, approximately 15%–40% of patients with MCL have malignant B cells that carry IGHV hypermutations, and, similar to CLL, there is a strong bias in the repertoire of IGHV gene usage. Furthermore, in 10% of MCL cases stereotyped complementarity-determining region 3 (VH CDR3) sequences have been recognized. Together, this data suggests that BCR is also a driver of disease pathogenesis in, at least, a subgroup of MCL patients.

1.11.1 MCL and CLL chromosomal and genetic abnormality:

MCL is characterized by developing pathognomonic chromosomal translocation, such as t (11;14) (q13; q32), which causes a fusion of the cyclin D1 gene on chromosome 11 to the immunoglobulin heavy chain promoter on chromosome 14. This fusion is a diagnostic hallmark of the disease, as abnormal cyclin D1 expression plays a major role in dysregulating the G1/S phase transition of the cell cycle, and therefore increases cell proliferation. The disease can be stable and asymptomatic for long periods, but some tumors may acquire additional genetic alterations which facilitate progression of the disease to more aggressive behaviour with a poor prognosis [121]. TP53 is often mutated in MCL, and as a tumor suppressor gene that pauses cell cycle progression and induces apoptosis depending on levels of genomic and cellular stress, its dysfunction can lead to greater genetic instability. [122].

A subset of MCL does not carry the t(11;14) translocation despite having similar pathological and clinical characteristics [123]. These cases overexpress the transcription factor SOX11 [124], and/or a combination of SOX11 mutation and cyclin D1 overexpression [125]. SOX11 acts as an oncogene in MCL promoting malignant cell growth and regulating broad transcriptional programs that induce cell proliferation. One direct target of SOX11 is the Paired box transcription factor PAX5, a regulator for B cell differentiation whose downregulation is required for plasma cell development [126]. PAX5 regulates expression of BLIMP1, which is a

master regulator of B cell differentiation to plasma cells [127, 128]. SOX11 upregulates expression of PAX5 which then suppresses expression of BLIMP1, and this maintains the differentiation status of MCL cells. This shows that SOX11 actively contributes in MCL pathogenesis and can serve as a specific biomarker for the diagnosis of MCL irrespective of the cyclin D1 presence.

In CLL, by applying classical cytogenetic techniques, it is revealed that clonal chromosome abnormalities have been identified in more than 80% of the cases. Four main chromosomal abnormalities are usually observed in CLL cytogenetic analysis, trisomy of chromosome 12 and deletions of chromosomal regions 11q, 17p, and 13q which usually affect the progression and future prognosis of the disease [129]. The most frequent chromosomal abnormality observed in CLL is deletion of 13q14 resulting in loss of expression of DLEU7 and miR15/16a. DLEU7 is a master inhibitor for the NF-κB pathway [130], and functions by physically interacting and inhibiting B-cell maturation antigen (BCMA) and transmembrane activator and calcium-modulator and cyclophilin ligand (TACI) [131]. BCMA and TACI are receptors for B-cell activating factor (BAFF) and A Proliferation-Inducing Ligand (APRIL), respectively. miR15 and miR16a regulate expression of Bcl2. Importantly, mouse studies where syntenic regions of 13q14 have been deleted, or APRIL expression upregulated, lead to development of CLL-like disease. Whereas BAFF overexpression does not result in neoplastic transformation of cells, it does accelerate development of CLL-like disease in mouse models. Deletion of 11q22 is associated with

dysfunction of the ATM gene, whereas deletion of 17p13 is associated with dysfunction of TP53, both lead to genomic instability and, ultimately, more aggressive disease behaviour. [132, 133]As mentioned previously in MCL, TP53 mutations in CLL well-established prognostic markers and inform on the appropriate course of treatment for patients as their major role in cell cycle control [134].

1.11.2 CLL and MCL Microenvironment support:

The fact that CLL/MCL cells are long-lived in vivo but rapidly undergo apoptosis in vitro clearly indicates they rely on the microenvironment to provide survival signals [135]. Malignant cells recirculate between peripheral blood and tissues, mainly lymph nodes and bone marrow, where they receive these survival and proliferation signals. These crucial interactions mainly occur in the proliferation centres of lymph nodes which contain a variety of follicular dendritic cells (FDC), a variable number of T cells, and other stromal cells. CLL cells crosstalk with activated T cells, for example, via CD40/CD40L interaction to promote cell survival [136] and receive secretion of several cytokines essential for cell proliferation such as IL-4 and IL-10 [137]. Stromal cells provide adhesive ligands and other factors that support CLL/MCL cell survival. For example, interaction between α4β1 on CLL and VCAM-1 on stromal cells mediate the adhesion of the former to the latter cells [138]. Moreover, microenvironment support provides migration signals to these malignant cells where α4β1 helps them to migrate into proliferation centres.

Stimulation of BCR may also occur during these interactions, thereby stimulating CLL/MCL cell activation and proliferation if sufficient T cell help is available [139]. Establishment of BCR signaling as a key player in the pathogenesis of B cell malignancies has resulted in development of therapies that target components of the signaling pathway that is intitiated following BCR engagement. Some of these therapies, such as ibrutinib, have shown clinical success in treating CLL and MCL, where lymphnode-resident tumour cells are released into circulation to an important role for BCR signaling in maintaining malignant cell residency within tissues [140].

Tumour cells in proliferation centres can expand in number are result in lymphadenopathy, splenomegaly and/or bone marrow suppression. Rai and Binets systems of stage classification in CLL link tissue involvement with more severe disease and potential aggressive behaviour depending on the extent of microenvironment-induced activation of NFκB, AKT and MAPK pathways [141]. [142]. Taken together, it is clear that microenvironmental support is critical for supplying survival and proliferation signals to CLL and MCL cells, therefore, disruption of these signals is likely to improve disease outcomes.

1.12 BCR signaling in CLL and MCL:

It is widely accepted that the majority of B cell malignancies remain highly dependent on abnormal activation of BCR signaling which controls neoplastic B cell growth, their proliferation, and inhibits their death [143, 144]. The key factors of aberrant BCR signaling are abnormalities in BCR

expression and/or changes in the activity of proteins within the signaling pathway [118, 143].

The role of BCR in CLL and MCL pathogenesis was discovered in studies that some cases have identical or quasi-identical amino acid sequences of the complementary determining region 3 (CDR3) within IGHV. This indicates strong antigen-driven selection and is explained by the propensity of the malignant cells in these diseases to use a restricted, or stereotyped, repertoire of IGHV gene segments [145, 146]. This repertoire of IGHV gene segments is shown to have reactivity with autoantigens where somatic hypermutation determines specificity, and with respect to CLL, created subgroups of patients where disease outcome is different (mutated CLL has good prognosis whilst unmutated CLL has poor prognosis) [147, 148]. This holds true also for MCL where there is biased usage of specific Ig heavy chain genes IGHV3–21, IGHV4–34, and IGHV3–23 [149, 150].

Recently, Syk, BTK, and PI3K were found constitutively activated in cells from a subgroup of patient in malignancies, and that this was associated with poor prognosis indicating constant BCR engagement [25, 151]. Such BCR engagement likely participates development of lymphadenopathy where BCR signals encourage malignant cells to remain within lymphoid tissues. [152]. Thus, treatments targeting BTK (ibrutinib) and PI3Kδ (idelalisib) cause release of the malignant cells in CLL and MCL into the periphery [153], which could lead to a rapid and sustained reduction of lymphadenopathy and ultimately suppresses disease progression [154,

155]. Combination of Ibrutinib affects α4β1, integrin-mediated adhesion and retention of malignant cells caused by BCR induced activation is disrupted [156]. With Idelalisib the arrest process of cells which occurs because of BCR stimulation is suppressed through upregulating sphingosine-1-phosphate receptor 1 (S1PR1) [140]. Moreover, according to the Food and Drug administration, BCR inhibitors are considered as second line treatment for CLL and MCL [157], whereas Chemotherapy treatment is the first line treatment. In combination with chemotherapy, Patients with CLL and MCL are often treated with immunotherapy drug rituximab to keep the leukemia/lymphoma in remission [158, 159]. Rituximab is a monoclonal antibody that selectively binds to CD20 protein expressed on the surface of B cells [160]. The interaction between CD20 and Rituximab facilitates the destruction of those malignant cells by immune cells.

Therefore, it is reasonable to target these kinases activity to at least prevent malignancy progression and improve survival rate.

1.13 Normal / CLL and MCL B cell migration:

Migration and trafficking of normal B cells is regulated via the interplay between chemokine networks and BCR signaling. Migration of malignant and normal B cells to the bone marrow and secondary lymphoid tissues is controlled by CC and CXC chemokines such as CCL21 and CXCL12. These chemokines bind to their receptors on B cells, CCR7 and CXCR4 respectively, and modulate intracellular pathways integral to chemotaxis [161]. For example, the interaction of malignant cells through CXCR4 and

CXCL12, which is secreted mainly by nurse-like cells facilitates the activation of PI3K-Akt, Raf/Ras/MEK1/2/ERK1/2, leading to key survival pathways [162].

Genes mutations affect CLL/MCL cells migration. Neurogenic locus notch homolog protein (NOTCH1) is a member of notch receptors family that are involved in B cell migration. It is frequently mutated in CLL/MCL cells and could influence their migration [163]. In glioma, a study has shown that NOTCH1 requires Arp2/3 complex activity to maintain stem cell phenotype as Arp2/3 complex regulate these malignant cells migration and thus invasion [164]. This study indicates to the link between NOTCH1 and Arp2/3 complex in solid tumor, and can be also investigated in CLL/MCL cells to further explain the migration phenotype in these cells.

The exact mechanism controlling migration/retention of CLL and MCL cells within lymphoid tissues is not fully clarified but BCR signaling may play a role because of its known function in reprogramming normal B cell migration [165]. Therefore, it is important to understand how BCR signaling and what are the components that affect malignant cell trafficking through lymphoid tissues to regress these diseases' progression.

1.14 ARPC5 paralogue in human cancer:

Only a few studies have highlighted the active role of ARPC5 paralogues in cancer progression and more investigations are needed to demonstrate how each paralogue influents actin dynamic in a variety of cancers. Apart from the vaccinia virus study on ARPC5 paralogues which has been done

in Hela cells, human cervical carcinoma cell line, another study has demonstrated the contribution of ARPC5 in head and neck squamous cell carcinoma (HNSCC) progression. Immunohistochemistry results show that the levels of ARPC5 expression were significantly higher in invasive cancer cells, and genome-wide gene expression analysis and bioinformatics study pointed out that ARPC5 is a candidate target of tumor-suppressive microRNA-133a (miR-133a) which is frequently observed downregulated in cancer cells. Restoration of miR-133a or silencing ARPC5 revealed significant inhibition of cell migration and invasion in HNSCC cell lines [166]. In addition, in Multiple Myeloma (MM), a malignancy of plasma cells, the expression level of ARPC5 highly determines the disease prognosis. ARPC5 level is significantly increased in relapsed MM cells compared to baseline MM cells, and patients with ARPC5 high expression are associated with poor overall survival [167]. Based on genomic data derived from the Cancer Cell Line Encyclopaedia (CCLE), a collection of information from 947 human cancer cell lines (114), shows a variety between ARPC5 paralogues mRNA expression with ARPC5L being highly expressed in B cell malignancies [168]. Potentially these paralogues could function in regulating actin dynamics in the same way as was described using a Vaccinia virus actin motility model (see section 1.10) or as characterised in other types of cancers (as mentioned up in this section).

These discoveries are expected to be extremely important in B cells since ARPC5 paralogues could influence how the actin cytoskeleton responds to BCR stimulation, and understanding their functional role provides a

comprehensive picture of the molecular mechanism underpinning B cell activation.

1.15 ARPC5 paralogue in MCL:

ARPC5 paralogues seem to have an important function in MCL. An open investigation had been done in our lab on the proteomics approach to globally characterise active BCR signaling in JeKo-1 cells, MCL cell lines. Using anti-phospho-tyrosine (p-Tyr) beads to immunoprecipitate phospho-tyrosine proteins and their associations we found that among 856 proteins that precipitated seven percent showed differential accumulation within BCR-stimulated compared to unstimulated cells which considered as a responsive group of proteins. Specifically, the strong enrichment of phospho-tyrosine associated ARPC5L in stimulated cells compared to unstimulated cells. (Fig1-7) [169]. As shown in that study, analysis of the peptide sequence of ARPC5L using the PHOSIDA and PhosphoSitePlus databases revealed that this protein did not contain tyrosine residues within consensus phosphorylation sites of known tyrosine kinases. This suggests that the representation of ARPC5L within the group of BCR responsive proteins is not because it is directly phosphorylated. More likely, ARPC5L is associated with tyrosine-phosphorylated proteins [170, 171].

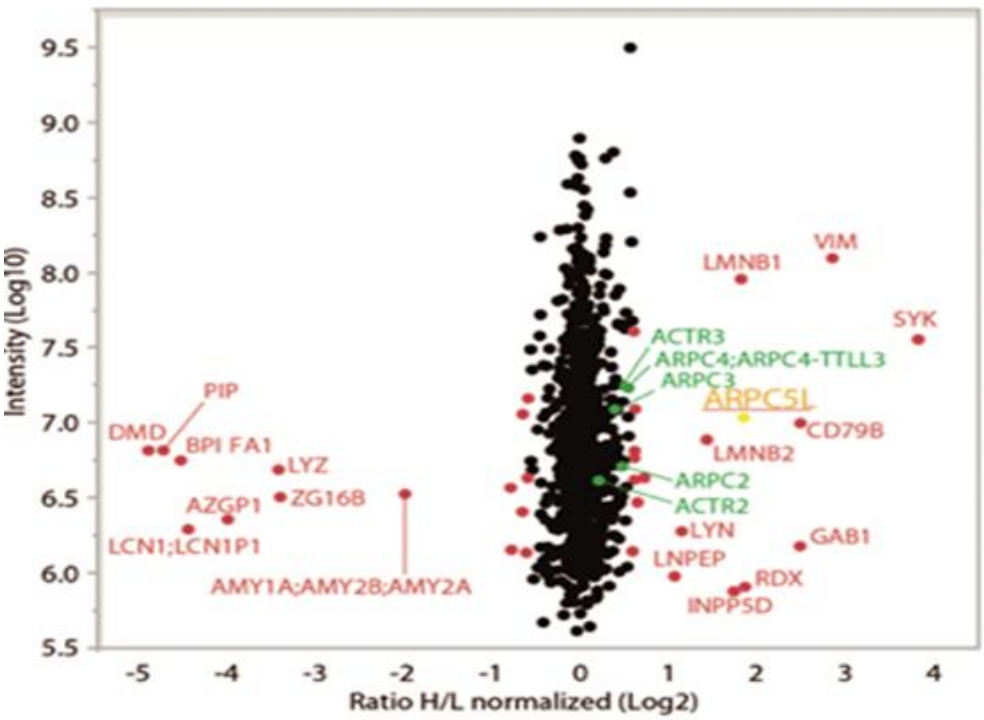

Figure 1-7: **A strong enrichment of phospho-tyrosine associated ARPC5L after BCR stimulation in Jeko-1 cells**. Jeko-1 cells were left untreated or treated with 20µg/ml of anti-IgM antibody for 15minutes. Lysates from both conditions were combined and subjected to immunoprecipitation using phospho-tyrosine antibody beads. Proteins in red and yellow are those categorized as changing. Proteins shown in green are members of the Arp2/3 complex (that are unchanged). Taken from [169].

1.16 Hypothesis and aims:

The finding in section 1.15 points to a selective role of ARPC5L in BCR signaling among other Arp2/3 complex subunits. ARPC5L and its paralogue ARPC5 are unstudied proteins in BCR signaling, therefore, I decided to dedicate the work of this thesis to characterise the functional role of these paralogues in BCR signaling that furthermore suggest a distinct link between BCR signaling and the actin cytoskeleton. Moreover, since one of the major issues in MCL and CLL is the residency of malignant cells within the lymph nodes seeking for survival signalling and the enrichment of ARPC5L as a member of cytoskeleton proteins after BCR stimulation, it would be rational to understand the biology of these paralogues in MCL/CLL and target the cytoskeleton to effectively suppress malignant cells retention within the survival area specially such BCR inhibitors including idelalisib is reported with complicated site effects.

ARPC5 paralogue could reciprocally interact with BCR signaling and may have functional importance for B cell biology. Following the proteomic finding (Fig1.7), I aimed in this study to

characterise ARPC5 isoforms after BCR stimulation, speculating that BCR signaling governs actin dynamics through manipulating ARPC5 paralogue.

ARPC5 paralogue could influence BCR signaling, thus determining the functional role of ARPC5 isoforms in BCR signaling is crucial to provide a novel insight into malignant CLL and MCL cells activation.

Chapter 2: Material and Methods

2.1 Tissue culture

2.1.1 Cell lines:

The details of cell lines used in this thesis including origin, growth pattern, and doubling time are listed in Table 2.1. Both the suspension cell line (MAVER-1) and adherent cell line (HeLa) were purchased from the American-type culture collection (ATCC). Cell lines were cultured in a vented culture flask in a sterile tissue culture cabinet at 37° and 5% CO_2. MAVER-1 cells were grown in Roswell Park Memorial Institute Medium (RPMI-1640) (Sigma life science, UK) which was supplemented with L-glutamine (2mM). Hela cells were maintained in Dulbecco's Modified Eagle Medium (DMEM) with GlutaMAX™, Pyruvate, and glucose. All growth mediums were premixed with 100IU/ml penicillin and 100 µg/ml streptomycin (Sigma Aldrich, USA), and 10% fetal bovine serum (FBS) (Life Technology, USA).

Cell Line	Cell type	Patient age/sex	Doubling time (h)	Karyotype
MAVER-1	Mantle Cell Lymphoma	77/Male	24h	t(11;14)
HeLa	Adenocarcinoma	31/Female	24h	t(1q;3q)

Table 2-1: **Features of cells lines used in this study.**

2.1.2 Maintenance of cell lines

MAVER-1 cells were passaged every three days to maintain optimal growth reaching 16 passages before discarding. They were split by re-suspending the cells 1:3 in a fresh RPMI-1640 medium. Hela cells passaged 1:5 every 3-5 days reaching about 24 passages and then discarded. These cells were split by aspirating the growth medium and washing twice with sterile PBS. 2ml of Trypsin-EDTA solution (Sigma Aldrich, UK) was added to the cells and returned to the incubator with 5%CO_2 and 37^{o} until cells are detached. Fresh DMEM medium was added to the cells suspension and mixed gently. An appropriate volume of cells suspension is transferred into a new flask with adding a fresh volume of DMEM to reach the desired dilution for optimal growth.

2.1.3 Cell viability and live-cell count

Assessment of cell viability and count were done by using a plastic SD100 cell counting chamber (Nexcelom Biosciences, UK) with using trypan blue dye (Sigma Aldrich, UK) which is only able to stain dead cells and not live cells. Cells were diluted to 1:1 with trypan blue and 20µl of the mix loaded into the chamber. Both cells viability (%) and count were measured through Nexcelom apparatus (Nexcelom Biosciences, UK) and Cellometer Auto T4 software.

2.1.4 Mycoplasma test

As a quality control, every six weeks our lab required testing for Mycoplasma infection which could affect cells' growth and/or their biological function. The test run used an eMycoTM Mycoplasma PCR Detection Kit (ver. 2.0) (Life Diagnostics, iNtRON Biotechnology, Korea) following the manufacturer's protocol guidelines.

2.1.5 Buffers

Phosphate-buffered saline (PBS-): 137mM NaCl, 2.7mM KCl, 10mM Na_2HPO_4, 1.8 mM KH_2PO_4.

Phosphate-buffered saline (PBS+): Dulbecco's Phosphate Buffered Saline, with MgCl2 and CaCl2, liquid sterile-filtered, suitable for cell culture (Sigma-Aldrich D8662).

5X Reducing Sample Buffer 15% Sodium dodecyl sulfate: 312.5mM Tris-HCL PH 6.8, 50% Glycerol, 15% SDS, 16% β -Mercaptoethanol.

50x Tris-Acetate –EDTA (TAE) Buffer: To Make 1 L - 242 g Tris-Base, 57.1 mL Acetic Acid, 100 mL 0.5 MEDTA.

RIPA Lysis Buffer: 150mM NaCl, 1.0% (v/v) NP-40, 0.5% (w/v) Sodiumdeoxycholate, 0.1% Sodium dodecyl sulfate, 50 mM Tris pH 8.0.

1x Turbo-Transfer buffer: 200ml 5xTurbo-Transferring buffer, 200 ml 100% pure Ethanol, 600ml distal water.

10X Gel running Tris-Glycine-SDS (TGS) Buffer: To make 1L, 10xTG buffer (BioRad, UK, 161771), 10g SDS.

Tween- Tris Buffer Saline(T-BST): 20mM Tris, 150mM NaCl, 0.1% Tween.

1x FACS buffer in PBS: 1%BSA, 4mM EDTA, 0.15mM NaN3

Lysis buffer (CoIP): 10mM Tris/HCL PH7.5, 150mMNaCl, 0.5mMEDTA, 0.5%NP-40.

Dilution/ Wash buffer: 10mM Tris/HCL PH7.5, 150mMNaCl, 0.5mMEDTA.

Glycine-elution buffer: 200mMglycine PH:2.5.

2.2 BCR stimulus

One of the ways to study the biology of B cells is to stimulate these cells through their IgM/BCR activation. BCR can be activated in vitro through crosslinking the Fc domain within IgM receptor by commercially available Anti-human IgM antibody which induce signalling pathway required for B cell activation. This experiment was generally performed to measure the phosphorylation level of significant kinases as well as the protein, transcription, and distribution level of ARPC5 and ARPC5L after BCR stimulation.

$2x10^6$ MAVER-1 cells were re-suspended in 200µl of RPMI and plated in 48 well plates. The cells were stimulated with 20µg/ml of unlabeled Goat F(ab)2 Anti-human IgM antibody (Southern Biotech, UK) and incubated at 37° for indicated timepoints. The cells were collected after the ending of each time

point and added to pre-cooled 1.5ml Eppendorf tubes with ice-cold PBS and lysates were prepared.

2.3 Cycloheximide (CHX) treatment

Cycloheximide can be used to block protein translation and hence determine protein level stability. This is useful for knockdown studies. The aim was to determine the protein stability of ARPC5/L. $5x10^6$ MAVER-1 cells were re-suspended in 500µl of RPMI and plated in 24 well plates. 100µg/ml of CHX was added to the cells and the cells were incubated for different timepoint at 37°. The cells were collected after each time point and added to pre-cold 1.5ml Eppendorf and lysates were prepared.

2.4 Knockdown studies by small interfering RNA (siRNA)

Protein knockdown can be achieved by using siRNA. The siRNA is a short single oligo complementary to specific messenger RNA (mRNA) used to destroy this mRNA and prevent protein translation (gene silencing). In this experiment, the aim is to knockdown ARPC5 and ARPC5L protein level for functional studies using siRNA. MAVER-1 cells were transfected through two rounds of transfection to achieve the maximum possibility of transfection efficacy. These cells were transfected by nucleofection. $8x10^6$ cells/condition were washed twice with sterile pre-warm PBS at 37º. For each transfection, the cells were resuspended in 100 µl of nucleofection solution V at 20º (Lonza Group, Switzerland) which was premixed with 60nM of the siRNA as a final concentration (Table 2.2). Cells were transferred into a sterile cuvette and program X-01 was used for nucleofection using the

Amaxa nucleofector (Lonza Biologics plc, UK). Immediately following the nucleofection, the cells were transferred to 2ml of pre-warmed fresh RPMI 1640 medium within 6 well plates and maintained for 24h under optimum culture conditions. After 24h 2ml of pre-warmed fresh RPMI 1640 medium was added to the cells to enhance their growth. The next day, the procedure of transfection was repeated on previously transfected cells with 8_X10^6 cells/ condition and cells were cultured in the same optimal conditions. After 24h of transfection, cells were ready for performing a further experiment, and thus the total time from starting the first hit of the knockdown until the cells be ready for the experiment is 96 hours.

Target Protein	Target sequence	Oligonucleotide feature
NT	UGGUUUACAUGUCGACUAA	ON-TARGETplus Nontargeting siRNA #1 D-001810-01-20
ARPC5	GCAGGCAGCAUUGUCUUGA	ON-TARGET plus SMART pool siRNA J012080-05
ARPC5	GUGUGGAUCUCCUAAUGAA	ON-TARGETplus SMARTpool siRNA J012080-06
ARPC5	GAAUAUGACGAGAACAAGU	ON-TARGETplus SMARTpool siRNA J012080-07
ARPC5	GCAGUUCAAUCUCUGGACA	ON-TARGETplus SMARTpool siRNA J012080-08
ARPC5L	UCGACGAAUUUGACGAGAA	ON-TARGETplus SMARTpool siRNA J014690-17
ARPC5L	CUUAGCAGUAGGAGGACUA	ON-TARGETplus SMARTpool siRNA J014690-18
ARPC5L	GCGUUGACUUGUUAAUGAA	ON-TARGETplus SMARTpool siRNA J014690-19
ARPC5L	GAUCCAAGGGCUGUGGUAA	ON-TARGETplus SMARTpool siRNA J014690-20

Table 2-2: **siRNA sequences for control siRNA and ARPC5 isoforms**. All siRNAs including a non-targeting control (NT) were purchased from Dharmacon (GE Healthcare UK Limited, Buckinghamshire). siRNAs against ARPC5 and ARPC5L were purchased as pools of 4 individual siRNAs (smartPOOL®).

2.5 Western blotting (WB)

2.5.1 Preparation of cells lysate

MAVER-1 cells were washed once with cold and sterile PBS and centrifuged at 1500rpm for 5 minutes at 4° to remove the medium. The cells were lysed with 100µl of Radio immunoprecipitation (RIPA) buffer supplemented with 1x HALT Phosphatase and protease inhibitors (Thermo Scientific, UK). The cells were lysed directly in the 1.5 Eppendorf tubes. The lysate was incubated on ice for 10 minutes and centrifuged at 14000rpm for 10minutes at 4°. The supernatant was transferred into a fresh pre-cold Eppendorf tube and stored at -20° for further use.

2.5.2 Protein concentration quantification

The concentration of proteins was calculated by using Bio-Rad laboratories DC protein assay kit (Bio-Rad Laboratories Ltd, Hertfordshire, UK). In brief, following the manufacturer's instructions, 5µl of Bovine Serum Albumin BSA as the standards and the sample were added separately to 96well plate followed by adding 25µl of premixed 20µl of reagent S with 980µl of reagent A, and 200 µl of reagent B. After incubation in dark for 15 minutes, absorbance readings were taken at 490nm. Proteins concentrations were quantified by comparison with the standards curve prepared with BSA standards. Measurements of concentrations were considered reliable if there were a linear doubling of absorbance with doubling of protein standard concentrations.

2.5.3 Gel electrophoresis

Samples were run in 4-15% gradient Mini Protein TGX Precast Gel (BioRad, UK) and 50µg of protein lysate was loaded. Proteins were premixed with 1x sample buffer and boiled for 5min at 95-100 C°.

2.5.4. Protein transfer

The gel was then transferred onto Amersham™ Protran® nitrocellulose membrane with a pore size of 0.45 µM (Sigma Aldrich, UK) using a Trans-blot turbo transfer system (BioRad, UK). Proteins were transferred for 10min at 1.3 Amp using the recommended transfer buffer.

2.5.5 Protein detection:

Membrane was then incubated in 5% of milk (Marvel, UK) mixed with T-BST to block unspecific binding for 45 minutes on a rocker. Membranes were placed in 50 ml falcon tubes with 2 ml of primary antibody solution and rolled overnight at 4°C (Table 2.3). The membrane was washed in T-BST for 5 min three times. A secondary antibody was added according to the species and detection system and incubated for one hour. The membrane was washed 3 times (5min each) with T-BST on a rocker. Visualising of bands was performed by scanning the blot through Odyssey infrared scanner (LICOR-Bioscience, USA) or ChemiDoc™ Touch Imaging System (BioRad, UK).

Primary Antibody	Host species	Dilution	Buffer	Supplier	Catalog number
ARPC1A	Rabbit	1:250	5%Milk in TBST	Sigma	HPA004334
ARPC2/p34-Arc	Rabbit	1:2000	5%Milk in TBST	Millipore	07-227
ARPC3/p21-Arc	Mouse	1:1000	5%Milk in TBST	BD-Transduction lab	612234
ARPC4	Rabbit	1:1000	5%Milk in TBST	Sigma	SAB1100901
ARPC5/ p16-ARC	Mouse	1:1000	5%Milk in TBST	Synaptic Systems	305011
ARPC5L	Rabbit	1:1000	5%Milk in TBST	Abcam	169763
Arp2	Rabbit	1:2000	5%Milk in TBST	Abcam	129018
Arp3	Mouse	1:1000	5%Milk in TBST	Sigma	A5979
p-Syk (Tyr525-526)	Rabbit	1:1000	5%BSA in TBST	Cell Signalling	2711
t-Syk	Mouse	1:1000	5%BSA in TBST	Cell Signalling	80460
p-Lyn (Tyr507)	Rabbit	1:1000	5%BSA in TBST	Cell Signalling	2731
t-Lyn	Mouse	1:1000	5%BSA in TBST	Santa Cruz	7274

p-Plcγ2 (Tyr1217)	Rabbit	1:1000	5%BSA in TBST	Cell Signalling	3871
t- Plcγ2	Rabbit	1:1000	5%BSA in TBST	Cell Signalling	3872
p-AKT (Ser473)	Rabbit	1:1000	5%BSA in TBST	Cell Signalling	9271
t-AKT	Mouse	1:1000	5%BSA in TBST	Cell Signalling	2920
p-BTK (Tyr223)	Rabbit	1:1000	5%BSA in TBST	Cell Signalling	D9T6H
t-BTK	Mouse	1:1000	5%BSA in TBST	Cell Signalling	D6T2C
p-Erk (1/2) (Tyr204)	Mouse	1:2000	5%BSA in TBST	Santa Cruz	7383
p44/42 MAPK (Erk1/2)	Rabbit	1:3000	5%BSA in TBST	Cell Signalling	9102
GAPDH	Rabbit	1:20000	5%Milk in TBST	Proteintech	10494-1-AP
c-Myc	Rabbit	1:1000	5%Milk in TBST	Cell Signalling	18583
β-Actin	Mouse	1:20000	5%Milk in TBST	Sima Aldrich	A1978

Table 2-3: Immunoblotting primary antibodies. p-Phosph, t-Total.

2.5.6 Immunoblotting secondary antibodies

Depending on the primary antibody species and desired detection system, membrane blots were incubated with IRDye® 680RD or 800CW (LICOR-Bioscience, USA) or HRP secondary antibody (Invitrogen, UK) for 1hour diluted 1:10.000 or 1:1000 respectively. The secondary antibody was diluted in the same buffer as the one used in the primary antibody.

2.6 Surface marker quantification

2.6.1 Surface marker quantification using CyTof

The aim of this experiment is to test the effect of ARPC5/L on surface receptor expression in MAVER-1 cells. Following adjusting MAVER-1 cell count to a 5 x 10^6 cells/ml, they were washed with 300µl PBS followed by room temperature (RT) centrifuging at 550xg for five minutes and the supernatant were discarded. The cells were resuspended in 300uL of room temperature PBS-Cisplatin solution (1:1000 in PBS) to stain the dead cells and centrifuged at (550g/3mins/RT) and washed with 500uL ice-cold Cell Staining Buffer (Maxpar® CSB) to remove extra staining of Cisplatin and by centrifugation removing as much supernatant from the sample to avoid unnecessary dilution of the antibody's concentration in later addition. The cells then resuspend with 45 µl of CSB and 5 µ FcX Fc blocker was added to them to block antibody from falsely binding to Fc receptor and incubated on ice for 10 minutes. The cells then mixed with 5µg/ml of CD45 antibody tagged with metal and incubated for 30 minutes on ice. The cells then washed twice with CSB by centrifugation at 550xg/4° for three minutes and

supernatant was discarded. The cells were resuspended with 300µl of cold CSB and pooled with the other cells (with different condition) in one tube. The cells then spined down at (550g/3minutes/4°) and the supernatant was removed as much as possible for the next staining step. The tube was mixed with 5µg/ml of antibodies cocktail made in CSB (23µl antibodies cocktail and 77µl CSB for each condition) and incubated on ice for 30 minutes. The cells were washed twice with cold CSB and once with PBS and fixed with 300µl of cold Paraformaldehyde (PFA) 5X Fix I buffer for each condition. The cells then were washed once with PBS and resuspended with Intercolator-Ir solution mixed with Fix and Perm buffer to detect singlet cell by DNA staining and incubated for one hour at RT. Cells were then run through mass cytometry and analysed using Cytobank ™ software.

	Metal	CD markers
1	149Sm	CCR4 (CD194)
2	141Pr	CCR6 (CD196)
3	167Er	CCR7 (CD197)
4	163Dy	CXCR3 (CD183)
5	175Lu	CXCR4 (CD184)
6	153Eu	CXCR5 (CD185)
7	154Sm	CD62L
8	174Yb	CD49d
9	172Yb	IgM
10	146Nd	IgD
11	142Nd	CD19
12	143Nd	CD5
13	144Nd	CD38
14	171Yb	CD20
15	173Yb	HLA-DR
16	150Nd	CD43
17	151Eu	CD69
18	155Gd	CD45RA
19	152Sm	CD21
20	159Tb	CD22
21	164Dy	CD23
22	166Er	CD24
23	158Gd	CD27

Table 2-4: **Mass Cytometry antibodies**. Each antibody was tagged with metal to upon detection. The antibody with tagged metals were purchased from (FLUIDIGM, UK).

2.6.2 IgM surface marker quantification using Flow Cytometry

2.6.2.1 Conjugation of anti-human IgM antibody with Alexa Fluor dye

Unlabelled Goat F(ab)2 Anti-human IgM antibody (Southern Biotech, UK) was labeled with Alexa-488 fluor using Alexa Fluor™ 488 Antibody Labeling Kit (Thermo Fisher Scientific, A20181, UK) to visualise the antibody bound to IgM receptor in FACS machine. Briefly, Sodium Bicarbonate was resuspended in 1ml of deionized water to reach the solution concentration of 1M. 1:10 (100 µl) dilution of the solution volume was added to the Anti-human IgM antibody and 100 µl of this antibody mix was added to the vial of Alexa Fluor® dye. The mix was inverted and incubated for 1 hour in dark at room temperature (RT). 1.5 ml of the resin bed was prepared after assembling the purification column and centrifuged at 1100xg for 3 minutes at RT. The mix of the antibody with dye was added to the column and centrifuged at 1100xg for 5 minutes at RT to collect the labeled antibody. The concentration of the labeled antibody was measured using the Nanodrop system.

2.6.2.2 Surface IgM quantification

MAVER-1 cells concentration was adjusted to 3_x10^6 cells/ml in all the conditions. 100µl of cell suspension was stimulated in 48 well plates with 5µg/ml of labeled anti-human IgM pre-mixed with 100µM of Primaquine to block receptor recycling. At the end of each time point cells were added to 1.5 eppendorf tubes which already have 100 µl of ice-cold FACS buffer, and the volume was separated into two 1.5 eppendorf tubes (Unquenched and

Quenched) which were prepared for each time-point on ice. For time point 0, 200 µl of cells suspension were added to unquenched tube on ice and stimulated with 5µg/ml of labeled anti-human IgM pre-mixed with 100µM of Primaquine and mixed gently. 100 µl of ice cells suspension were transferred to the time-point 0 quenched tube. As a negative control, unstimulated cells were prepared for each condition.

Cells then were subjected to centrifugation at 1500rpm for 5 minutes and the supernatant was taken off. Cells resuspended with 100µl cold FACS buffer containing 2.5µl of Alexa 488 antibody (Thermo Fisher Scientific, Cat: A11094, UK) and added to only quenched tubes and incubated in the dark for 30min on ice. Incubation of quenched tubes with Alexa 488 antibody prevents any surface IgM from getting measured during sample reading and hence the measurement in quenched tubes will be only for internalised IgM receptors. Unbound antibodies were removed by adding 200 µl of cold FACS buffer and centrifugation at 1500rpm for 5 minutes. After the supernatant was taken off, cells were resuspended in 500 µl of cold FACS buffer prior FACS analysis using Attune™ flow cytometer (Life Technologies Ltd, Paisley UK).

2.7 Analysis of stimulated IgM induced intracellular calcium flux

To test the BCR efficacy, intracellular calcium level can be measured. During BCR signling, calcium is released from endoplasmic reticulum to catalyse the signaling pathway reaction. In this experiment, the effect of ARPC5/L on Calcium release was measured using the fluorophore dye,

Fluo4-AM (Life Technologies Ltd,Paisley, UK) as a calcium indicator. MAVER-1 cells at 6_x10^6 cells/ml were incubated with 2 µM Fluo4 -AM for 20 minutes at 37°C. These cells were washed and resuspended in 1ml of warm RPMI medium-1640 and incubated for another 20 minutes at 37°C. The cells were placed in a heat block with shaking at 1100 rpm for 5 minutes at 37°C before the first one-minute acquisition which determined the basal fluorescence of non-stimulated cells, followed by the addition of 20 µg/ml goat F(ab′)2 anti-human IgM and data acquisition recorded for 10 minutes. Data were acquired on a BD FACSCalibur and analyzed using Flowjo software.

2.8 Adhesion assay

The performance of this experiment was to measure the adherence ability of MAVER-1 cells to their legends under silencing of ARPC5/L level. 96 well plates (Greiner bio-one) were coated overnight at 4° with a mix of 100µl of (PBS+) with 10µg/ml Fibronectin, 1µg/ml VCAM-1, 5 µg/ml anti- IgM, combination of 10µg/ml Fibronectin with 5 µg/ml anti- IgM, combination of 1µg/ml VCAM-1 with 5 µg/ml anti- IgM, and 100µl of PBS- mixed with 1%BSA (as a negative control). The next day, the plates were washed twice with PBS-. 4_x10^6 cells/2ml of MAVER-1 cells were resuspended with RPMI-1640 medium containing 1% BSA and 10 µg/ml Calcein-AM (C1430, Thermo Scientific, UK) to stain living cells and incubated in dark at 37°C for one hour. The cells then subjected to centrifugation for 5 minutes at 1500rpm to remove unbound Calcein-AM and resuspended with 1ml the

same medium. After saving 600µl of cells suspension for calibration and the positive control in the incubator, 100µl of cell suspension was added to the 96 well plates in technical duplicate and incubated for 30 minutes at 37°C. After finishing the 30 minutes timepoint, 100µl of PBS- was added to the wells and the plate subjected to the upside-down centrifugation at 100rpm for 2minutes to remove non adherent cells. This step was repeated one more time. 100µl of positive control (cells in uncoated well) were added to the well. For the calibration, the cells added to the well and topped up with PBS- to reach the final volume of 100 µl in a specific amount in each well shown in table 2.5. The microplates were read at absorbance 495/515nm using an Omega microplates reader instrument. The number of adherent cells in each condition was quantified by a comparison with the standard curve prepared with a calibration (Table 2.5).

Cell suspension	PBS-	Number of cells
50 µl	50 µl	100000
40 µl	60 µl	80000
30 µl	70 µl	60000
20 µl	80 µl	40000
10 µl	90 µl	20000
5 µl	95 µl	10000
2 µl	98 µl	4000
1 µl	99 µl	2000

Table 2-5: Number of cells added in calibration for adhesive cells quantification.

2.9 Molecular biology

To determine the effect of BCR signaling on ARPC5/L transcription, q-PCR technique was used to quantify mRNA level of these proteins.

2.9.1 Primer design for q-PCR

Using NCBI (primer design blast) website, Primers for ARPC5\L were designed with the specific condition including amplicon size from (100-300bp), a continent of (50%-55%) GC, and optimum melting temperature is between (60°-63°). The specificity of these primers was confirmed using the same website. The primers were purchased from Integrated DNA Technology (IDT) (Table2.6). The primers for GAPDH and Egr1 were used as reference gene and positive control respectively.

Name	Description	Sequence
ARPC5	forward primer	GTCGGGATTGGGATGTCGAA
ARPC5	Reverse primer	GTCATGTTTCCTTGCCGCAG
ARPC5L	forward primer	AACCTTGGCGGACAACTGAA
ARPC5L	Reverse primer	GCTGGAGAGGCACATCTTGA
GAPDH	forward primer	CCTCTGACTTCAACAGCGACA
GAPDH	Reverse primer	TGGTCCAGGGGTCTTACTCC
Egr1	forward primer	ACAGCAACCTTTTCTCCCAG
Egr1	Reverse primer	CCAATAGACCTTCCACTCCAG

Table 2-6: Primer sequences of q-PCR. Purchased from Invitrogen.

2.9.2 Total RNA extraction

Cells were harvested from the experiment in section 2.2.3 in 1.5 Eppendorf tubes. Total RNA was isolated from these cells using an RNAeasy mini kit (Qiagen, UK). Following the manufacturer's instructions, in brief, the cell pellet was lysed with 350µl of RNA lysis buffer, the whole solution was transferred to the Zymo Spin III-C column and centrifuged at 12000g for 1min. The flow-through was mixed with 350µl of 70%Ethanol and transferred to Zymo Spain II-C column followed by centrifugation for 30seconds at 12000g. At this stage, RNA was attached to the column and then washed with 700µl of RW1 wash buffer followed by two washes with 500µl of RPE washing buffer. RNA was transferred to a 1.5 nuclease-free Eppendorf tube and eluted with 30µl of elution buffer and centrifuged at 12000g for one minute. The isolated RNA was then immediately stored at -80C° for further assessment.

2.9.3 Measuring RNA purity and quantity

Nanodrop 2000 spectrophotometer machine was used to assess RNA purity and quantity (Thermo scientific, UK). Isolated RNA is considered pure if the absorbance ratio 260/280nm is ~2. A value less than 1.7 indicates high protein contamination. Additional absorbance was taken at 230/260 and a considered ratio fill within 2. A lower value than expected indicated contamination which might be absorbed in 230nm.

2.9.4 Synthesis of complementary DNA (cDNA) from RNA

To synthesize cDNA from Isolated RNA, 1µg of RNA was mixed with 1µl of oligo T and heated at 70° for 5 minutes. This mix was then mixed with 1µl of nucleotides Dntp (mix of nucleotides), 1µl Reverse Transcriptase (RTase), 0.5µl RNAse, 4 µLof 5X RT buffer, and top up with Nuclease free H_2O to reach the final volume of 20µl. The sample was incubated for one hour at 42° followed by incubation at 95° for five minutes. Synthesized cDNA was then stored at -20 until further use.

2.9.5 Quantitative Polymerase Chain Reaction (q-PCR)

A master mix was prepared from 4µl of evagreen dye (Biorad), 1µl of respective primers, and 13µl of nuclease-free H_2O. 2µl of c-DNA was added to the 96 well PCR plate with 18 µl of master mix. The sample in 96 well PCR plate was run using q-PCR instrument AriaMx (Agilent, UK). The machine took in the beginning 1 cycle include warming the sample at 95°for 10 minutes followed by 40 cycles including 3 steps as shown in table 2.7.

Step	Seconds	Temperature
Denaturing	10	95°
Annealing	15	60°
Extension	20	72°

Table 2-7 Steps followed in q-PCR for amplicon replication.

2.9.6 Agarose Gel Electrophoresis

Agarose gel electrophoresis was used to separate DNA fragments. The procedure was an electrical field where DNA fragments are separated based on their size because usually, a high percentage is used for small fragment size, and a low percentage is used for large fragment size. In this experiment, the use of agarose gel was to confirm the specificity of the primers used in this technique by measuring the amplicon band which expected to have a size between 100-300 bp as designed in section 2.9.1. 2% of agarose gel was used by weighing 2g of agarose and mixing it with 100 ml of 1X TAE buffer. The agarose was melted by heating it in a microwave and leaving it to cool down but not to solidify. At this moment 5µl of sybr safe (Invitrogen) was added to the agarose gel to stain the DNA, and the gel was poured into the tray slowly and allowed to solidify for 1 hour. The gel was then transferred to an electrophoresis tank and filled with 1X of TAE. Carefully, samples (the remnant samples taken from q-PCR plate after running in the q-PCR machine) were mixed with1x of loading dye and 10µl of this mix loaded into the gel. 5 µl of the 100Bp ladder was added as well. Samples were then run at 100 volt for 35 minutes and the gel was visualised using blue light.

2.10 Lentiviral constructs for ARPC5/L overexpression tagged with a fluorescent protein.

The constructs were designed using a plasmid designing tool (Vector builder) to study ARPC5/L distribution following BCR stimulation. The plasmid maps are provided in the appendix (Fig A4).

2.10.1. Plasmid DNA Maxi prep

The bacteria containing the construct for ARPC5/L overexpression were injected into 300 mL of LB Broth containing the appropriate antibiotic. In a bacterial shaker incubator, the bacteria were allowed to grow overnight at 37°C. Bacteria were pelleted using centrifugation (10 minutes, 3000xg) and then processed or kept at -20°C. Plasmid DNA was extracted from bacterial pellets according to the manufacturer's instructions using a PureLink®HiPure Plasmid Maxiprept kit (Invitrogen, K210007).

2.11 Live Hela cell transfection

2.11.1 Hela cell transfection using CRISPR methodology

For ARPC5/L localisation, three vectors were designed and kindly granted by Takashi Yamamoto group [172] to endogenously tag ARPC5 and ARPC5L proteins. The vectors sequences and the gene locus targeted by the Cas9 are provided in the appendix (FigA1, A2, and A3). Live Hela cells were cultured in 6 well plate until reaching healthy 40% confluency level. The cells were transfected with 2µg of three vectors at the same time, the PITCh donor vector carries the mNeonGreen or mKATE tag sequence, the

all-in-one CRISPR vector contains the guide RNA (sgRNA) to direct the Cas9 protein to bind and cleave a particular DNA sequence and the CtIP vector was used as a strong enhancer for the other vectors (Fig 3.1). After incubating the cells in an optimal culture environment for 2 days, the expression and incorporation of tagged protein into the Arp2/3 complex was validated using tagged fusion protein immunoprecipitation assay (section 2.12).

2.11.2 Transient transfection and cell compartment labelling in Hela cells expressing ARPC5 mNEON green

Cell compartments were labeled in Hela cells (knock-in) expressing ARPC5 mNEON green, either through transient transfection or direct labeling. For transient transfection, Hela cells were plated in a confocal imaging dish and transfected with appropriate plasmid. The next day the cells were subjected for imaging. For direct labeling ER, Mitochondria, cell Membrane, and Actin, the cells were labeled according to the manufacturing instructions and imaged. Table 2.8 shows the details for each marker used for each compartment. Airyscan LSM-900 microscopy was used for the imaging.

Marker	Organelle	Detection	Type	Manufacturing
EEA1	Early endosome	561nm	plasmid	Supplied in the Lab
Rab7	Late endosome	561nm	plasmid	Supplied in the Lab
Membrane	Membrane	590nm	Direct labeling	Lipilight Idylle
SiR-Actin	Actin	640nm	Direct labeling	Cyotoskeleton, Inc
Endoplasmic reticulum (ER)	ER	580nm	Direct labeling	Abcam,139482
Mitochondria	Mitochonderia	633nm	Direct labelling	EMD Millipore, SCT137

Table 2-8 Markers used for live imaging.

2.12 Immunoprecipitation of mNeonGreen-Fusion Proteins using mNeonGreen-Trap_A

We followed the protocol that was supplied with the mNeonGreen-Trap beads_A (Chromotek, UK), briefly 1_x10^7 of Hela cells were washed with cold sterile PBS- and subjected for centrifugation at 1500rpm for five minutes. The pellet was resuspended in 200µl ice-cold lysis buffer and incubated for 30 minutes with extensively pipetting every 10 minutes. The cell lysate was centrifuged at 20.000xg for 10 min at +4°C, 30µl was saved for the input condition and the remaining volume was transferred to precooled tube. 300µl of dilution buffer was added to the lysate. The mNeonGreen-Trap beads were vortexed and 25µl of beads were added into 500µl ice-cold

dilution buffer. The mix was subjected to centrifugation at 2.500xg for 2 min at 4°C. The diluted lysate was added to equilibrated mNeonGreen-Trap beads_A beads and incubated for one hour at 4° with gentle mixing.

The mix was then centrifuged at 2.500x g for 2 minutes at 4°C and the precipitated beads were washed with resuspending in 500 µl ice-cold dilution buffer and subjection to centrifugation at 2.500x g for 2 min at 4°C. The precipitated beads were resuspended with 50µl 2xSDS-sample buffer and boiled for 10min at 95°C. The beads then were collected by centrifugation at 2.500xg for 2 min at 4°C and the gel was run with the supernatant.

2.13 Microscopy

2.13.1 TIRF microscopy

Marinas spinning disc imaging system (3i) with an attached motorised TIRF module was used to do total internal reflection fluorescence (TIRF) imaging. The TIRF objective was a Plan-Apochromat 100x/1.46 oil (Zeiss). A Hamamatsu ORCA Flash 4.0CMOS camera with 2x binning was used to capture the images.

2.13.2 Airyscan laser scanning microscopy (LSM)

A Zeiss LSM 800 or LSM 900 imaging system with a 63x oil or 10x objective was used to image the samples. The number of acquisition tracks, laser wavelengths (405nm, 488nm, 561 nm, 640 nm), and emission detection window were all determined automatically using Zen software (Ziess) by

selecting the desired fluorophores from the pre-loaded library and selecting the smartest setup.

2.14 Live cell protein distribution measurement using TIRF microscopy

For protein distribution measurement, MAVER-1 cells overexpressing ARPC5-GFP or ARPC5L-GFP were plated on an imaging dish pre-coated with 20µg/ml of anti-IgM overnight at 4°C. Following 3 minutes of stimulation, the cells imaged until 20 minutes of stimulation using TIRF microscopy. The protein distribution was analysed using ImageJ software.

2.15 Cell spreading assay

Four compartment imaging dishes (Cellvis, D35C4-20-0-N) were coated with 10µg/ml F(ab′)2 anti-human IgM (Southern biotech, UK) overnight at 4°C. $2x10^5$ of MAVER-1 cells were incubated with 1µM SirActin for 45 minutes at 37°C. Cells were then allowed to spread by incubating them on imaging dishes for 30 minutes at 37°C. Cells were imaged using an Airyscan LSM800 microscope and analysed at 30 minutes of cell spreading using ImageJ software.

2.16 Migration assay

2.16.1 Pillar forests device preparation and cell loading

The pillar forests are Polydimethylsiloxane (PDMS)-based setups in which arrays of micrometre-sized pillars connect two closely neighbouring

surfaces. This technique mimic 3D cell environment. The advantages of 2D cell migration tests are combined with the precise determination of 3D environmental parameters in this new technique. The device used for cell migration was prepared following the published protocol involving Fabrication of Pillar forests, cutting and dicing the PDMS device. [173]. Accurate preparation of the PDMS device is required since changing the pillar shape, size, height, and inter-pillar distance can manipulate microenvironmental parameters. Luckily, this device was kindly prepared and granted by Dr. Anne Reversat who actively contributed to discovering it. Figure 2.1 shows a diagram of the pillar forest device pore size 5µm I used in this study.

RPMI-1640 medium was added to the device and incubated for one hour at 37°C. Cells were stimulated either with 10µg/ml of anti-IgM or anti-IgG, loaded into the entry hole in the device, and incubated for four minutes. Images were taken every minute for 30 minutes using an Airyscan LSM-900 microscope. Single-cell movement was tracked using ImageJ software.

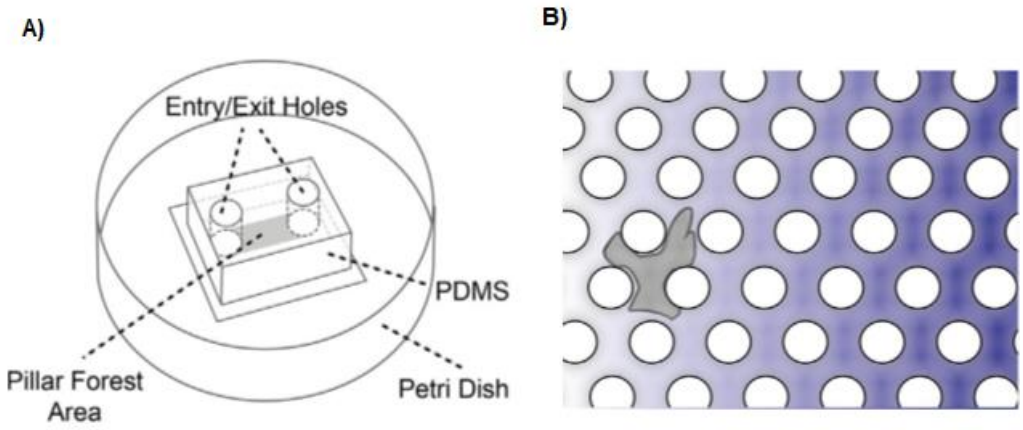

Figure 2-1: Pillar forests to study cell migration. A) Overview of a pillar forest device (with two entry/exit holes) attached to a Petri dish. B) Top view onto the pillar forest area, showing the cell migrating through location the manually punched holes in the pillar array. The diagram was adapted with permission from [173] (figure1).

2.17 Statical analysis

In this study the error bar within each graph is represented by standard error of mean (SEM) to measure the variability in the sample means as a result of experimental biological repeats. The SEM was obtained using GraphPad Prism software. The statistical analysis was generated using GraphPad Prism software based on the number of comparisons within the experimental study (student's t-Test, One-way ANVOA). The result value is considered statistically significant if the P value is 0.05 or less.

Chapter 3: ARPC5 isoform characterisation and identifying their distribution during BCR signaling

3.1 Introduction:

The Arp2/3 complex nucleates new actin filaments from the sides of pre-existing ones and thus produces a branched actin network. In B cells, F-actin in synapses generates a highly dynamic pattern composed of actin foci formed by the Arp2/3 complex [49] . ARPC5 and ARPC5L as complex isoforms that can be integrated into the complex resulting in two different subcomplexes [49]. The role of the Arp2/3 complex within a cell is considerably dependant on which ARPC5 paralogue is included in the complex [97].

A phospho-proteomic study shown in section 1.16 in figure 1.5 indicates a link between induction of phosphorylation signaling cascades in B cells and cytoskeletal reorganization. In that expriment, the strong enrichment of phospho-tyrosine associated ARPC5L but not ARPC5 indicates to selective use of one paralogue rather than the other after BCR signaling activation [169]. This points to a functional distinction between these two paralogues in B cell biology. However, it is still undefined how BCR signaling control actin dynamic through influencing the isoforms. Understanding the relationship between BCR signaling and cytoskeleton organisation might provide an explanation for CLL and MCL cells behaviour in motility and retention through Arp2/3 isoform manipulation. Thus, it is important to investigate these isoforms by determining their localisation, identifying their expression level after BCR stimulation, and observing whether these

phenotypes are different between the isoforms to explore their different contribution to B cell function.

3.2 Aim of this chapter

To characterise the ARPC5 isoform expression level and distribution after BCR stimulation in MAVER-1 cells. Charctrisation of the isoform addresses the question whether BCR signalling controlling the isoforms via manipulating their expression. This investigation could be a foundation to determine the functionality of the isoform with MAVER-1 cells.

3.3 Result

3.3.1: Establish mNeonGreen ARPC5 knock-in Hela cells using the LoADed PITCh system.

In this investigation, I decided to tag endogenous ARPC5 and ARPC5L with fluorescent proteins to determine the cellular localization of the isoforms. Determining the cellular localization of the isoforms provides information about protein characterization and ultimately their function. The tagging process was achieved using the selective genome editing way (gene knock-in) [172]. The technique is based on using local accumulation of DNA double-strand break (DSB) repair molecules called (LoAD system). The repairing way for the DNA break was through microhomology-mediated end-joining (MMEJ) repair. Three vectors were used for transfection at the same time, the PITCh donor mNeonGreen vector carries the tag sequence, the all-in-one CRISPR vector contains the guide RNA (sgRNA) to direct the Cas9 protein to bind and cleave a particular DNA sequence and the CtIP vector was used as a strong enhancer for (MMEJ) (Fig 3.1). these vectors were kindly prepared and granted by Takashi Yamamoto group [172]. To transfect these vectors, Hela cells and MAVER-1 cells were selected to be host cells. Hela cells were chosen to confirm the functionality of the constructs as they are convenient to use by being an adherent epithelial cell line that is easy to transfect with one or multiple vectors. Unfortunately, MAVER-1 cells did not survive after sorting the transfected cells which limits the localisation study of ARPC5 only in Hela cells.

After the three vectors were transfected into HeLa cells and the recovery of cells in an optimal culture environment (2 days), the expression and incorporation of tagged protein into the Arp2/3 complex was validated. In the beginning, the aim was to tag both ARPC5 and ARPC5L with fluorescent proteins but was only successful in ARPC5 tagging as the red signal was not detectable in the confocal microscopy and the immunoprecipitation experiment did not show any pulldown of mKate2 fused ARPC5L signal.

I pulled down mNeonGreen-proteins and their association from Hela knock-in cells lysates using mNeonGreen beads. Lysates from control Hela cells that did not express mNeonGreen-tagged ARPC5 were used as a negative control by subjecting them as well to the pulldown process. Both control and expressing Hela cells showed the presence of endogenous ARPC5 protein at a molecular weight of 16kDa. However, only expressing Hela cells showed mNeonGreen fused with ARPC5 signal at a molecular weight ~ 43kDa (Fig 3.2b). To further confirm the specificity, the blot was incubated with other Arp2/3 complex proteins antibodies (Arp2, Arp3, ARPC1A, and ARPC2). According to the study [97], all these protein members are bound to ARPC5 and subsequently subjected for co-immunoprecipitation which is what we can infer from (Fig3.2c). The cells were placed into glass bottom imaging dishes and imaged using spinning disk confocal microscope which showed live Hela cells expressing green fluorescent on ARPC5 protien (Figure 3.2a).

These observations indicate the specific successful tagging of ARPC5 with mNeonGreen and thus these HeLa cells could be used for localisation studies.

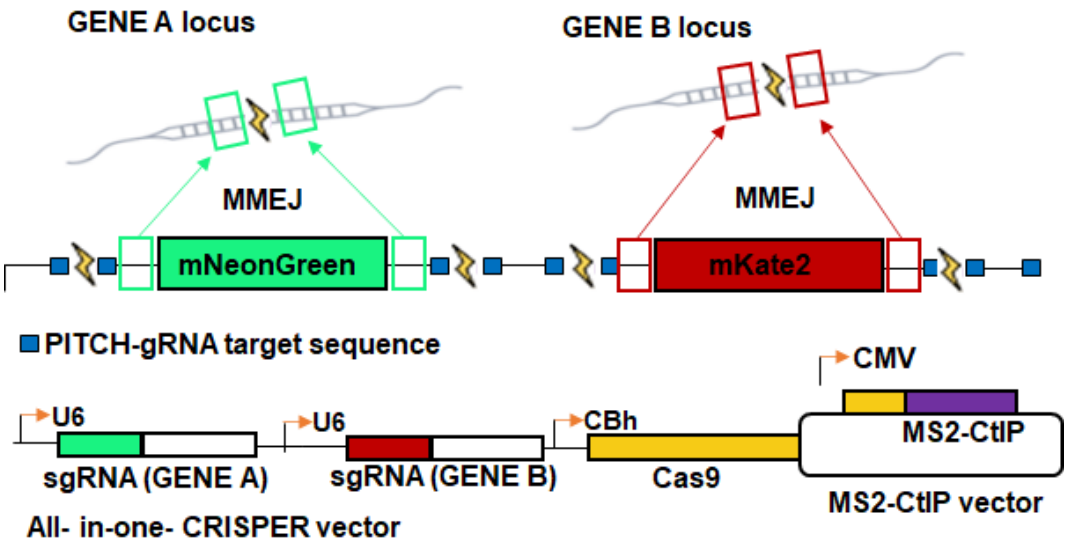

Figure 3-1: **Schematic of double gene knock-in with the enhanced PITCh system**. Two independent loci were targeted by a single-donor vector containing green and red fluorescent protein genes flanked by specific microhomologous arms for each gene locus. Douple gene knock-in was achieved by co-transfection of the integrated donor vector, all-in-one CRISPR vector, and MS2-CtIP vector. U6, Human U6 promoter, CBh, chicken beta-actin short promoter, CMV, cytomegalovirus promoter. Adapted from *[172]***.**

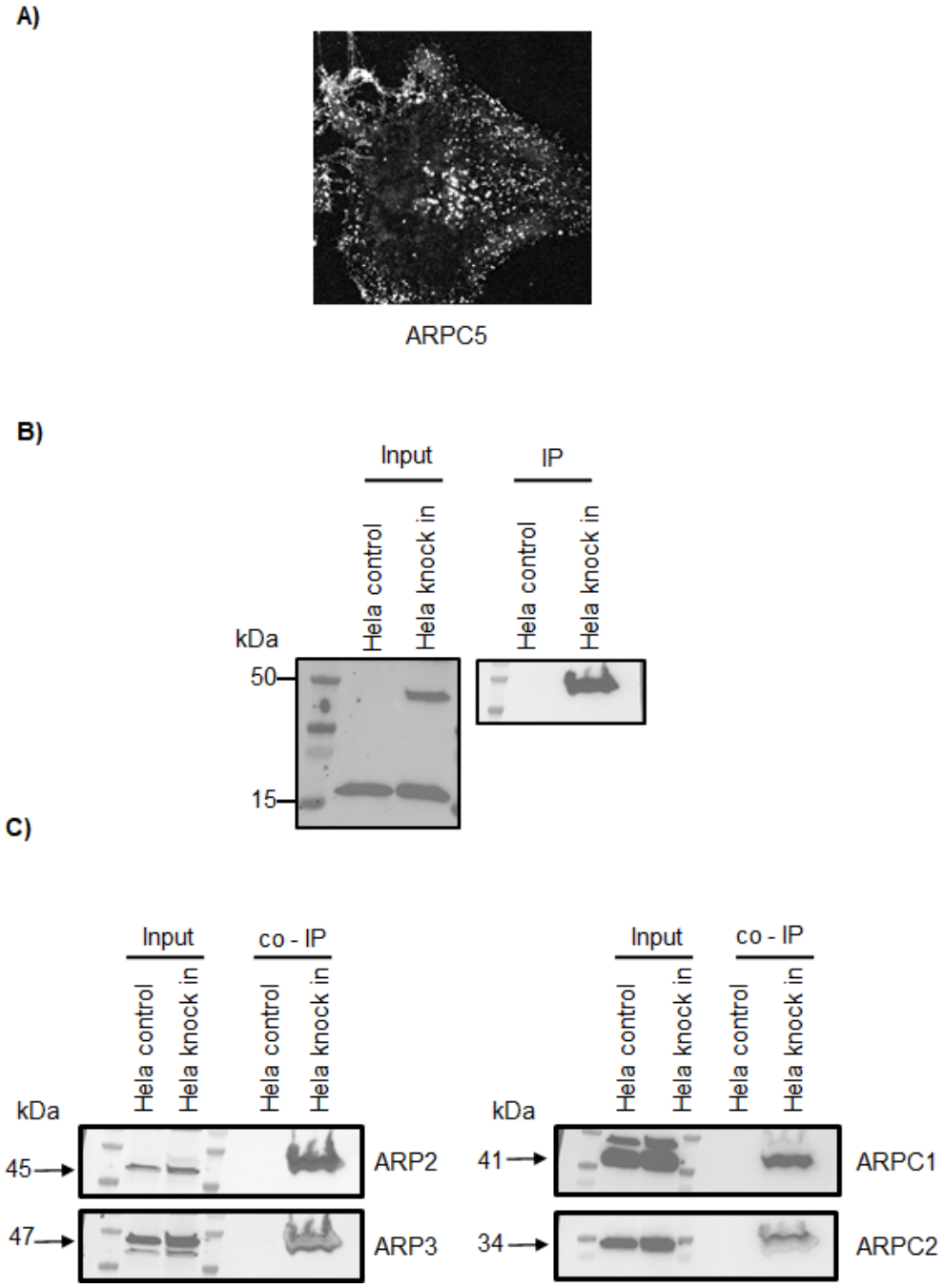

Figure 3-2: Generation mNeonGreen ARPC5 knock-in HeLa cells using the LoADed PITCh system. Hela cells were transfected with three vectors (PITCh donor mNeonGreen vector, CRISPR vector, and CtIP vector). A) Spinning disk confocal microscopy showing Hela cell expressing mNeonGreen-tagged ARPC5. B) mNeonGreen-Trap pulldowns from HeLa cells lysate expressing mNeonGreen-tagged ARPC5 using mNeonGreen beads. C) Co-IP of Arp2/3 complex proteins in Hela cells lysate. IP: immunoprecipitation.

3.3.2: Determine endogenous ARPC5 localisation with mNeon-Green-ARPC5.

Establishing Hela cells expressing mNeon-Green endogenous ARPC5 facilitates the determination of ARPC5 localisation to Hela cell compartments. I labeled the compartments either with plasmid transfection as in EEA1-RFP and Rab7-RFP as markers for early and late endosomes respectively or used fluorescent dye protein as in labeling the plasma membrane, actin, mitochondria, and endoplasmic reticulum. Figure 3.3 shows Hela cells expressing mNeonGreen endogenous ARPC5 knock-in Hela cells with organelle markers. This qualitative figure indicates strong localisation of ARPC5 to actin while there is partial localisation to the early endosome while it does not seem to indicate the presence of ARPC5 in the other compartments.

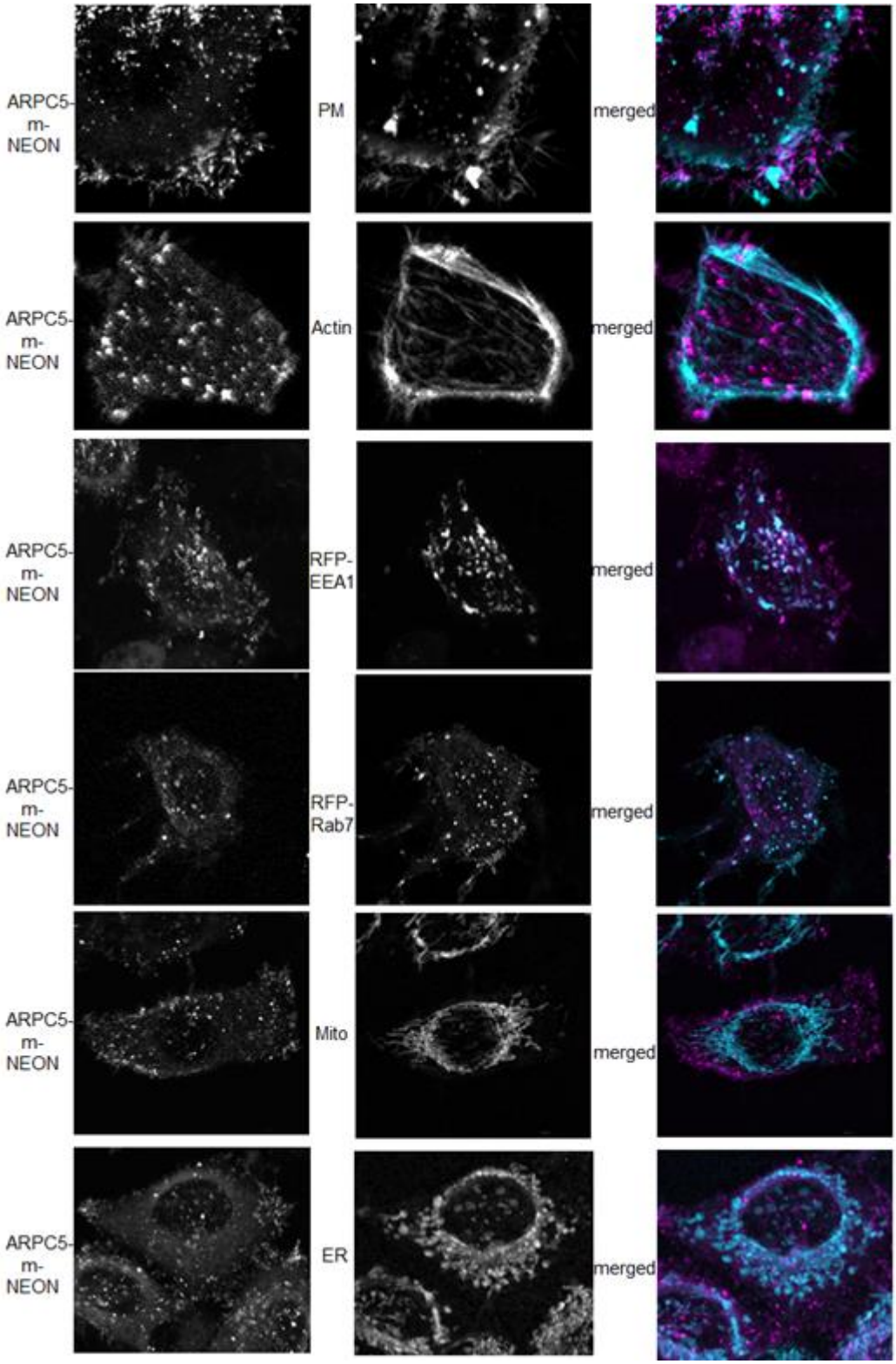
ARPC5-m-NEON
PM
merged
ARPC5-m-NEON
Actin
merged
ARPC5-m-NEON
RFP-EEA1
merged
ARPC5-m-NEON
RFP-Rab7
merged
ARPC5-m-NEON
Mito
merged
ARPC5-m-NEON
ER
merged

Figure 3-3: Determine ARPC5 localisation in mNeonGreen ARPC5 knock-in Hela cells. Using the indicated organelle marker to identify ARPC5 localization. Hela cells were put in confocal imaging dishes and allowed to spread, and organelles were labeled as indicated. Images were obtained on a Zeiss LSM 900 system. Images were background subtracted, adjusted for brightness and contrast using ImageJ software. Scale bar: 6µm. in merged images magenta color: ARPC5, cyan color: compartment marker. PM: Plasma membrane, Mito: Mitochondria, ER: Endoplasmic Reticulum.

3.3.3: Determine the concentration of Anti-Human IgM antibody used for BCR stimulation in MAVER-1 cells.

Antigenic stimulation of the BCR is a central part of CLL cell biology. In vivo, this stimulation is a major driver of the proliferation and survival of CLL cells. [25, 151]. Receptor stimulation of lymphocyte cells can induce strong or weak signals that determine the response outcome of that cell [174]. Therefore, in this investigation, before deciding to understand how BCR signaling influences the ARPC5 paralogues, it is important to accurately determine the right and appropriate quantity of antigen. In-vitro, crosslinking of the BCR with either immobilized or soluble bivalent anti-IgM F(ab')2 fragments, induces BCR signaling and ultimately B cell activation [175]. I decided to determine the appropriate concentration of anti-IgM F(ab')2 fragments in two-time points (5 and 60) minutes attempting to determine a strong BCR signaling and the maximum phosphorylation status of downstream kinases such as ERK and Akt after BCR stimulation, kinases which act as downstream effectors of BCR signaling and these kinases are traditionally used as markers for BCR activation [176, 177].

The fact that CLL cell lines are either unable to induce BCR signaling or continuously induce signaling even in the absence of BCR stimulation [178], makes them hard to use as a model to study BCR signaling. MCL cells lines are responsive to BCR stimulation and mimic in vivo kinases phosphorylation in CLL make them a good model in understanding BCR signaling and the effect of this signaling on isoform expression. Thus, I decided to use MAVER-1 cells (MCL cell lines) as a model to better understand the behaviour of the isoforms during signalling because these cells respond to BCR stimulation like in vivo CLL cells.

Cultured MAVER-1 cells were stimulated with different anti-IgM F(ab')2 fragments concentrations for 5 and 60 minutes. Lysates were prepared from collected cells and subjected to western blotting (Fig 3.4 A&B). At concentration 20µg/ml of anti-IgM F(ab')2 fragments at 5 and 60 minutes, the maximum phosphorylation level of ERK and AKT was observed which indicates that this concentration is sufficient to induce appropriate and strong BCR signaling.

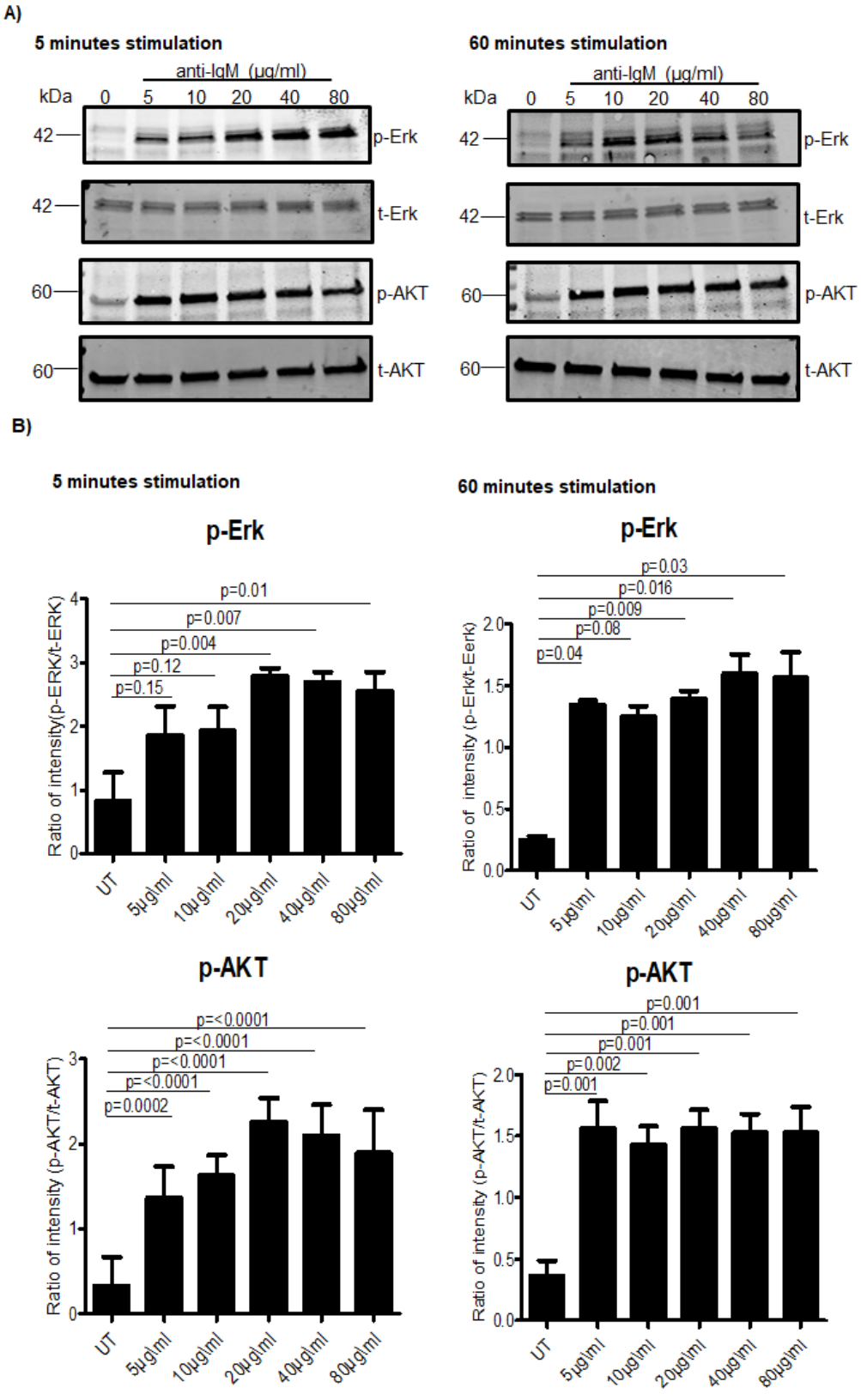
A)
5 minutes stimulation
anti-IgM (µg/ml)
kDa 0 5 10 20 40 80
42 p-Erk
42 t-Erk
60 p-AKT
60 t-AKT
60 minutes stimulation
anti-IgM (µg/ml)
kDa 0 5 10 20 40 80
42 p-Erk
42 t-Erk
60 p-AKT
60 t-AKT
B)
5 minutes stimulation
p-Erk
Ratio of intensity(p-ERK/t-ERK)
p=0.01
p=0.007
p=0.004
p=0.12
p=0.15
UT 5µg/ml 10µg/ml 20µg/ml 40µg/ml 80µg/ml
60 minutes stimulation
p-Erk
Ratio of intensity (p-Erk/t-Eerk)
p=0.03
p=0.016
p=0.009
p=0.08
p=0.04
UT 5µg/ml 10µg/ml 20µg/ml 40µg/ml 80µg/ml
p-AKT
Ratio of intensity (p-AKT/t-AKT)
p=<0.0001
p=<0.0001
p=<0.0001
p=<0.0001
p=0.0002
UT 5µg/ml 10µg/ml 20µg/ml 40µg/ml 80µg/ml
p-AKT
Ratio of intensity (p-AKT/t-AKT)
p=0.001
p=0.001
p=0.001
p=0.002
p=0.001
UT 5µg/ml 10µg/ml 20µg/ml 40µg/ml 80µg/ml

Figure 3-4: Determine the concentration of anti-IgM F(ab')2 fragments used for BCR stimulation in MAVER-1 cells. MAVER-1 cells were incubated at 37° with different anti-IgM antibody concentrations for two-time points as indicated. A) A western blot image showing phospho-kinases and total-kinase levels before and after BCR stimulation. B) Quantification analysis of the western blot images. All WB images were visualised and band intensity quantified using the LI-COR imaging system. All experiments n=3, statistics performed using PRISM (SEM). Statistical tests performed are one-way ANOVA's with Dunnetts multiple comparison post-test. SEM: standard error mean.

3.3.4 ARPC5 protein level is reduced after BCR stimulation while ARPC5L protein level is unchanged.

In this experiment, I aimed to determine the effect of BCR stimulation on the ARPC5/L expression level. Understanding the connection between BCR stimulation and ARPC5/L expression level manipulation explores one possible way that BCR signaling is controlling actin dynamics.

MAVER-1 cells were conjugated with 20µg/ml of anti-IgM F(ab')2 fragments for different time points (15,30, and 60 minutes). Since actin reorganisation after BCR stimulation is a fast process [179], it is important to determine the paralogues expression in such shorter time points. To detect if the level of the isoforms is changing when BCR is stimulated, they were compared with their level before BCR stimulation (0minutes). p-AKT measurement was used as a positive control for the experiment to show successful BCR signaling induction.

The experiment showed a slight trend toward reduction of ARPC5 level in 15 and 30 minutes while this level is significantly reduced in 60 minutes after BCR stimulation. The level of ARPC5L is unchanged in the same time points

of BCR stimulation (Fig 3.5 A&B). The phenotype was confirmed with only focusing on testing the level of the isoforms in 60 minutes after BCR stimulation (Fig 3.5 C&D).

This novel observation from the experiment suggests that BCR signaling influences the expression level of ARPC5 paralogues by selective reducing of one paralogue and maintaining the other one.

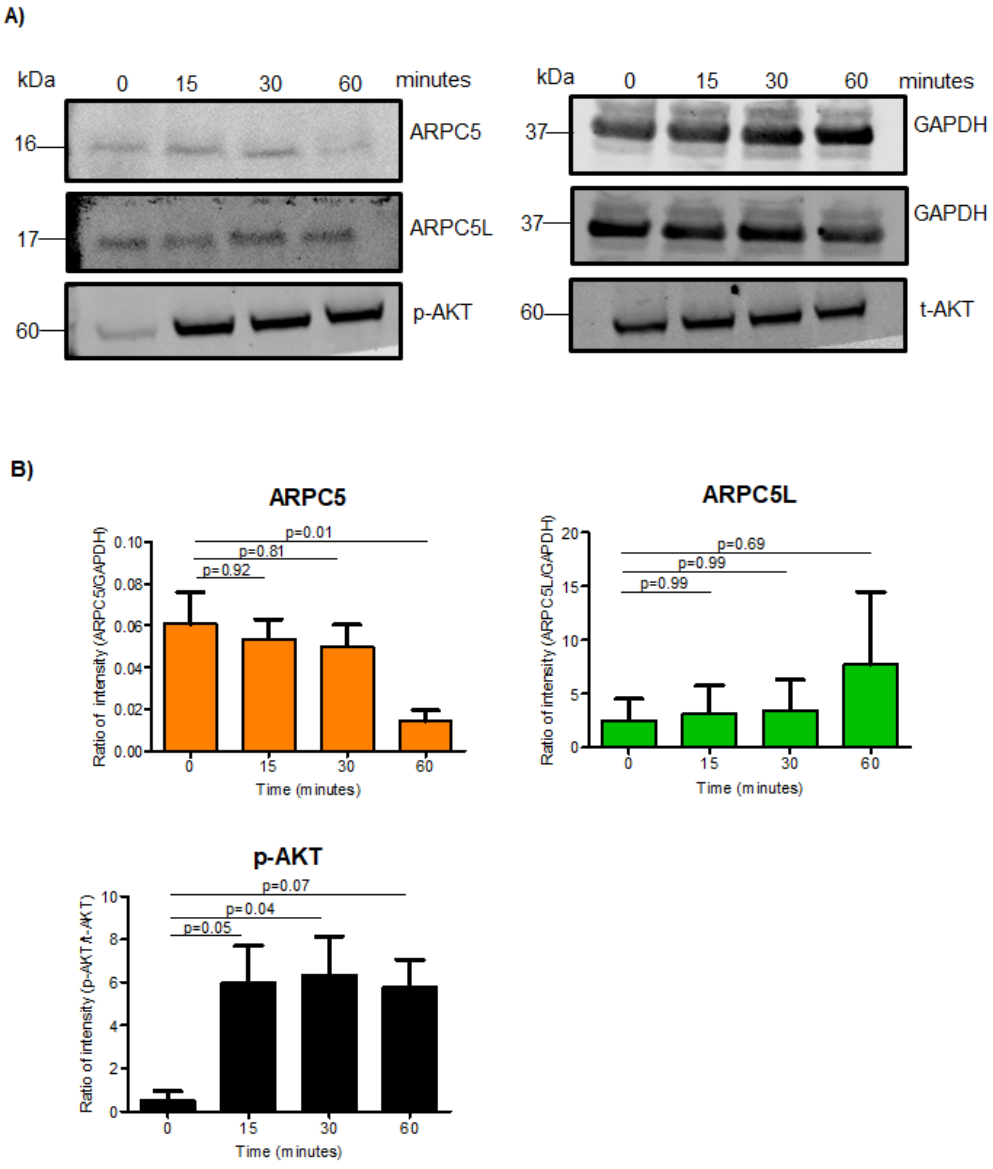

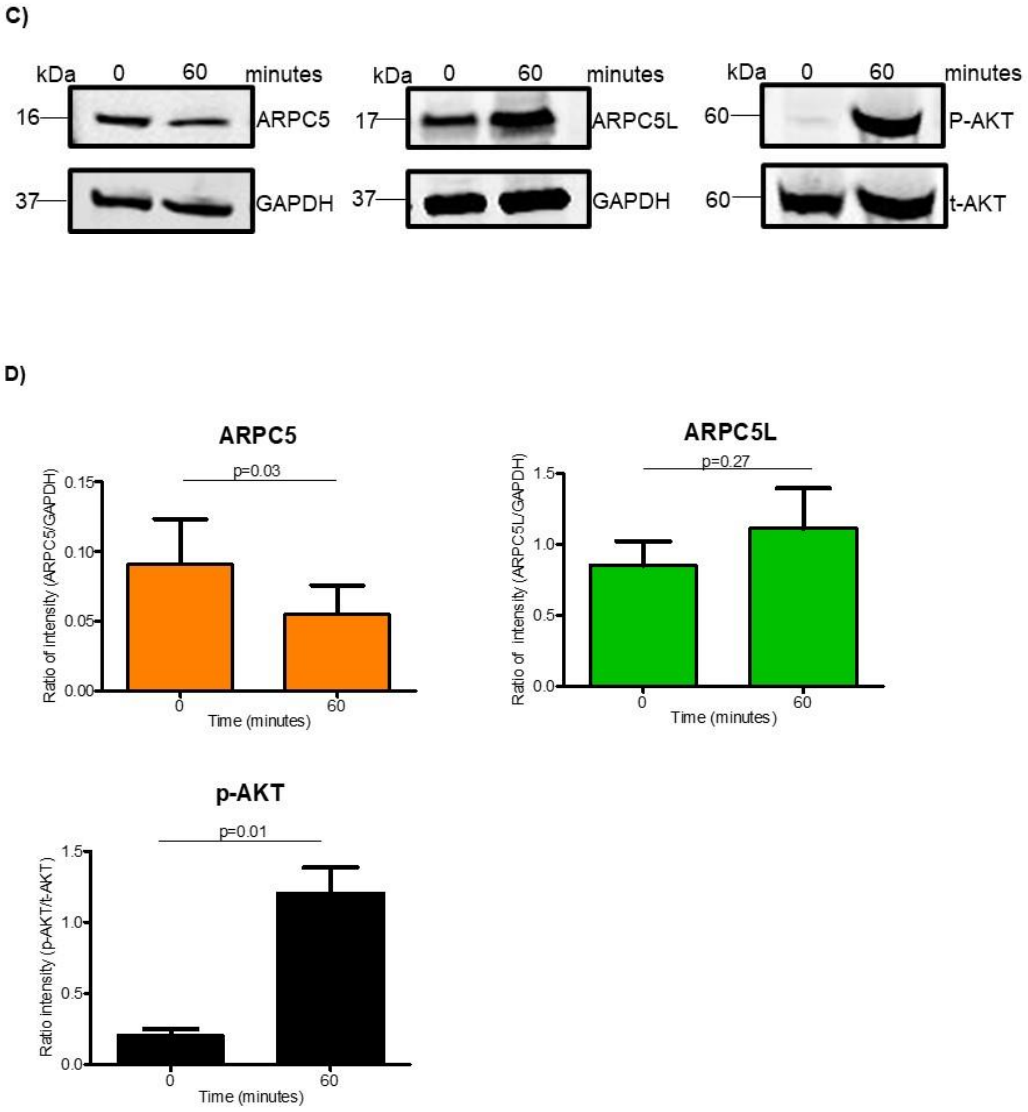

Figure 3-5: **ARPC5 protein level is reduced after BCR stimulation while ARPC5L protein level is unchanged**. MAVER-1 cells were incubated with 20µg/ml of anti-IgM antibody. The stimulation reaction was stopped by adding cold PBS and the lysates were prepared for WB. A) WB images show the level of ARPC5/L before and after different time points of BCR stimulation as indicated. B) Quantification analysis of western blotting. C) WB images show the level of ARPC5/L before and in 60 minutes after BCR stimulation. D) Quantification analysis of WB images. p-AKT was used as a positive control for BCR stimulation. GAPDH is used as a loading control for WB. All WB images were visualised and band intensity quantified using the LI-COR imaging system. All experiments n=3, statistics performed using PRISM (SEM). Statistical test performed is one-way ANOVA's with Dunnetts multiple comparison post-test in B and paired T-test in D. WB: Western blot. SEM: standard error mean.

3.3.5 ARPC5/L mRNA level is unaffected after 60 minutes of BCR stimulation.

The reduction of ARPC5 level after BCR stimulation raised the question of what the underlying reason could be. At the cellular level, the reduction of any protein level can be connected to reduced synthesis or a higher degradation rate. Therefore, I decided to investigate the ARPC5 isoforms production level by measuring the mRNA level of the isoforms before and after BCR stimulation.

MAVER-1cells were incubated with anti-IgM F(ab')2 fragments for 60 minutes. q-PCR was used to synthesise cDNA from isolated RNA. I used the NCBI (primer design blast) website to construct the primers with the appropriate conditions indicated in section 2. The primer specificity for Early growth response (Egr) was confirmed by Dr. Andrew Duckworth who used it in his study and kindly supplied it to me for use in the experiment. The mRNA level of Egr was used as a positive control for BCR signaling induction since its level is upregulated after 60 minutes of BCR stimulation [180].

After testing the specificity of the primers by visualising (Fig 3.6), the cDNA level for the isoforms was quantified by dividing the cDNA of each isoform by the cDNA level of GAPDH which was used as a reference gene in this experiment.

The mRNA level of ARPC5/L was unaffected after BCR stimulation (Fig3.7). This excludes the possibility that the reduction of ARPC5 protein level is due

to less protein synthesis. It was also attempted to test whether the ARPC5 protein reduction is due to degradation, but experimental variation made it hard to achieve a conclusion.

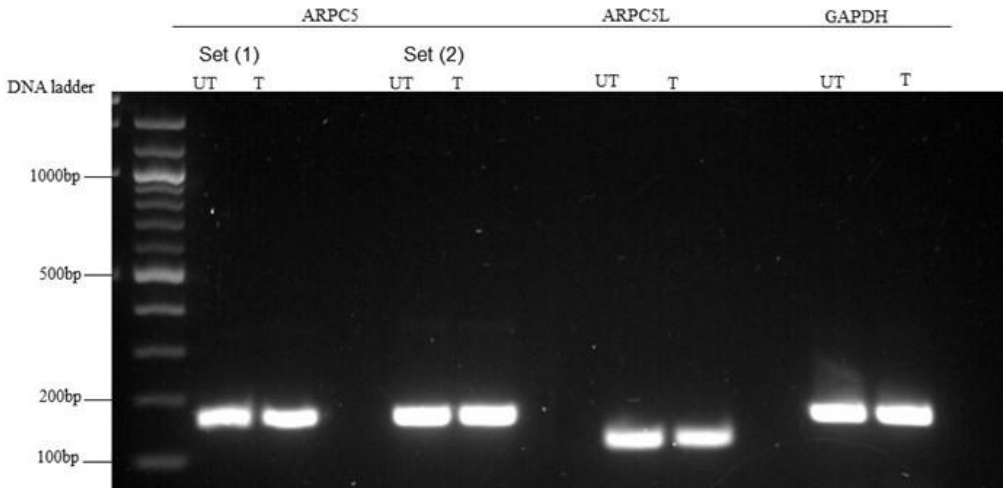

Figure 3-6: An image of an agarose gel showing the specificity of the primers used in qPCR. The gel was visualized using blue light. UT: untreated, T: treated.

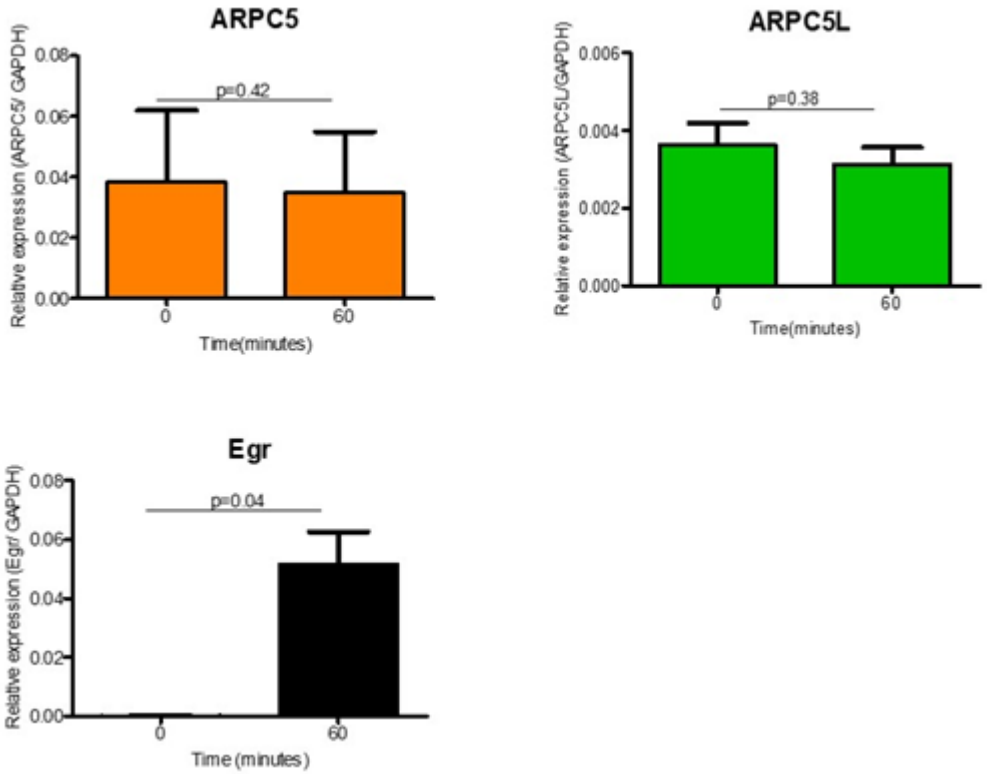

Figure 3-7: ARPC5/L mRNA level is unaffected after 60 minutes of BCR stimulation. MAVER-1 cells were incubated with 20µg/ml of anti-IgM antibody for 60minutes, and RNA was extracted from zero and 60 minutes. After cDNA was synthetised, it was amplified using qPCR. Egr mRNA expression level was used as a positive control for BCR signaling and GAPDH was used as a reference gene. Egr: Early growth response. The experiment was done in (n=3), the statistic was achieved using PRISM (SEM). The statistic test performed was paired T-test. SEM: standard error mean.

3.3.6 ARPC5 has a faster turnover than ARPC5L in MAVER-1 cells.

Part of the characterisation of proteins is to identify their stability. In this test, I decided to determine ARPC5/L turnover. Understanding the differences in protein stability may give indications as to their differential function in actin reorganisation.

In this experiment, I treated MAVER-1 cells with 100µg/ml of Cycloheximide, a protein translation blocker to test the turnover rate of ARPC5/L. in Western blot on the prepared lysates both isoforms seem to be stable in shorter time points (Figure 3.8 A&B). In longer time points, however, ARPC5 seemed to be degraded after 12 hours while ARPC5L was stable in the same time points (Figure 3.8 C&D). c-Myc was used as a positive control.

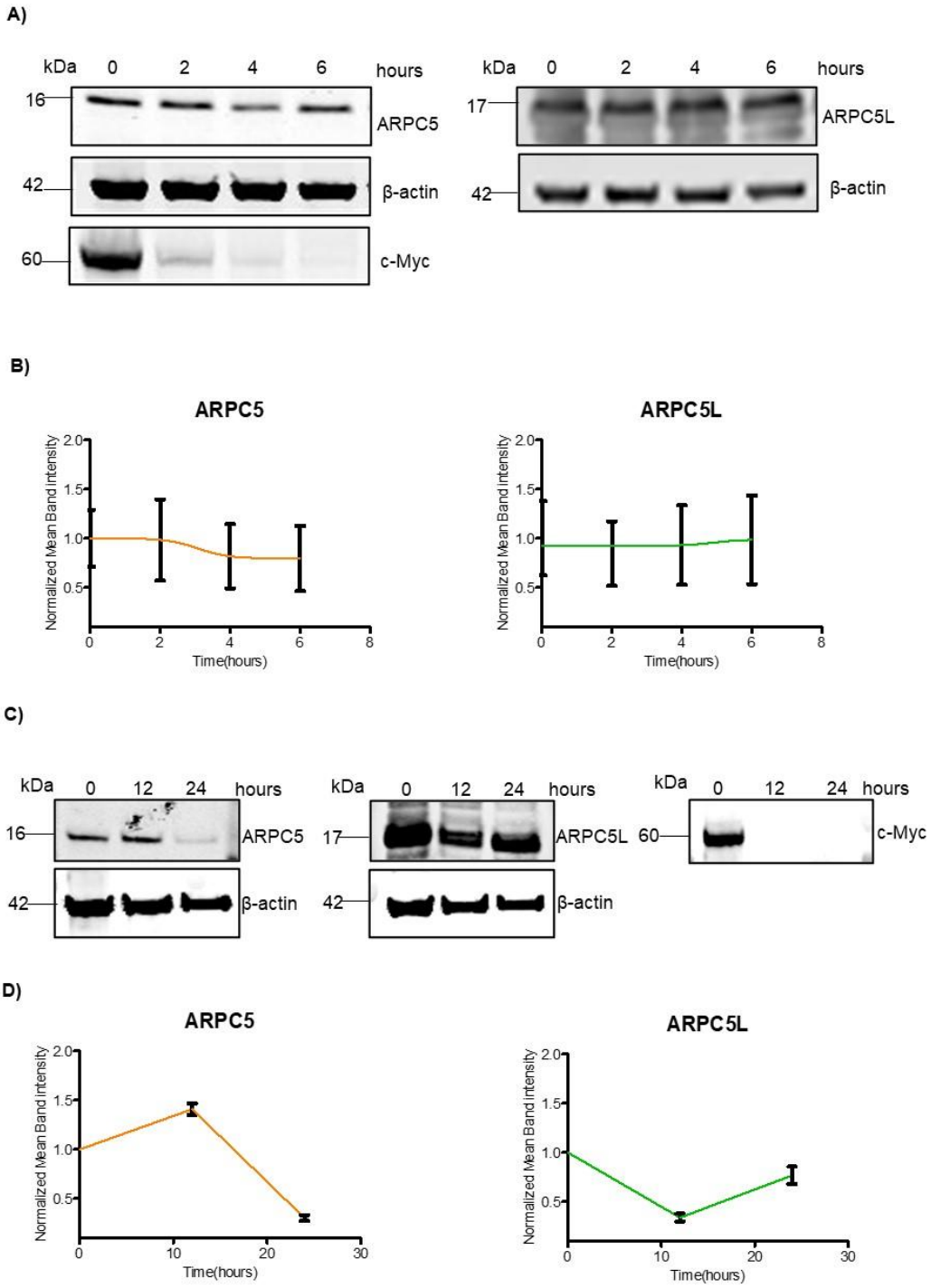

Figure 3-8: ARPC5 has a faster turnover than ARPC5L. MAVER-1 cells were treated with 100µg/ml of CHX and incubated at 37 for a different time. A) A western blot image showing ARPC5/L level before and after CHX treatment addition for shorter time points (2,4, and 6 hours). B) Quantification analysis of the western blot images in A. C)) A western blot images showing ARPC5/L level before and after CHX treatment addition for longer time points (12 and 24hours). D)Quantification analysis of the western blot images in C. c-Myc is used as a positive control for

proteins translation blocking. β-actin is used as a loading control. All WB images were visualised, and band intensity quantified using LI-COR imaging system. A was done experiments N=7, and C was done N=3. Error bar represents SEM using PRISM. SEM: standard error mean. CHX: Cycloheximide.

3.3.7 An increase of ARPC5 paralogue protein expression when the expression of the other is reduced.

To enable studies into the functional roles of ARPC5 isoforms, MAVER-1 cells were treated with small interference RNA (siRNA). Figure 3.9 showed that I was able to significantly reduce the expression of ARPC5 and ARPC5L with the use of pooled siRNA oligonucleotides (Fig 3.9 a). In addition, I noticed that when the expression of one of the paralogues is reduced upon transfection, an increase is observed in the protein expression of the other paralogue, thus potentially pointing at a possible compensation mechanism between the paralogues (Fig 3.9b).

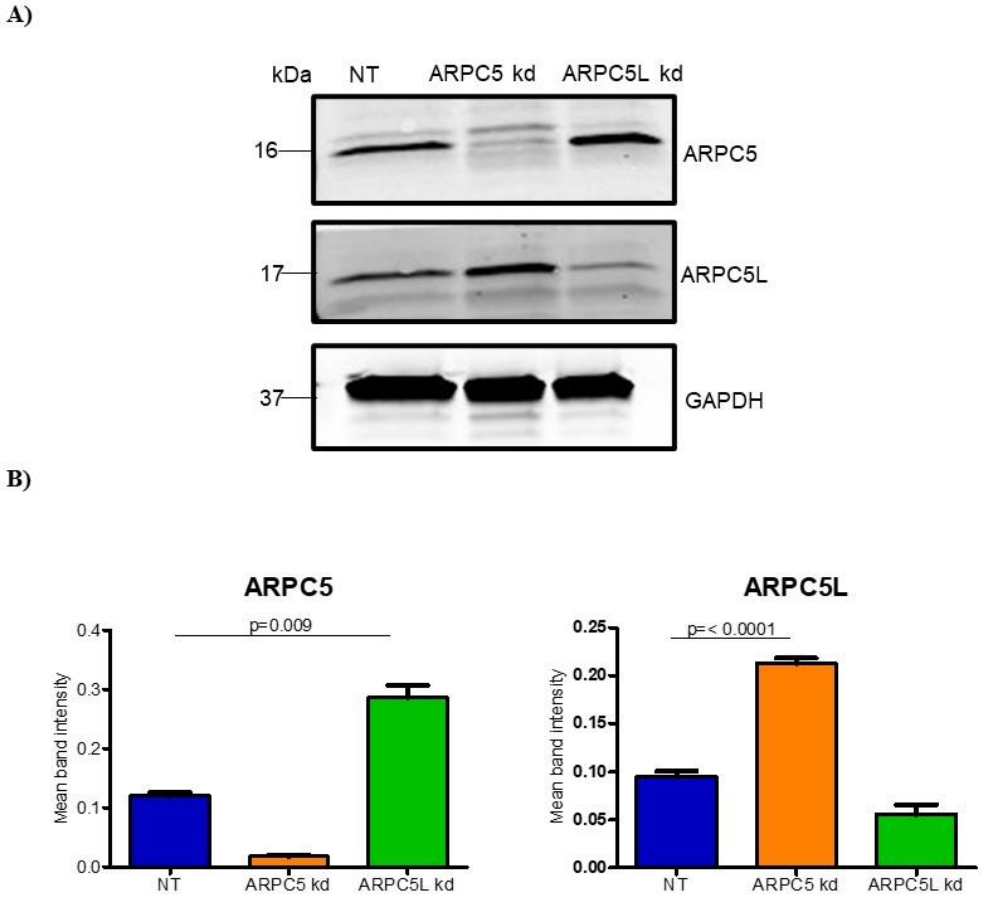

Figure 3-9: An increase of ARPC5 paralogue protein expression when the expression of the other is reduced. A. Western blot analysis of ARPC5/L proteins within lysates of MAVER-1 cells treated with the indicated siRNAs against NT, ARPC5, and ARPC5L. GAPDH is used as a loading control. B) Quantification of western blot analysis. Compendium of N=3 experiments using siRNA to ARPC5 and ARPC5L. Error bars represent the standard error of the mean. Statistical analysis was performed using paired T-test. NT: non-targeting control, kd: knockdown.

3.3.8 ARPC5/L isoforms show a distinct localisation after BCR stimulation in MAVER-1 cells overexpressing ARPC5/L.

In B cells, BCR stimulation induces sequential events including actin cytoskeleton reorganisation. In this test, I aimed to determine ARPC5/L distribution within the cell membrane at BCR activation site. Thus, to understand if ARPC5/L are redistributed upon BCR stimulation, MAVER-1 cells are stably overexpressing ARPC5 and ARPC5L-GFP.

MAVER-1 cells overexpressing ARPC5-GFP or ARPC5L-GFP were plated on an imaging dish pre-coated with 20µg/ml of anti-IgM and imaged using TIRF microscopy. Three minutes after BCR stimulation, both ARPC5 and ARPC5L were spread across the cell membrane with a distinct accumulation in the centre area. 20 minutes after BCR stimulation as the cell were fully spread, ARPC5 relocalised from the center toward the edge while ARPC5L is continued to be distributed within all of the spread area (Fig 3.11A &B). For the quantification, the centre area was defined as half of the total cell area from the point of the center (inner ring) while considering the other half the edge of the cell (outer ring) (Fig 3.10).

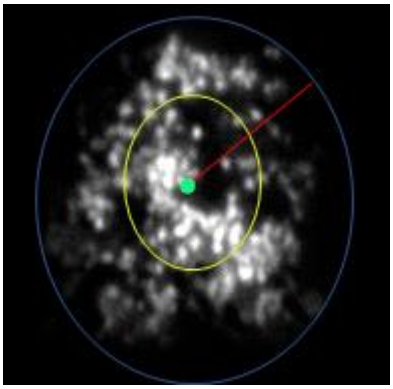

Figure 3-10: A diagram showing the different areas of the MAVER-1 cell selected for ARPC5 and ARPC5L distribution analysis. Manual determination of the cell area. center point of the cell, the distance between the center point and the edge of the cell, area of the center area (inner ring), and area of the edge area (outer ring).

Depleting the respective other isoform in each overexpressing cell (ARPC5L knockdown in ARPC5 overexpressing cells) did not change the phenotype observed in wildtype (Fig 3.11B).

By dividing the total fluorescent intensity in three minutes by 20 minutes, I noticed that there is no difference in isoform fluorescent intensity between the overexpressed paralogues (Fig 3.11C). To confirm BCR stimulation within analysed cells (positive control for BCR stimulation), the total area of the cell was measured in three and 20 minutes which showed an increase in cell area size indicating cell spreading after BCR stimulation (Fig 3.11D).

These experiments suggested that after BCR stimulation, the level of overexpressed ARPC5 and ARPC5L are not changing, but their distribution is significantly different within the cell membrane. Such a finding possibly

points to different the isoform's contributions in actin reorganisation as the BCR signaling is proceeding.

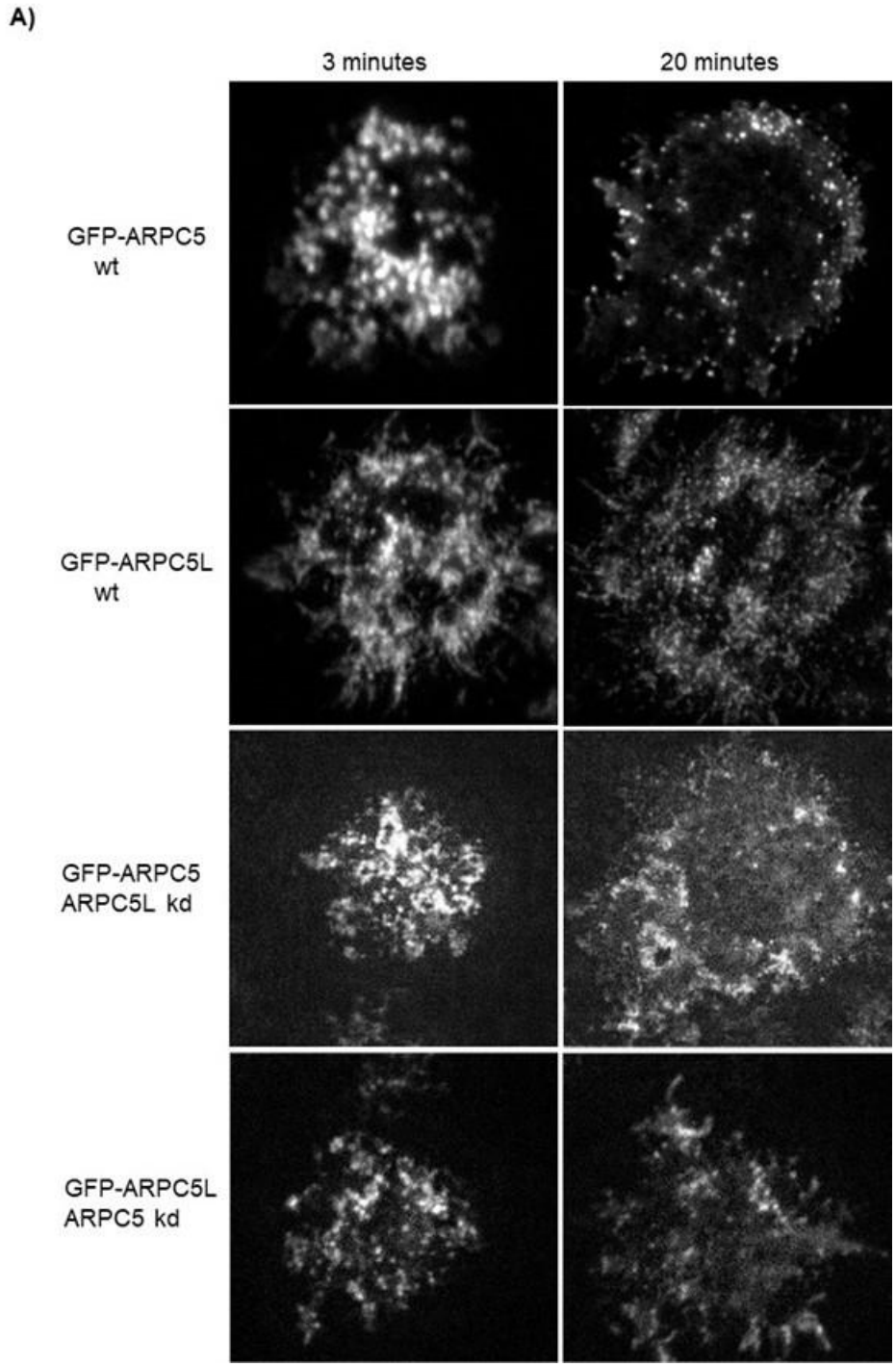

B)

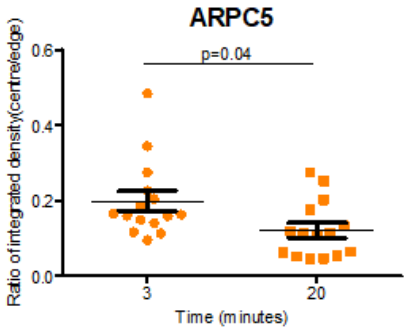
ARPC5
p=0.04
Ratio of integrated density(centre/edge)
0.6
0.4
0.2
0.0
3
20
Time (minutes)

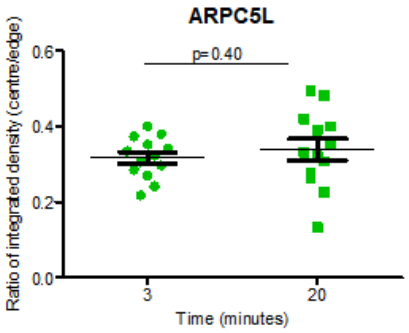
ARPC5L
p=0.40
Ratio of integrated density (centre/edge)
0.6
0.4
0.2
0.0
3
20
Time (minutes)

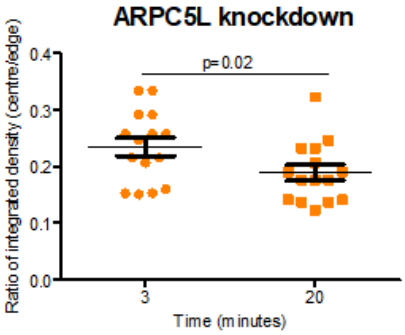
ARPC5L knockdown
p=0.02
Ratio of integrated density (centre/edge)
0.4
0.3
0.2
0.1
0.0
3
20
Time (minutes)

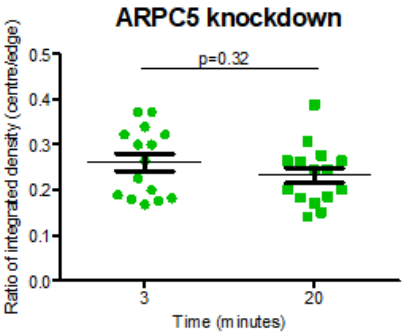
ARPC5 knockdown
p=0.32
Ratio of integrated density (centre/edge)
0.5
0.4
0.3
0.2
0.1
0.0
3
20
Time (minutes)

C)

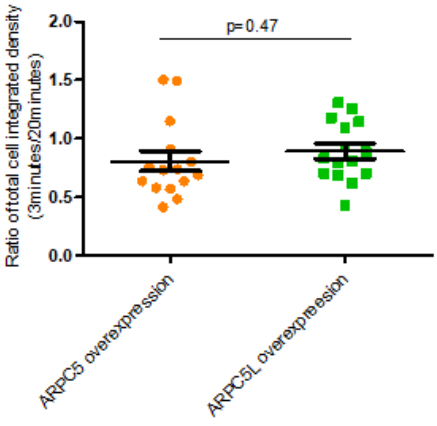
p=0.47
Ratio of total cell integrated density (3minutes/20minutes)
2.0
1.5
1.0
0.5
0.0
ARPC5 overexpression
ARPC5L overexpression

D)

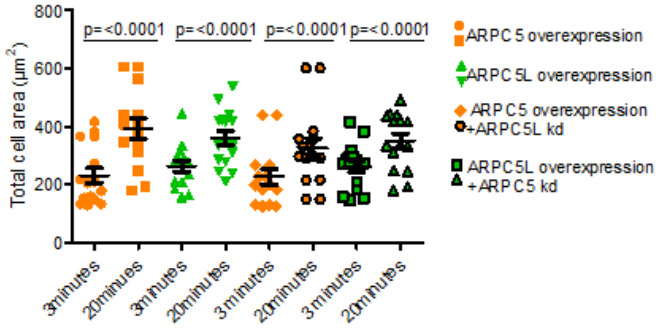
p=<0.0001
p=<0.0001
p=<0.0001
p=<0.0001
Total cell area (μm²)
800
600
400
200
0
3minutes
20minutes
3minutes
20minutes
3minutes
20minutes
3minutes
20minutes
ARPC 5 overexpression
ARPC 5L overexpression
ARPC5 overexpression +ARPC5L kd
ARPC5L overexpression +ARPC5 kd

Figure 3-11: ARPC5/L are distributed differently after BCR stimulation in MAVER-1 cells overexpressing ARPC5/L. MAVER-1 cells were added to the imaging dish pre-coated with 20µg/ml of anti-IgM, allowed to settle for two minutes, and imaged. A)TIRF images of MAVER-1 cells overexpressing ARPC5/L in indicated time points after BCR stimulated. B) A quantification analysis of the integrated density of ARPC5/L in the center and the edge of the cell. C) The ratio of integrated density of the ARPC5 and ARPC5L in 3 and 20 minutes of BCR stimulation. D) The total cells area measurement in 3 and 20 minutes after BCR stimulation was used as a positive control for BCR stimulation and cell spreading. ImageJ software was used for the analysis. Cells were background subtracted, bright/ contrast adjusted, and corrected for bleaching using (simple method). Images of cells were taken using spinning disk confocal microscopy N=3. Number of analysed cells 15 cells. The statistic was performed using PRISM (SEM), statistical test used is paired T-test in A,B,and C. in D one-way ANOVA's with Tukey's multiple comparison Test. TIRF: Total internal reflection fluorescence. SEM: standard error mean. wt: wildtype. kd: knockdown.

3.4 Discussion:

In this chapter, I investigated the effect of BCR stimulation on the behaviour of ARPC5/L in MAVER-1 cells. A principal finding is the role of BCR signaling in regulating ARPC5 and its paralogue ARPC5L expression level and their distribution. ARPC5 is downregulated after BCR stimulation and seems to redistribute toward the periphery of B cell synapse whereas ARPC5L expression level remain stable, and the distribution does not change after BCR stimulation. This provides a potential explanation for relative enrichment of ARPC5L in the phospho-proteome after BCR stimulation that our group observed previously (Fig 1.7). Moreover, the distinction in the isoforms turnover rate indicates to their different properties that could contribute to actin dynamics. This data gives rise to the possibility that BCR signaling controls actin dynamic through manipulating ARPC5 and ARPC5L expression levels.

Upon BCR stimulation, the ARPC5 level is reduced while the level ARPC5L is maintained. In the previous proteomic study, only ARPC5L is strongly enriched with phosphotyrosine (Fig 1.5) pointing toward an important function of ARPC5L in B cells after BCR engagement. Moreover, differences in isoform distribution after BCR stimulation, with ARPC5 accumulation at the edge of the cell membrane and ARPC5L being distributed within the cell membrane emphasize the selective ability of BCR signaling to manipulate ARPC5/L distribution within the actin cytoskeleton. Maintaining ARPC5L within the centre and the edge of the contact

membrane could imply the contribution of ARPC5L in mediating stabilisation of BCR central cluster formation. The preference of BCR signaling to stabilise and sustain ARPC5L over ARPC5 could be due to its known more efficient property in promoting actin polymerisation than ARPC5 [97]. Such a process could be essential for the signal activation and the merger of BCR micro clusters into the central cluster during B cell activation [70].

The quantification of the mRNA level of ARPC5 excludes the possibility of less ARPC5 transcription underlying the protein level reduction after BCR stimulation. The novel result of using cycloheximide treatment suggests different isoforms have different turnover properties that could affect actin stabilisation. Shorter ARPC5 half-life than ARPC5L indicates that ARPC5 could be degraded after BCR stimulation leading to its level reduction when B cells are activated. Moreover, analysing the amino acid sequences of ARPC5 and ARPC5L using the sequence alignment tool website showed that the amino acid sequence of ARPC5 contains five lysine residues that are replaced with another amino acid at the same positions within the ARPC5L amino acid sequence (Fig 3.11). The presence of these lysine residues potentially enhances the possibility that ARPC5 more susceptible for ubiquitin-mediated protein degradation when compared to ARPC5L. This possibility was subjected for testing through the inhibition of either ubiquitin-proteasomal or lysosomal pathways. However, due to experimental difficulties, the conclusion could not be achieved.

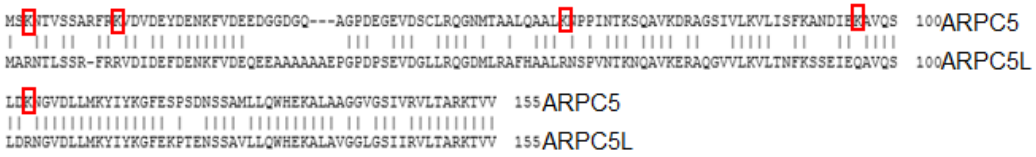

Figure 3-12: Comparison of the amino acid sequence of ARPC5 and ARPC5L.

The maintenance of one of the paralogues could be pivotal for the cell. The fact that when one paralogue expression is depleted, an increase in the other paralogue is observed suggests possible compensation or distinctive function between the paralogues within the B cell. However, the role of these isoforms in B cells and during BCR signaling is unclear. Therefore, the work in the next chapter will be dedicated to understanding the functional role of ARPC5 and ARPC5L in BCR signaling.

Chapter 4: Determine the functional role of ARPC5 isoforms in BCR signalling

4.1 Introduction

Finding differences in turnover and localisation between ARPC5 and ARPC5L after BCR crosslinking point to separate functional role in BCR signaling. The ARPC5 isoforms are unstudied proteins whose role in B cell biology is unknown. This chapter, therefore, examines the functional role of these proteins in BCR signaling and in the downstream events particularly cell adhesion and migration.

At the molecular level, actin networks are required in multiple steps during BCR signaling including BCR receptors internalisation, B cell spreading, and they greatly affect the signaling outcomes such as B cells adhesion and migration [85, 181]. With respect to CLL cells, cells trafficking occurs between various blood tissues to ensure access to the support they need from stromal cells [182]. When these malignant lymphocytes are retained in the nodes, this leads to lymphadenopathy, a sign of progressive disease and poor prognosis [183]. Although this process is vital and its mechanism very important, little is known about the dynamics of CLL cell retention, migration, and the influence of the actin cytoskeleton on retentions of these cells into the lymph node microenvironment.

The generation of branched actin networks during B cells activation occurs through the activation of the Arp2/3 complex which consists of 7 different subunits. ARPC5 and ARPC5L are paralogues that share 67% homology, and they are part of this complex. It is well known that these paralogues differentially influence the actin nucleating activities of the Arp2/3 complex

through the selective ability of cortactin to stabilise the ARPC5L isoform within the Arp2/3 complex, forming actin branching [97].

4.2 Aim of this chapter

To establish the role of ARPC5 and ARPC5L in B cell biology by investigating their function in MAVER-1 cells in the presence of BCR signaling, and then examining how these paralogues affect MAVER-1 cell adhesion and migration. the investigation in this chapter provides insight into the pathological behaviour of malignant MCL cells signalling/migration that could be beneficial for future therapeutic options.

4.3 Result

4.3.1 Cell surface markers level are unchanged after ARPC5/L depletion in MAVER-1 cells.

This investigation was dedicated to determining the role of ARPC5/L on the phenotypic changes of surface markers expression in MAER-1 cells. Cell-surface proteins including activation markers, chemokines markers, and adhesion receptors are required for B cell function in the absence or presence of BCR signaling. The actin cytoskeleton is required for surface markers stability on the cell surface and their internalisation [184], and thus it is important to explore the role of the isoforms in cell surface marker expression.

To determine the surface expression of MAVER-1 cells, a new technology, mass cytometry was used which can detect up to 40 antibodies binding to cell-surface proteins of multiple samples in one go without interference or overlap between different samples.

After the ARPC5/L knockdowns, samples were barcoded before pooling, and subsequent staining according to the protocol. The samples were then analysed by mass cytometry. Figure 4.1 shows the gating strategy for non-targeted MAVER-1 cells (NT), ARPC5 knockdown, and ARPC5L knockdown. For NT, the barcode used was a combination of metals ^{115}In and $^{+89}$Y, for ARPC5 knockdown the barcode combination was $^{+165}$Ho and $^{+89}$Y, and for ARPC5L $^{+165}$Ho and ^{115}In. These combinations were tagged to CD45 antibodies. CD45, commonly known as Leukocyte Common Antigen,

is strongly expressed on all blood cells except for mature erythrocytes and plasma cells. The bivariate dot blot and drawn gate indicate the population of cells that were then taken forward for further analysis using Cytobank software.

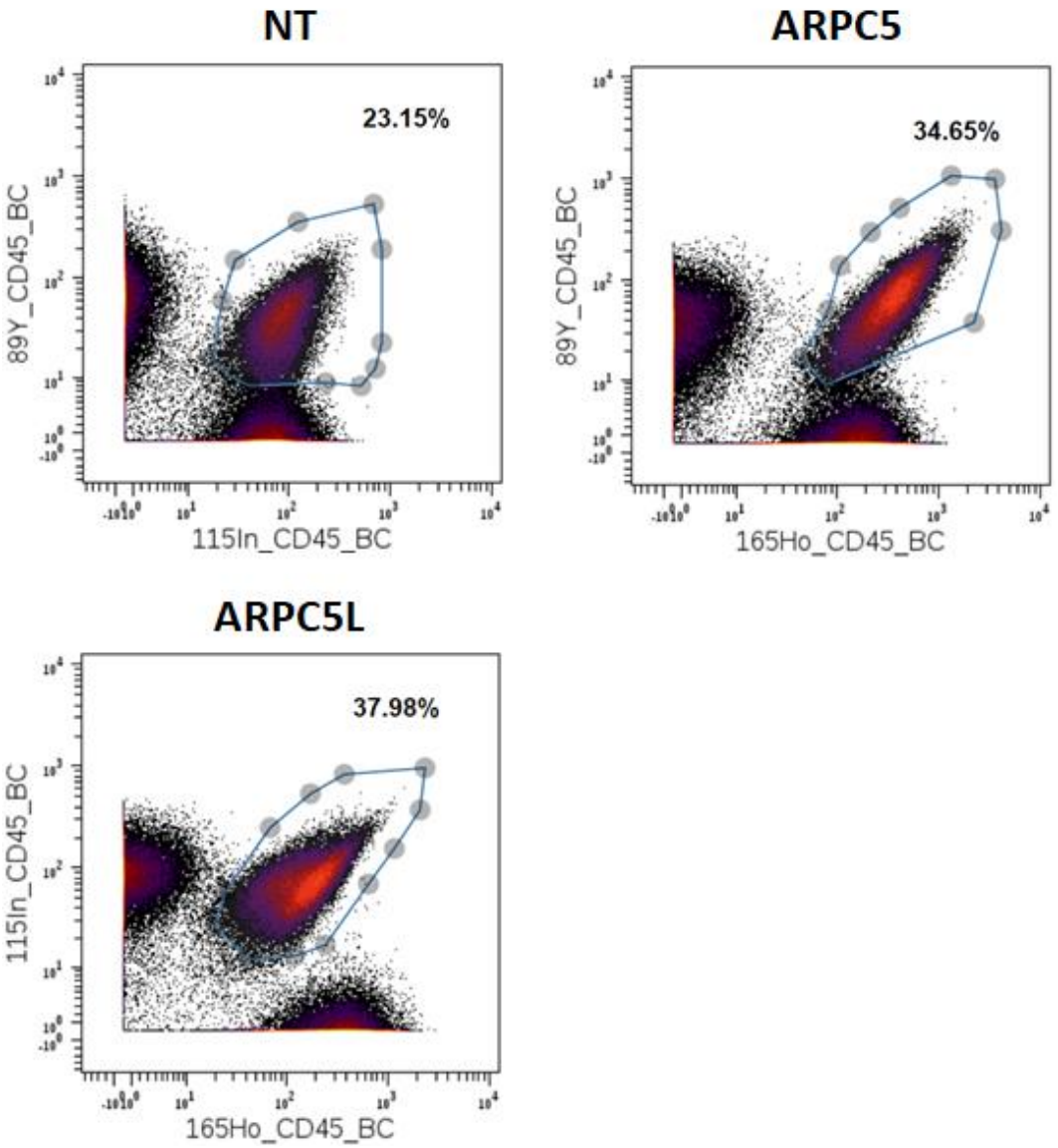

Figure 4-1: Manual gating strategy to identify live MAVER-1 cells (NT). Using mass cytometry to gate on live singlets cells. The gating strategy was based on barcoding multiple samples with metals combinations NT (^{115}In and $^{+89}$Y), ARPC5 ($^{+165}$Ho and $^{+89}$Y), ARPC5L ($^{+165}$Ho and ^{115}In) CD45 positive cells. The gating and the surface markers expression were identified using Cytobank software. NT: non-targeting.

Analysis of surface antigen expression on NT and ARPC5/ARPC5L knockdown MAVER-1 cells revealed each population to be highly similar. There was no overall phenotypic change in the wild-type cells compared to the knockdown cells (Figure 4.2) which rule out an effect of ARPC5/L on MAVER-1 cells surface antigen expression.

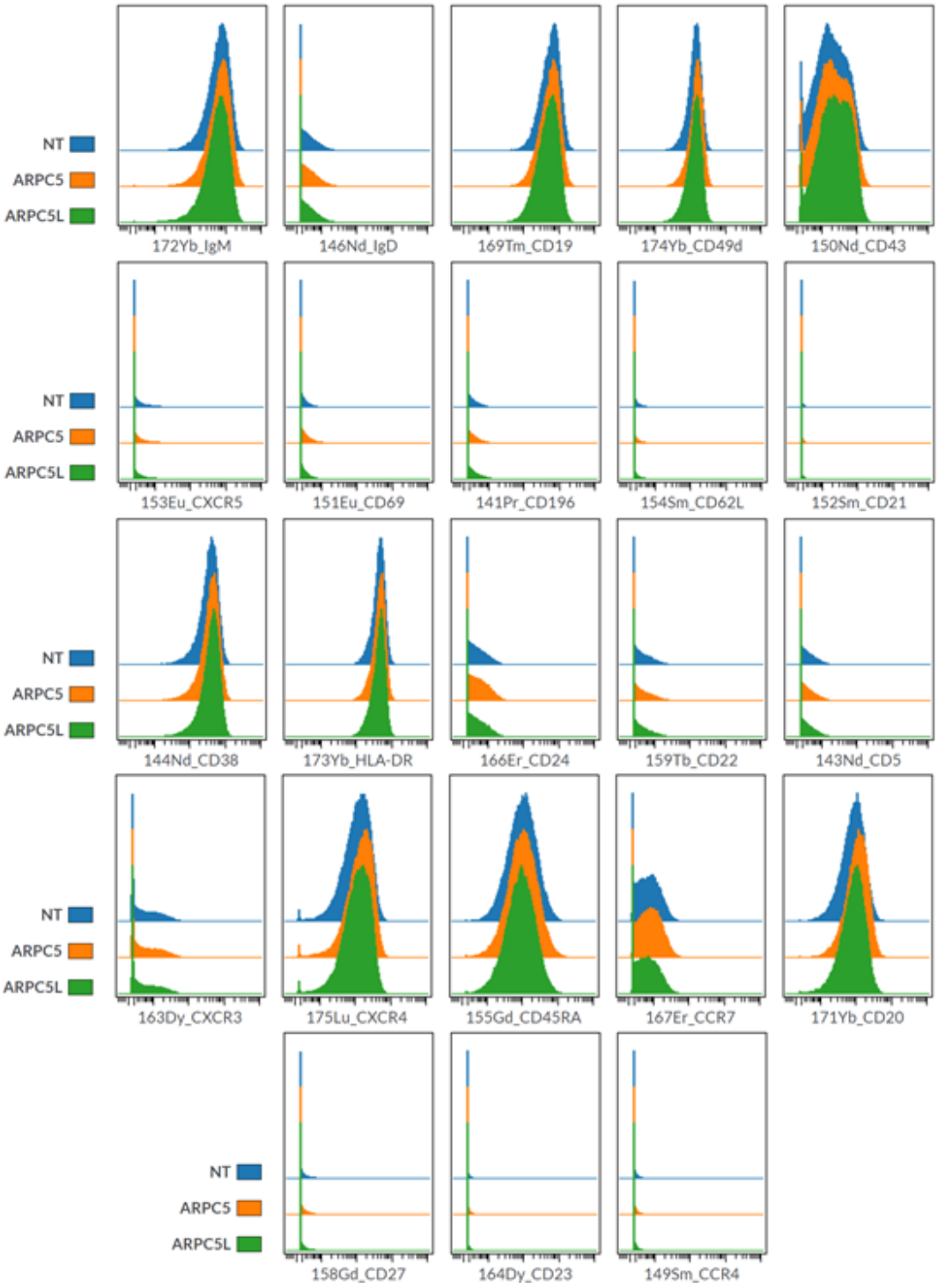

Figure 4-2: The surface expression markers (CD) are unchanged with ARPC5/L depletion in MAVER-1 cells. Following knockdowns hits, MAVER-1 cells from different conditions were prepared for mass cytometry analysis using antibodies panel. Samples from the three different conditions were differentially barcoded prior to the mass cytometry analysis. The Cytobank software was used to analyse the phenotypes of each condition. NT:non-targeting, CD: cluster differentiation.

4.3.2 Surface IgM expression and receptors internalisation are unaffected when ARPC5 paralogue is depleted.

After having tested the effect of ARPC5/L on surface antigen expression on MAVER-1 cells in the absence of BCR stimulation, I decided to monitor the internalisation of the B-cell receptor after BCR stimulation. The internalisation of activated receptors by endocytosis has an important role in regulating the duration and the intensity of downstream signaling events [185].

Actin dynamic plays a role in BCR trafficking, in particular, Arp2/3 complex-mediated branched actin network regulating BCR internalisation [49]. Therefore, by using Flow cytometry technology, I planned to look at the influence of ARPC5/L depletion on the levels of BCR internalisation in the MAVER-1 cells at various time points after BCR crosslinking**.**

Anti-IgM F(ab')2 fragments were labelled with Alexa-488 so they can be used in Flow cytometry. BCR on MAVER-1 cells were incubated with this antibody for specific time points. Two technical repeats were generated from each time point. The first sample is to show the total amount of BCR within the cell (on surface and internal), and the second sample is to show only the internalised receptors by quenching the surface receptors in that sample using anti-Alexa-488. Figure 4.3 exhibits the gating strategy I used to gate on live MAVER-1 cells based on forward scatter (the size of the cell) and the side scatter (the granularity).

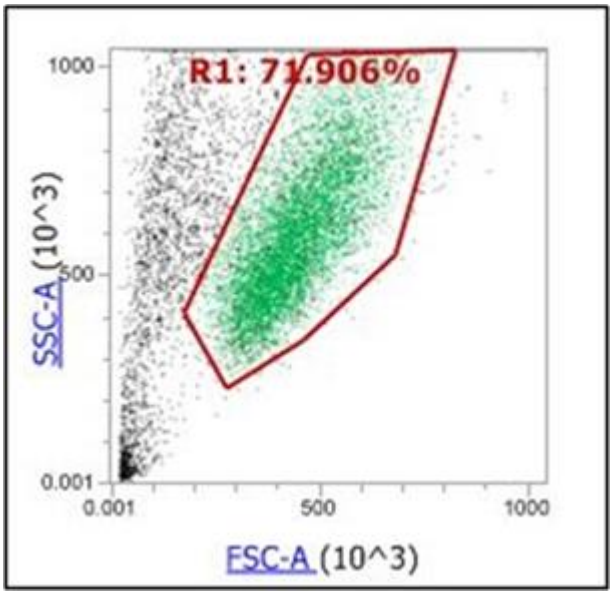

Figure 4-3: Manual gating strategy to identify live MAVER-1 cells in Flow cytometry. Using flow cytometry to gate on live cells based on the FS (the size of the cell) and the SS (the granularity). The gating strategy was identified using Flowjo software. FS: forward scatter. SS: side scatter.

Measuring the surface expression of BCR at zero minutes of BCR binding to anti-IgM F(ab')2 shows no difference in receptors expression between the wild type and the knockdown samples (Figure 4.4A). the level of surface BCR was then tracked on the MAVER-1 cells over time (Figure 4.4b), showing the ability of MAVER-1 cells to internalise BCR even with ARPC5/L knockdowns. This experiment excludes a functional effect of ARPC5/L in BCR internalisation after BCR stimulation.

A)

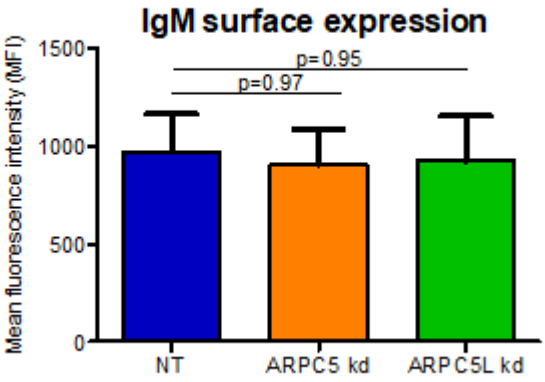

B)

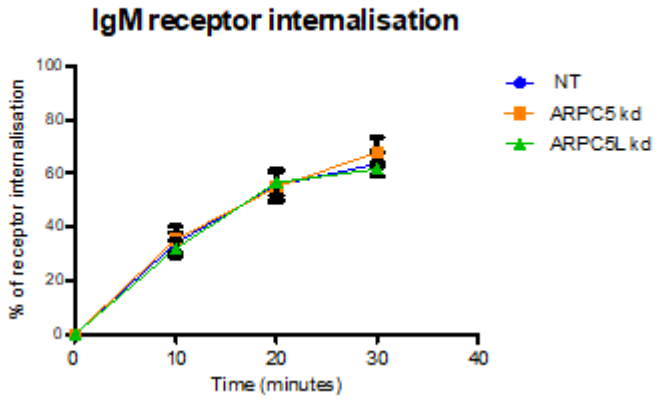

Figure 4-4: Surface IgM expression and receptors internalisation are unaffected when ARPC5 paralogue is depleted. MAVER-1 cells were treated with the indicated siRNA and stimulated with 20µg/ml of anti-IgM antibody conjugated with Alexa-488 for indicated time points. Half of the cells from each condition were incubated with anti-Alexa-488. IgM expression was determined on the gated live cells. A) The mean fluorescence intensity (MFI) of the surface IgM expression at zero minutes of BCR stimulated cells. B) Percentage of IgM receptor internalisation upon BCR stimulation. The surface expression o BCR was determined using Flowjo software. The experiment was done in (N=3), the statistic was achieved using PRISM (SEM) one-way ANOVA's with Dunnett's multiple comparison test. SEM: standard error of the mean. NT: non-targeting. Kd: knockdown.

4.3.3 ARPC5/L knockdown does not impair BCR-induced MAVER-1 spreading.

To further investigate the role of ARPC5 and ARPC5L in BCR signaling, I investigated how depleting these paralogues affected BCR-induced cell spreading. The role of ARPC5 and ARPC5L was tested by looking at the ability of MAVER-1 cells to spread on anti-IgM-coated coverslips following the knockdown of these paralogues with siRNA.

Following the protocol for ARPC5/L knockdowns, MAVER-1 cells were labeled with 1µM/ml of SiR-actin for 45 minutes, and then settled on coverslips precoated with anti-IgM. Cells were imaged after 30 minutes of BCR cross-linking, anti-IgG was used as a negative control for this experiment (Fig 4.5a). The quantification was performed by measuring the total area of the cell in each condition using ImageJ software (Fig 4.5b). Figure 4.6 shows there was no noticeable disruption in the ability of BCR signaling to the spreading of MAVER-1 cells after ARPC5/L knockdown.

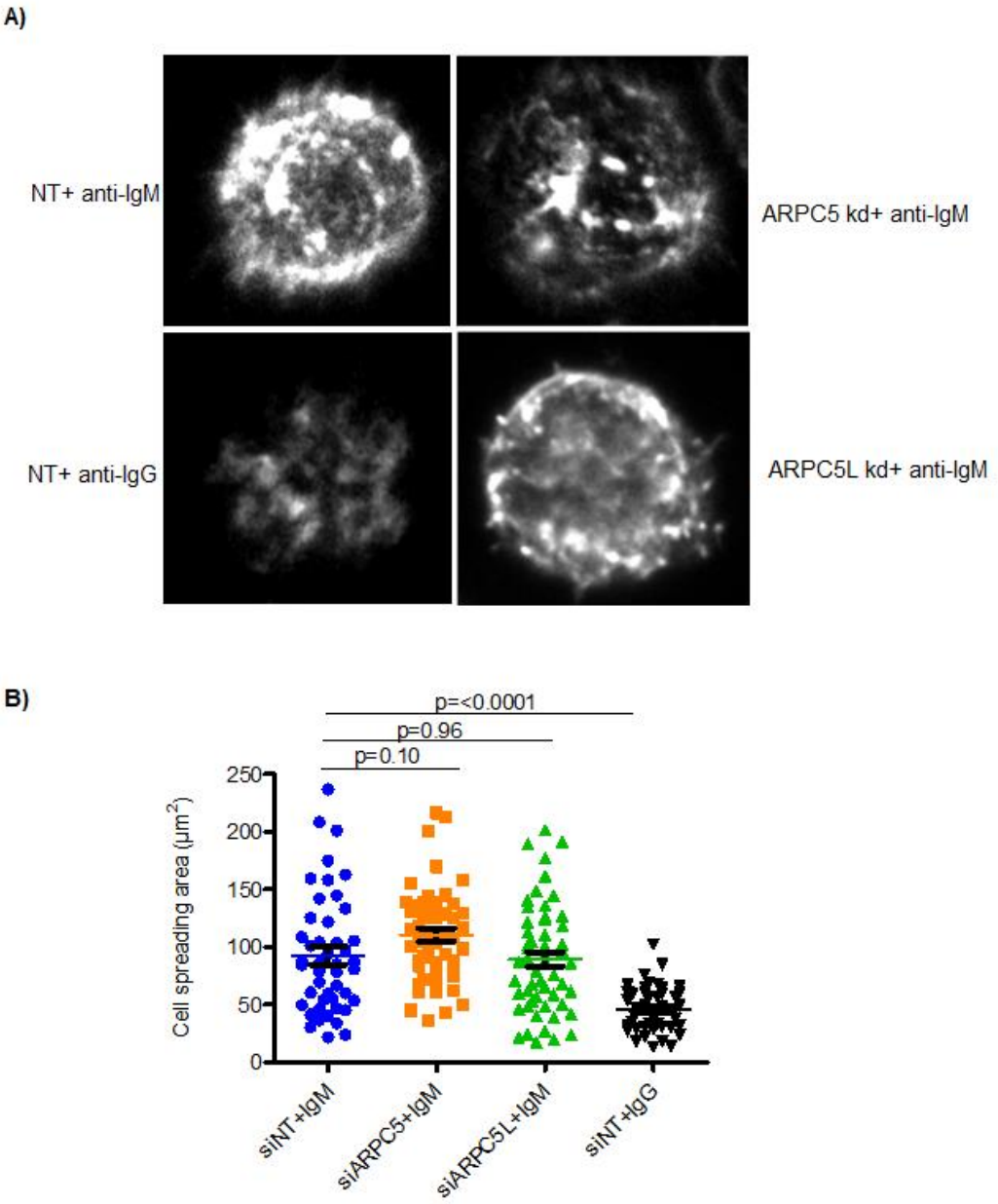

Figure 4-5: ARPC5A/L knockdown does not impair BCR-induced MAVER-1 spreading. A) Confocal image of MAVER-1 cells After ARPC5/L depletion and BCR stimulation., MAVER-1 treated with indicated siRNA and Actin was labeled with SiR-actin for 45 minutes. Cells were placed on coverslips precoated with anti-IgM and the negative control was treated with anti-IgG. Images were taken for each condition after 30 minutes of BCR stimulation using Zeiss LSM 800 system. B) Quantification of cell spreading by measuring the total area of the cell after 30 minutes using ImageJ software.The statistical analysis used was Prism One-way ANOVA with Dunnett's multiple comparison test. Error bars indicate th standard error of the mean and represent 3 independent experiments N=3. NT: non-targeted control. Kd: knockdown.

4.3.4 ARPC5/L depletion does not affect Calcium (Ca^{2+}) flux mediated by BCR stimulation.

Anti-IgM-induced calcium mobilisation can be used as an indicator of receptor signaling activity [6]. To test if this phenomenon is altered with ARPC5/L knockdown in MAVER-1 cells, I used Fluo-4-AM, a cell-permeable indicator that increases in fluorescence upon binding to released Ca^{2+}. After the knockdown of ARPC5 and ARPC5L, MAVER-1 cells were incubated with Fluo-4–AM dye for 20 minutes. The fluorescence of Fluo-4–AM-loaded cells was initially measured in non-stimulated cells, and then again, following the addition of 20 µg/ml goat F(ab′)2 anti-IgM. A rise in Fluo-4–AM fluorescence over baseline after BCR crosslinking indicated intracellular calcium release.

Figure 4.6 shows the intracellular calcium release in NT MAVER-1 cells and ARPC5/L knockdown cells. This figure showed that NT MAVER-1 cells are responded to BCR crosslinking in a similar way to that observed in cells where the ARPC5 paralogues had been knocked down, suggesting that ARPC5/L are not indispensable for Ca^{2+} release upon BCR cross-linking.

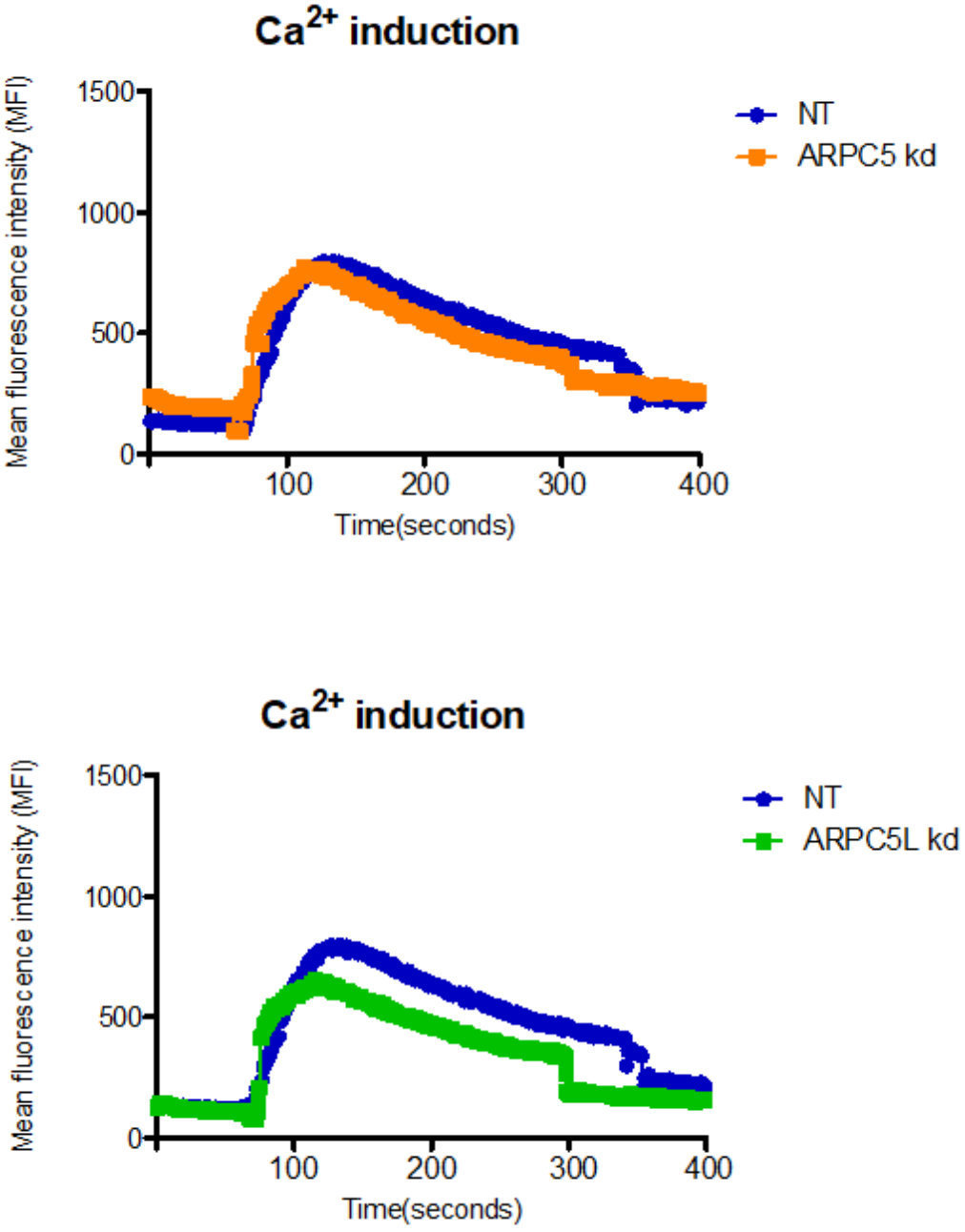

Figure 4-6: ARPC5/L reduction does not affect Calcium (Ca2+) flux mediated by BCR stimulation._Following knockdown hits, MAVER-1 cells were incubated with 2 µM Fluo4 –AM for 20 mints. Acquisition of the first one minute was performed without stimulation followed by the addition of 20µg/ml of anti–IgM to the same samples, and the acquisition was taken for 10minutes. Data were acquired on a Flow cytometry and analysed using Flowjo software. NT: non-targeting kd: knockdown.

4.3.5 ARPC5/L knockdown does not affect kinases phosphorylation level after BCR stimulation.

BCR engagement with antigen plays a crucial role in determining the fate of B cells by permitting many distinct outcomes including survival, proliferation, apoptosis, and differentiation [19]. Some of these pathways promote actin reorganisation suggesting the vital connection between BCR signaling and actin dynamic.

In this experiment, I aimed to understand the effect of ARPC5/L on BCR signaling mediated by BCR stimulation. I measured the phosphorylation level of major proximal and distal kinases, activated after BCR engagement. MAVER-1 cells were incubated with anti-IgM after depleting ARPC5 and ARPC5L. The incubation periods used in this investigation were 5 and 60 minutes according to the different time points in which some kinases reach their maximum phosphorylation level upon BCR stimulation. The total level of these kinases is used as loading control for western blotting.

This test showed no significant changes in the phosphorylation dynamic of the kinases (Fig 4.7A) across the conditions used in this experiment (Fig4.7B).

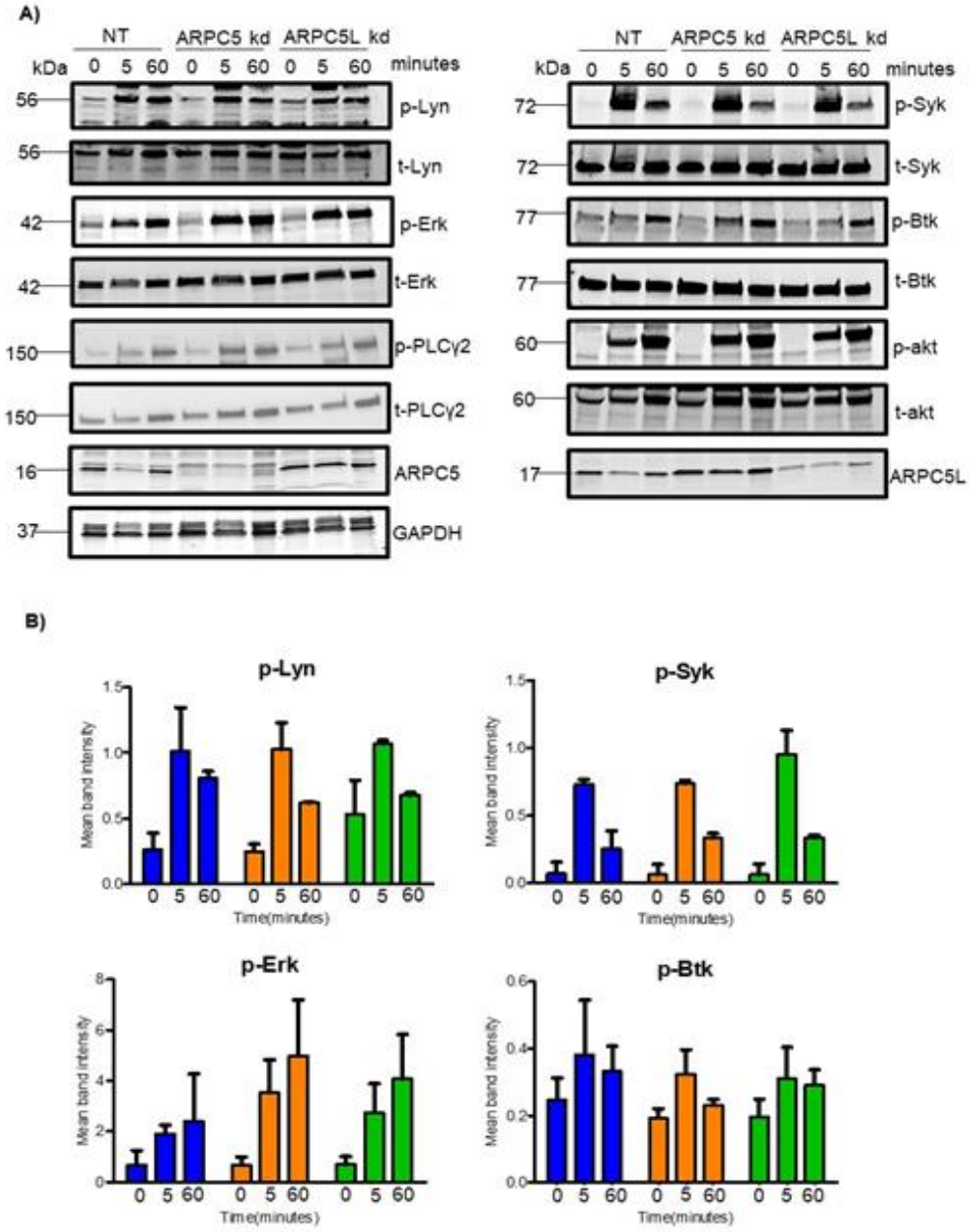
A)
NT
ARPC5 kd
ARPC5L kd
kDa
0 5 60 0 5 60 0 5 60
minutes
56
p-Lyn
56
t-Lyn
42
p-Erk
42
t-Erk
150
p-PLCγ2
150
t-PLCγ2
16
ARPC5
37
GAPDH
72
p-Syk
72
t-Syk
77
p-Btk
77
t-Btk
60
p-akt
60
t-akt
17
ARPC5L
B)
p-Lyn
p-Syk
p-Erk
p-Btk
Mean band intensity
Time(minutes)

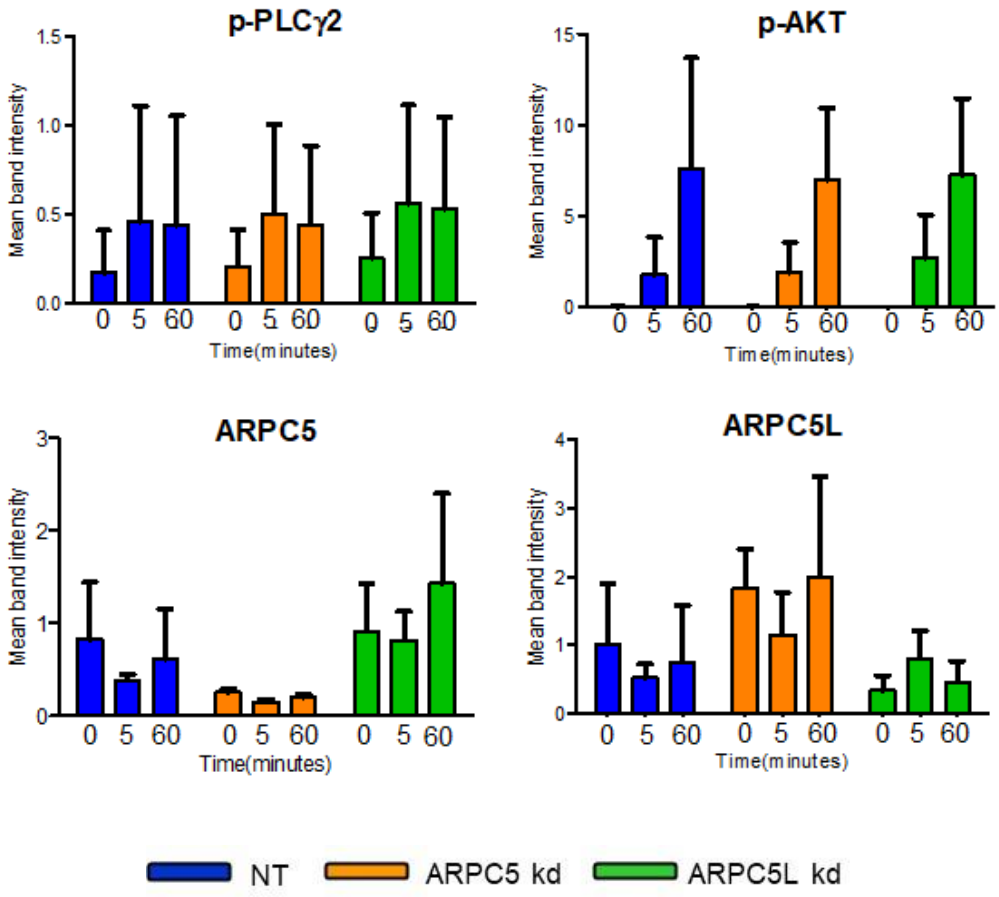

Figure 4-7: ARPC5/L knockdown does not affect the kinases phosphorylation level after BCR stimulation. A) Western blot analysis of ARPC5/L within lysates of MAVER-1 cells treated with the indicated siRNAs followed by BCR stimulation with anti-IgM antibody for 5 and 60 minutes. The Western Blot images were taken using the Li-COR Odyssey system. B) Protein levels were quantified by dividing the phosphorylated kinase level by the total level of the kinase. Statistical analysis was done using Prism software. Error bars indicate the standard error of the mean (SEM) and represent 3 independent repeats N=3. NT: None- targeted control, kd knockdown, p: phosphorylated kinase, t: total kinase.

4.3.6. MAVER-1 cells adhesion ability is not disrupted with ARPC5/L depletion.

The adhesion process in B cells is crucial for forming a central cluster of antigen receptors [186], and BCR signaling propagation. The involvement of the actin cytoskeleton is vitally important for successful adhesion formation [85]. Actin nucleating complex Arp2/3 is crucial for the generation of the actin ring and centripetal membrane flow for B cell adhesion [82].

I decided to measure the effect of ARPC5 isoforms, as Arp2/3 complex subunits in MAVER-1 cells adhesion. The selection of integrins ligends to be subjected to testing is based on their expression of the cognate integrin on MAVER-1 cells. MAVER-1 cells highly express Very Late Antigen-4 VLA-4 ($\alpha_4\beta_1$-integrin). The best-described ligands for VLA-4 are VCAM-1 and Fibronectin which are released by the surrounded stromal cells [187]. This integrin has been implicated in homing and retention of hematopoietic cells through binding to its ligends [188]. Moreover, BCR signaling promotes adhesion in B cells through controlling the integrin activity in particular α4β1 integrin [181].

Following ARPC5 and ARPC5L knockdown, MAVER-1 cells were stained with Calcein-AM, cell dye for one hour and replated into 96 well plates that were pre-coated with Fibronectin, VCAM-1, anti-IgM, ligends combinations, and BSA as a negative control. After incubation for 30 minutes, cells were subjected to washing steps to remove non-adherent cells. The stained cells also were added to non-coated wells for the calibration (shown in section 2)

and to the positive control. Using the FLUO star Omega microplate reader system, the absorbance reading was taken.

Figure 4.8 showed a successful adhesion ability of MAVER-1 cells through $\alpha_4\beta_1$-integrin activity. The experiment revealed that this adhesion ability is not impaired with ARPC5 and ARPC5L depletion factoring out their functional effect on these cells' adhesion.

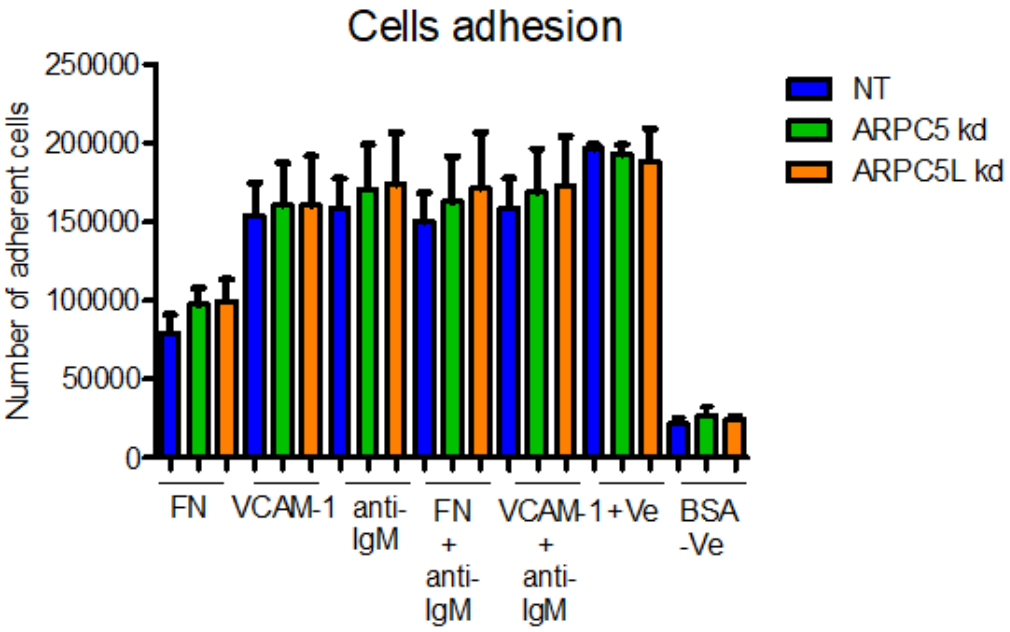

Figure 4-8: MAVER-1 cells adhesion ability is not disrupted with ARPC5/L depletion. MAVER-1 cells were stained with calcine-AM and added to 96 well plates which were pre-coated with different ligend combinations as indicated. After 30 minutes of incubation with the ligends at optimal conditions, cells were washed, and the number of stained cells was counted using FLUO star Omega microplate reader system. Statistical analysis was performed using Prism One-way ANOVA (Tukey's multiple comparison test). Error bars indicate the standard error of the mean and represent 4 independent experiments N=4. FN: Fibronectin, VCAM-1: Vascular cell adhesion protein 1, BSA: Bovin serum albumin, +Ve: Positive control, -Ve: Negative control.

4.3.7. Silencing of ARPC5 and ARPC5L impairs migration of MAVER1 cells.

BCR stimulation is reported to arrest B cell migration [189]. Since this chapter aims to understand the functional role of ARPC5/L in BCR signaling including cell migration, it was necessary to test the impact of BCR crosslinking on the migration of MAVER-1 cells.

To assess cell migration, I decided to use the method of "pillar forests" that mimic 3D cell environment. The pillar forests are Polydimethylsiloxane (PDMS)-based setups in which arrays of micrometre-sized pillars connect two closely neighbouring surfaces. The advantages of 2D cell migration tests are combined with the precise determination of 3D environmental parameters in this new technique [173], applicable for leukocyte migration studies [190]. Accurate preparation of the PDMS device is required since changing the pillar shape, size, height, and inter-pillar distance can manipulate microenvironmental parameters. Luckily, this device was kindly prepared and granted by Dr. Anne Reversat who actively contributed to discovering it [173]. Figure 2.1 shows the PDMS device with a specific design including the pore size 5µm I used in this study. The information of device preparation is stated in a detailed fashion in [173].

Following ARPC5 and ARPC5L knockdowns, MAVER-1 cells were either directly added or treated first with (anti-IgM or anti-IgG) and added to the device. In both ways, cells were incubated in the device at 37° for four minutes allowing them to enter the pillar and start to migrate. Images were

taken every minute over 30 minutes using widefield Zeiss microscope system. The images taken were adjusted for brightness and contrast and the analysis of the cell tracking was performed using Track mate (simple lab tracker) that allows cell tracking according to the time and distance using ImageJ software.

Figure 4.9 A&B shows the tracked cells after 30 minutes of imaging. Figure 4.9 c shows the quantifications of the migration speed which indicate MAVER-1 cells are free migratory cells meaning they are capable to migrate in the absence of chemokines. Knockdown of either isoform significantly slows the speed of the free migration indicating the requirement of ARPC5/L for the migration of MAVER-1 cells. BCR stimulation inhibited the migration of these cells, and depletion of ARPC5 or ARPC5L does not impair the BCR-mediated cell arrest. In this experiment, treating the cells with anti-IgG was used as a positive control pointing to the selective migration arrest of these cells to the BCR stimulation with anti-IgM.

Taken together, these results suggest the role of ARPC5/L in MAVER-1 cells migration. Crosslinking of BCR arrests these cells' migration regardless of ARPC5/L expression.

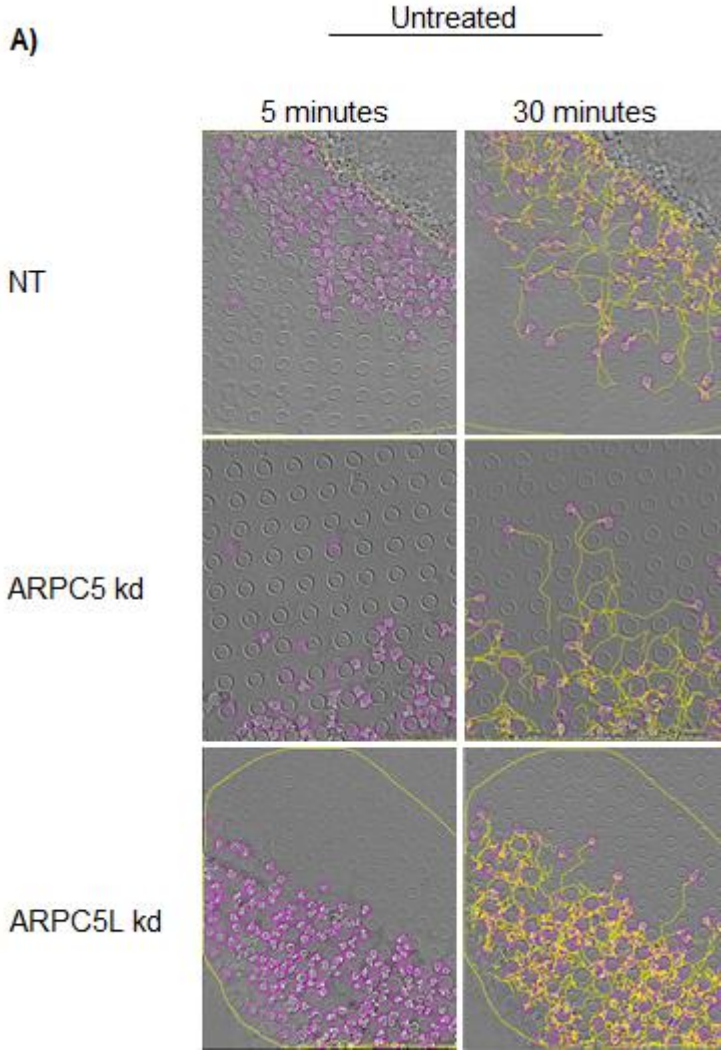
A)
Untreated
5 minutes
30 minutes
NT
ARPC5 kd
ARPC5L kd

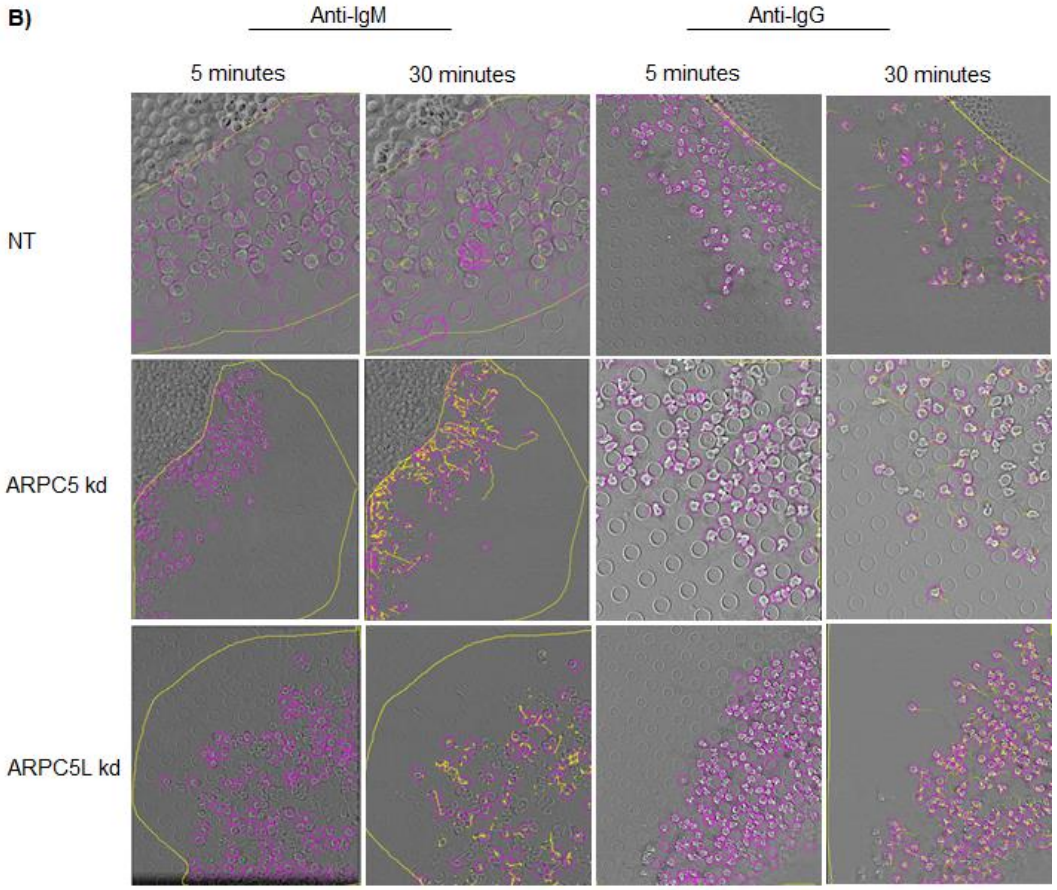
B)
Anti-IgM
Anti-IgG
5 minutes
30 minutes
5 minutes
30 minutes
NT
ARPC5 kd
ARPC5L kd

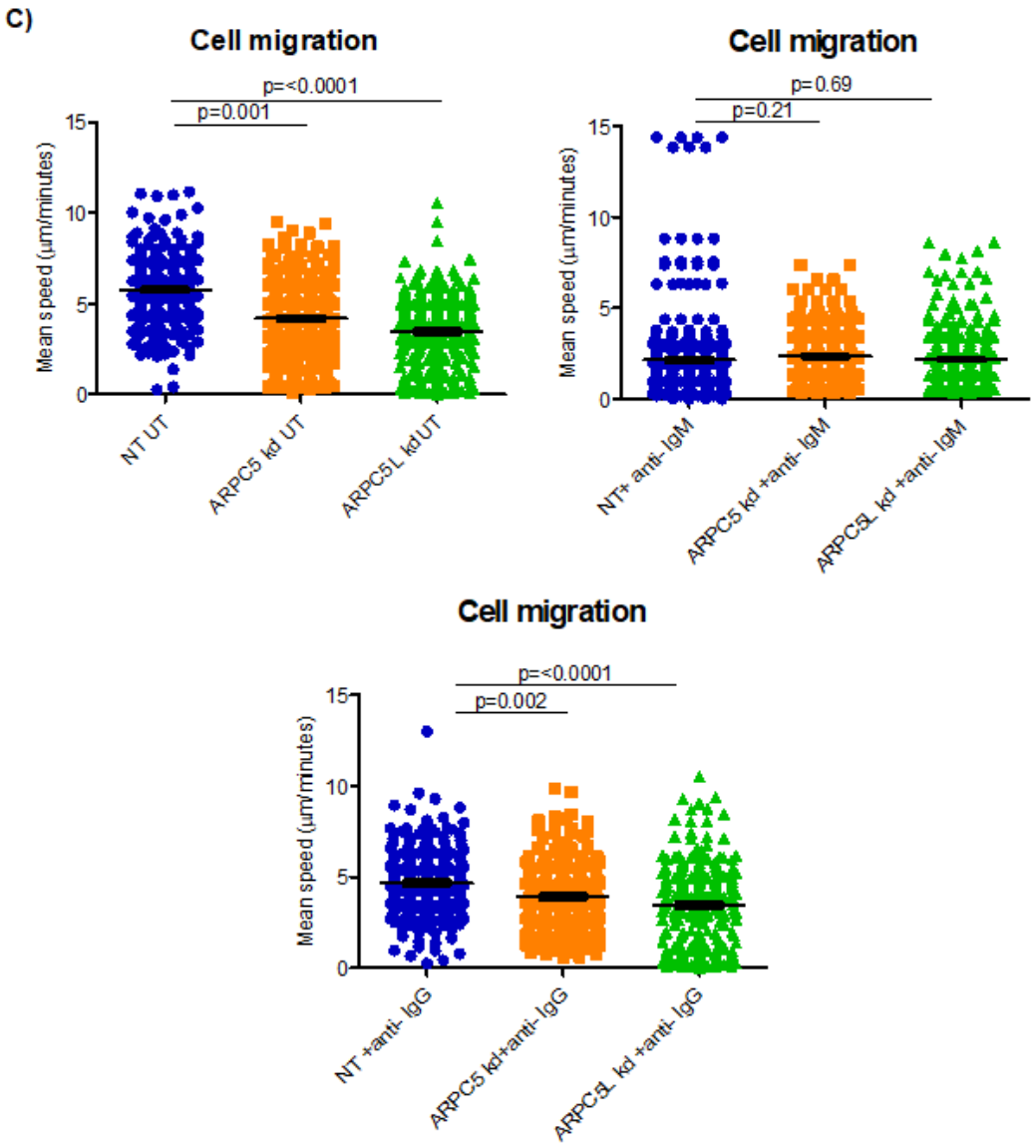

Figure 4-9: Depletion of ARPC5/L impair the free migration of MAVER-1 cells. MAVER-1 were cells treated with siRNA and left free or stimulated with (anti-IgM or anti- IgG). Cells were added to the chamber and incubated for four minutes to allow them to settle in the chamber. A&B) showing the snapshot of adjusted Bright and contract images of five minutes and 30 minutes tracked cells (in yellow), the images were taken every one minute over 30 minutes using Widefield Ziess LSM 900 system. C) is the tracks analysis of cell mean speed using Trackmate (Simple Lab Tracker) method in ImageJ software. The experiment was independently repeated three times (N=3). The error bar represents the SEM using PRISM and the statistical analysis was performed is one-way ANOVA's with Dunnetts multiple comparison test. SEM: standard error mean. kd: knockdown.

4.4 Discussion :

BCR signaling plays a crucial role in B cell activation which is initiated via the interaction of BCR with a specific antigen. It was found that the actin cytoskeleton changes dramatically during B-cell activation, and its reorganisation regulates BCR signaling in different stages of B-cell biology [191]. Since ARPC5 and ARPC5L are isoforms contributing to actin formation, in this chapter, I investigated their functional role in BCR signaling using MAVER-1 cells.

When BCR signaling is induced, B cells go through multiple changes facilitating their activation. It is shown that in T cells, Arp2/3 complex is required for maintaining surface TCR levels via regulating TCR endosome trafficking [192], and in B cells the complex is required for antigen-BCR complex internalisation [49]. These findings suggested the possibility that the isoforms as members of the Arp2/3 complex might be required for BCR trafficking either in their maintenance on the B cell surface or their internalisation. Upon antigen encounter, B cells undergo a spreading response and actin plays an essential role in this process. Inhibition of Arp2/3 complex alters BCR induced spreading in B cells [82]. A cytoplasmic free calcium level induced by BCR signaling is strongly connected to the generation of actin-based membrane protrusion, essential for B cell spreading and adhesion [193]. Moreover, BCR engagement leads to different kinases phosphorylation required for B cell activation and survival.

Some of these kinases induce actin reorgnaisation pointing to the link between BCR signaling and actin dynamic.

Although Arp2/3 complex is important for these changes, in my study, depletion of ARPC5 and ARPC5L did not affect these processes. This suggests that the Arp2/3 complex with the respective other isoform can still fulfil these functions to same degree. These observations opened the window for the necessity for further investigation.

The functional effect of ARPC5 and ARPC5L in MAVER-1 cells adhesion and migration was tested. A role for ARPC5/L isoform specificity in adhesion induction was excluded by measuring the ability of α4β1 integrin to induce MAVER-1 cells adhesion through binding to its ligands FN and VCAM-1 with and without BCR stimulation.

To test the effect of the isoforms on cell migration, MAVER-1 cells were tracked through “pillar forest” champers that mimic the confined migration of lymphocyte in tissue. ARPC5 and ARPC5L were shown to functionally affect MAVER-1 cells migration to similar degree, depletion of either isoform slowed the migration down. This was somewhat surprising since in [97] showed that ARPC5 isoforms differently affect actin polymerisation. BCR stimulation arrested both wildtype and knockdown cells indicating the strong controlling ability of this signaling on cell migration regardless of knockdown effect.

Chapter 5: General Discussion

The main aim of this study is to determine the functional differences between ARPC5 and ARPC5L in BCR signaling. The studies in this thesis further the previous findings which showed enrichment of ARPC5L in the phosphoproteomic study [169] (Fig1.5). I found that following 60 minutes of BCR engagement, ARPC5 levels are downregulated while the ARPC5L level remains constant. Moreover, a change in ARPC5 and ARPC5L distribution in cells is observed within 20 minutes of BCR stimulation where there is selective distribution of ARPC5 toward the edge of the cell membrane while ARPC5L remains diffused within the membrane. ARPC5 was shown to have a faster turnover than ARPC5L, and isoform depletion by siRNA leads to an increase of the protein level of the other respective isoform. Depletion of either paralogue significantly reduces the migration ability of B cells. Together these findings show BCR engagement induces a change in expression and distribution of ARPC5 and ARPC5L activity, however, the specific functional role of either ARPC5 paralogues in BCR signaling could not be elucidated.

To my knowledge, there are no reports characterising ARPC5 paralogues in CLL, MCL, or even within global B cell activation. Thus, the work presented in this thesis is of interest within this field because it attempts to make a connection between ARPC5 paralogues and BCR signaling specifically in the malignant cells of MCL. BCR engagement activates signaling pathways important to the behavior of normal and malignant B-cells [141]. This is particularly true of CLL and MCL where BCR signals

facilitate the growth and survival of malignant clones in these diseases. My work shows that BCR engagement induces differences in the turnover rate and a switch in ARPC5/L expression in the knockdown study that support the possibility of a role for these paralogues in MCL and CLL.

Findings in chapter 3 show that ARPC5 paralogues have differential protein expression and distribution following BCR stimulation. This evidence suggests that BCR signaling selectively requires ARPC5L activity during signaling induction. The reduction of ARPC5 levels in the face of maintained ARPC5L levels is in agreement with findings of a previous phosphoproteomic study (Fig1.5) performed in this lab. Here the high enrichment of ARPC5L that occurs in cells responding to BCR signaling supports the notion that such signaling maintains the level of ARPC5L. The lack of tyrosine residues associated with consensus phosphorylation sites within the amino acid sequence of this protein suggests that it is likely to be associated with proteins that are tyrosine phosphorylated rather than being directly phosphorylated itself. A possible explanation for why ARPC5L levels are maintained is through BCR-induced down-regulation of ARPC5 which may be analogous to experiments in the thesis showing that siRNA knockdown of ARPC5 leads to an increase in expression of ARPC5L. This apparent compensation of isoform expression points at diversity in function of the two paralogues despite their sequence homology.

In my work to characterise endogenous ARPC5 and ARPC5L I initially used Hela cells, human cervical carcinoma cells, because they are convenient to

use and easy to transfect in comparison to the MCL cell line I used in this thesis (MAVER-1 cells). Thus, the technical difficulties in tagging endogenous ARPC5 isoforms via CRISPER in MAVER-1 cells limited my observations of endogenous protein in those cells. Nevertheless, overexpression of either isoform in MAVER-1 cells was achieved successfully, and this allowed me to see different patterns of ARPC5 and ARPC5L distribution in the cell membrane during BCR signaling observed that ARPC5L becomes spread across the membrane in MAVER-1 cells responding to BCR engagement, and this allows the hypothesis that ARPC5L selectively could be required for BCR signaling stabilisation by contributing to the formation of central BCR clusters, required for signaling propitiation [70]. This is an attractive hypothesis that further supports isoforms functional variation in BCR signaling ARPC5 expression is downregulated is not a result of changes in gene transcriptions because q-PCR analysis of ARPC5 mRNA shows no change during BCR signaling. Because of experimental difficulties, I could not confirm that ARPC5 down-regulation after BCR stimulation due to higher protein degradation because of technical difficulties with the assay, but the evidence I present of the faster turnover of ARPC5 compared with ARPC5L observed in this study suggests this possibility. This suggestion is supported by studies of ARPC5 degradation in T lymphocyte cells [194]. Here ARPC5 is subjected to degradation in order to maintain the anergic state in T cells. The anergic state is crucial to keep the peripheral tolerance and avoid autoimmunity, this study indicated that ARPC5 becomes ubiquitinated by GRAIL (genes

related to anergy in lymphocytes), a family of E3 ubiquitin ligases that are required to sustain anergy in T cells. Downregulation of ARPC5 leads to less localisation of this isoform within immune synapse formed by T cells, and that greatly affects the responsive state of these T cells [194].

These findings collectively support the notion that BCR signaling, by maintaining the ARPC5L levels could exploit this paralogue for its distinct properties within the Arp2/3 complex. Arp2/3complexes containing ARPC5L are more efficient in promoting actin polymerisation than those containing ARPC5 and cortactin preferentially stabilises the complexes containing ARPC5L over complexes containing ARPC5 against coronin-mediating actin depolymerisation [97]. This may be particularly relevant in CLL where high levels of cortactin and its paralogue HS1 in malignant cells correlate to poor outcomes in this disease [195]. Importantly, both cortactin and HS1 are key substrates of Lyn in the signaling pathway induced by BCR [196].

Several lines of evidence support the concept that CLL and MCL are greatly dependent on BCR. Understanding the mechanism in which BCR signaling works may provide a clear insight into the pathogenesis of CLL and MCL [197, 198]. As actin cytoskeletal proteins, the Arp2/3 complex plays a role in the regulation of actin polymerisation [199], and subsequently controlling BCR signaling [82]. Thus, it is important to understand how Arp2/3 proteins subunits including ARPC5 and ARPC5L with their divergent properties affect BCR signaling. As shown in chapter 4, the functional role of ARPC5/L isoform specificity is not determined in BCR signaling. Knockdown of either

paralogue had no discernable effect on either BCR internalisation and MAVER-1 cells spreading, or on BCR induced signaling (ie intracellular Ca^{2+} flux and phosphorylation of BCR pathway mediators). However, using a unique assay of adhesion-free migration, I showed that these paralogues are required for B cell migration. The speed of MAVER-1 cell movement in the system I used is significantly reduced with siRNA depletion of either paralogue. However, the reduction of ARPC5L seemed to have a greater effect than the reduction of ARPC5. These results indicate the requirement of MAVER-1 cells for Arp2/3 complex generally and for ARPC5 paralogues specifically for actin dynamics that allow B cells to migrate. I found that BCR engagement inhibits MAVER-1 cell migration in my system, and the siRNA-mediated knockdown of ARPC5/ARPC5L seems to not have any effect on this phenomenon. This shows that although ARPC5 and ARPC5L play roles in B cell migration, they do not seem to mediate BCR arrest of migration. The contact of anti-IgM with BCR seems to control the migration of those cells regardless of the expression of the isoforms indicating the strong influence of BCR signaling on MAVER-1 cell migration.

The ability of MAVER-1 cells to adhere to the adhesion ligends (FN-VCAM-1) was also tested. MAVER-1 cells highly express α4β1 integrin and the majority of cell adhesion occurs through this receptor/integrin. The stimulation of this receptor-mediated cell adhesion occurs by either directly binding to its legend (outside-in signaling) or through BCR stimulation-induced α4β1 activation make it ready to bind to its ligends (inside-out signaling) [181]. Either mechanism of α4β1integrin activation involves the

cytoskeleton, but I found no contribution of ARPC5/L isoform specificity to MAVER-1 cell adhesion capability through this integrin regardless of how it was activated.

Although my experiments did not show ARPC5/L involvement with BCR internalisation, this does not rule out the role of these paralogues in antigen presentation to T cells that is necessary for the full activation of B cells which leads to their differentiation. Actin dynamics are required in multiple steps of the BCR signaling pathway [179], and the Arp2/3 complex plays a role in this signaling and B cells response [49, 82]. The findings, shown in chapter three suggest the need for further investigation in ARPC5 and ARPC5L function in the multiple signaling steps of BCR signaling, and this includes antigen presentation.

In general manners, ARPC5/L functionality within the indicated steps in the signaling pathway was not elucidated due to certain limitations. For example, depletion of either ARPC5/L isoform levels does not alter surface receptor's stability presumably BCR induction is also needed which could provide a clearer picture of paralogue contribution. A limitation of my study is that BCR stimulation mediated BCR internalisation was performed on a plastic surface which is considered a stiff surface. A study has shown that Arp2/3 activity is critical for the uptake of antigens only from soft substrates, such as plasma membrane sheets (PMSs), which promote mechanical antigen extraction similar to that occurring with live antigen-presenting cells [49]. However, testing the paralogue functionality in this thesis in a given

experimental environment confidently excludes their contribution in BCR signaling and opens the way to test their functionality in another possible context. One of the inherent limitations of my experimental design was the use of only one cell line of MCL. A study in our lab (unpublished data) shows kinases upregulation and downregulation differences between MAVER-1 cells and Jeko-1 cells line as a result of anti-IgM stimulation. These differences could affect the cytoskeleton dynamic and could participate in determining the role of ARPC5/L in BCR signaling globally in MCL and CLL.

For the future work, it could be interesting to investigate the importance of ARPC5 isoform interaction with other Arp2/3 complexes in BCR signaling, or generally in B cell activation. A study has shown that mutation within the ARPC1 binding site to ARPC5 results in unregulated nucleation activity of the Arp2/3 complex when WASp is not present. This observation may indicate the necessity of proper physical contact of ARPC1 with ARPC5 as ARPC5 functions, by keeping ARPC1 less active to hold the Arp2/3 complex in an inactive state, suppressing spontaneous nucleation activity until WASp activity is induced to trigger a conformational change within the Arp2/3 complex [200]. Thus, it is worth testing whether this contact site between ARPC1 and ARPC5 is crucial to prevent spontaneous actin nucleation by Arp2/3 complex in B cell and how it could manipulate BCR signaling by affecting Arp2/3 complex nucleation activity.

Since the single isoforms knockdown did not determine the functional differences in BCR signaling, the need for the double ARPC5/L depletion as

an effective positive control has become apparent. That double paralogue depletion may clearly explain if both isoforms are collaborating, or if they are functionally distinct in BCR signaling. A study of Arp2/3 complex partial subunits expression shows that ARPC5 (without isoform specification) functionality is important for the complex nucleation activity and the expression/stability of other Arp2/3 complex protein ARPC1. The same study excludes ARPC5 contribution in maintaining the structural integrity of the complex and branch actin formation [115]. Thus, this observation suggests that the Arp2/3 complex remains intact with ARPC5 paralogues depletion which supports the notion of the double ARPC5/L depletion and makes it feasible. Thus, these limitations can be exploited and taken into consideration for future work.

As mentioned earlier the HS1, a homolog of cortactin is highly expressed in CLL and cortactin selectively stabilise ARPC5L to maintain the long actin filament generated by Arp2/3 complex containing ARPC5L but not ARPC5. It worth to test if the functionality of HS1 is similar to cortactin in relation to ARPC5L. Moreover, actin cytoskeleton influences cell stiffness that could greatly affect it’s function. A study has shown that CLL cells have higher stiffness when compared with cells from healthy individuals [201]. This work could be further investigated to explore the effectiveness of ARPC5 paralogues as actin relating proteins on CLL/MCL cells stiffness and whether this biophysical alteration is correlated with the clinical symptoms of CLL and MCL and diseases outcomes.

In conclusion, in this thesis, I characterised the expression and the distribution of the ARPC5 isoforms in a B cell line which show the controlling ability of BCR signaling on the cytoskeleton dynamic and supports the link between them. These novel observations led me to further investigate their functional role in BCR signaling since the BCR signaling pathway actively contributes to the pathogenesis of CLL and MCL and ARPC5/L as actin rearrangement proteins could affect this pathway. The potential specifc mechanism of action of ARPC5 isoforms was not revealed by the experiments performed in this study, however, the isoform-specific differences we did find provide the groundwork for further exploration of Arp2/3-controlled cytoskeletal events in B cells to give further information on the pathophysiology of MCL and CLL cells.

Appendix

Supplementary figures

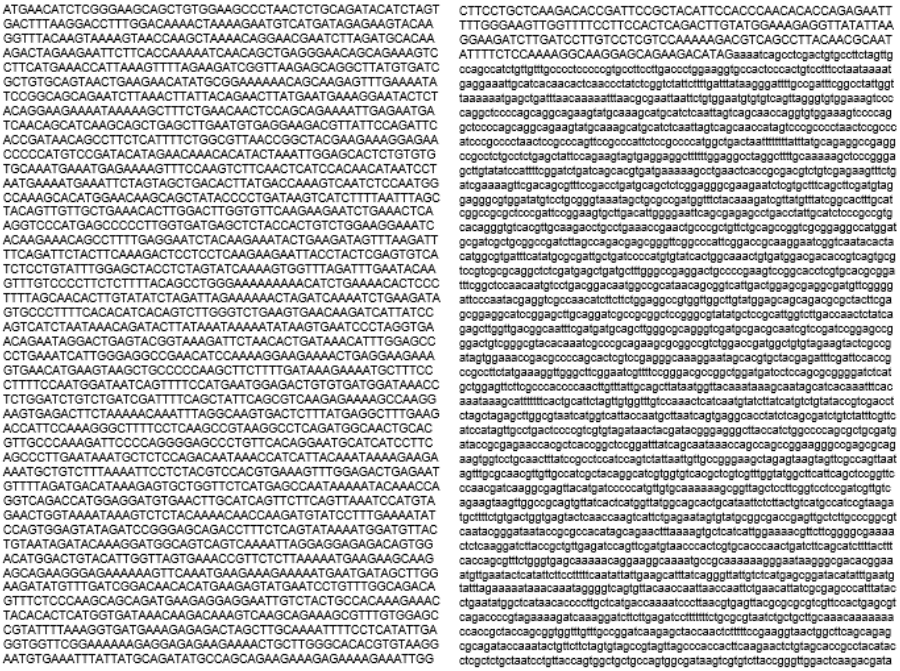

A1:CtIP vector sequence. The vector is used as a strong enhancer for (MMEJ) in tagging ARPC5/L.

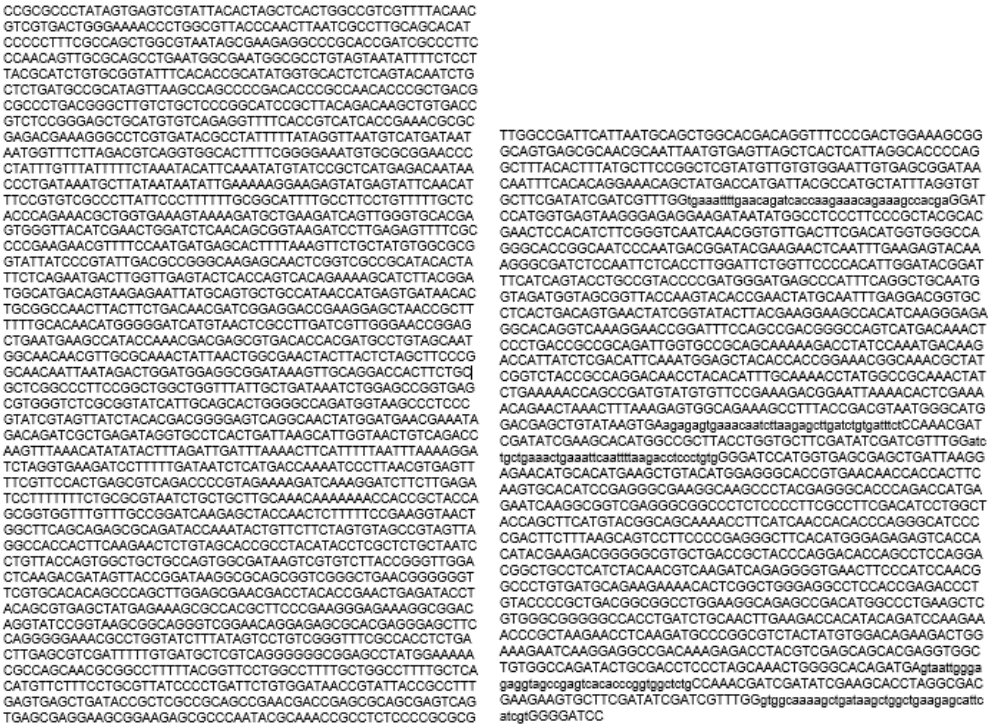

A2: PITCh donor vector (CANX-mNeonGreen, PARP1-mKate2) vector sequence. The vector is used to tag ARPC5/L.

ARPC5 locus

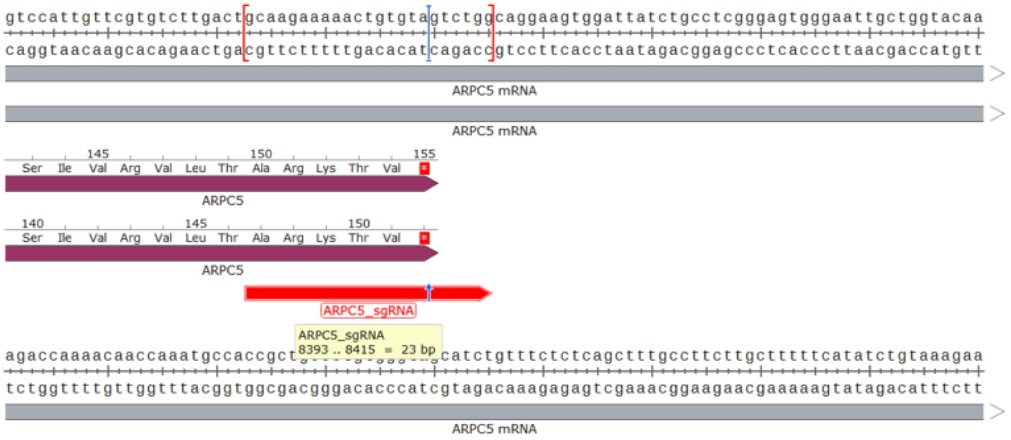

Top 3 potential off-target sites (analyzed by COSMID)

Result	Query tag	Search result	Query type	Mismatch	Ends with RG	Chr Position	Strand	Cut site	Score
ACAAAAAAGACTGTGTAGTCGGG -- hit GCAAGAAAAACTGTGTAGTCNGG -- query	Query: GCAAGAAAAACTGTGTAGTCNGG	hit: ACAAAAAAGACTGTGTAGTCGGG	No indel	3	Yes	Chr7:2576698- 2576720	-	2576704	0.66
GAAATAAAAAATGTGTAGTCAGG -- hit GCAAGAAAAACTGTGTAGTCNGG -- query	Query: GCAAGAAAAACTGTGTAGTCNGG	hit: GAAATAAAAAATGTGTAGTCAGG	No indel	3	Yes	Chr12:95819167- 95819189	-	95819173	1.02
GCAGGGAAACTGTGTAGTCAGG -- hit GCAGAAAAACTGTGTAGTCNGG -- query	Query: GCAGAAAAACTGTGTAGTCNGG	hit: GCAGGGAAACTGTGTAGTCAGG	Del 17, or Del 18	2	Yes	Chr3:42290564- 42290585	-	42290570	1.1

ARPC5L locus

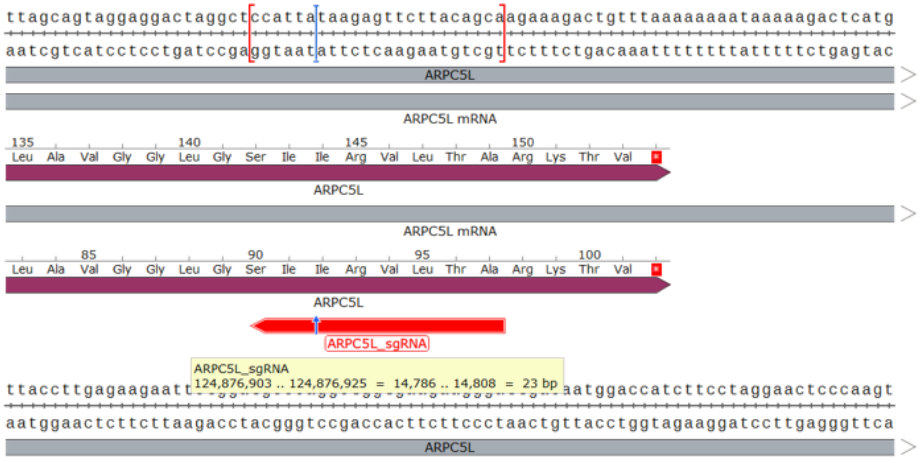

Top 3 potential off-target sites (analyzed by COSMID)

Result	Query tag	Search result	Query type	Mismatch	Ends with RG	Chr Position	Strand	Cut site	Score
TACTTTAAGAAGTCTTATAATGG -- hit TGCTGTAAGAACTCTTATAANGG -- query	Query: TGCTGTAAGAACTCTTATAANGG	hit: TACTTTAAGAAGTCTTATAATGG	No indel	3	Yes	Chr2:32735115- 32735137	-	32735121	1.12
TCTGAAAGTACTCTTATAAAGG -- hit TCTGTAAGAACTCTTATAANGG -- query	Query: TCTGTAAGAACTCTTATAANGG	hit: TCTGAAAGTACTCTTATAAAGG	Del 19	2	Yes	Chr3:54383200- 54383221	-	54383206	1.35
TGCTTTAGGAATCTTATAATGG -- hit TGCTGTAAGAATCTTATAANGG -- query	Query: TGCTGTAAGAATCTTATAANGG	hit: TGCTTTAGGAATCTTATAATGG	Del 9	2	Yes	Chr12:32562267- 32562288	-	32562273	1.77

A3: ARPC5/L gene locus targeted by sgRNA and Cas9.

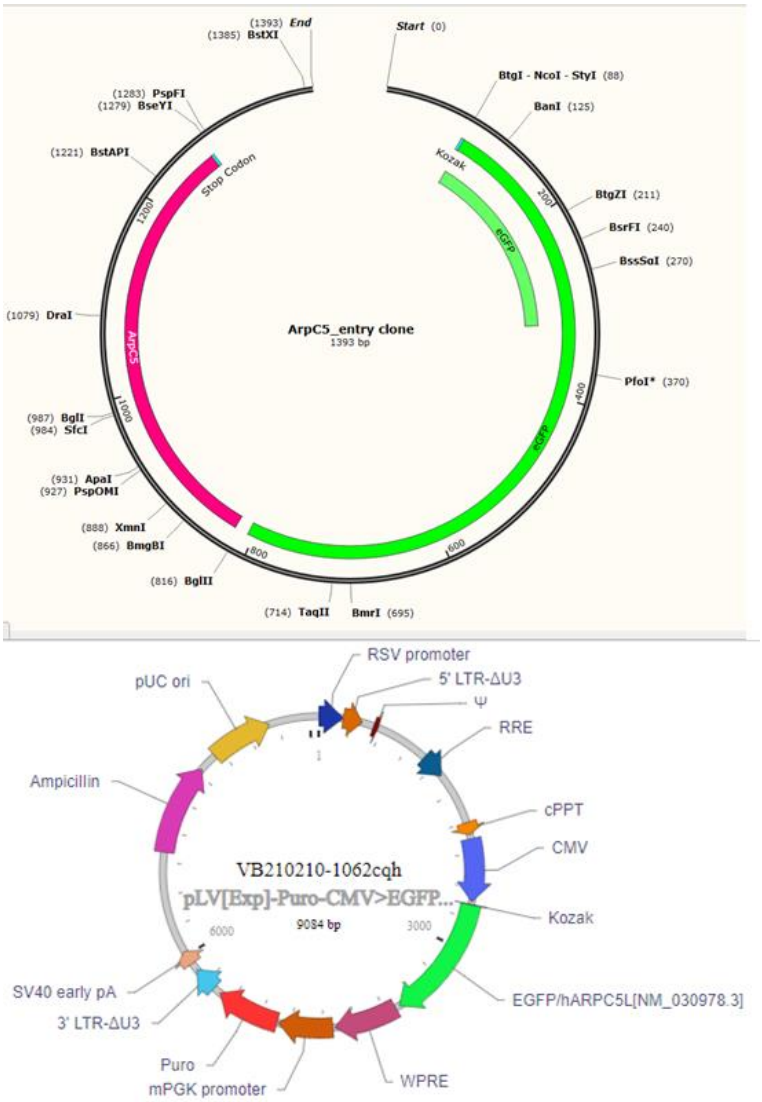

A4: ARPC5/L plasmid map for ARPC5/L overexpression.

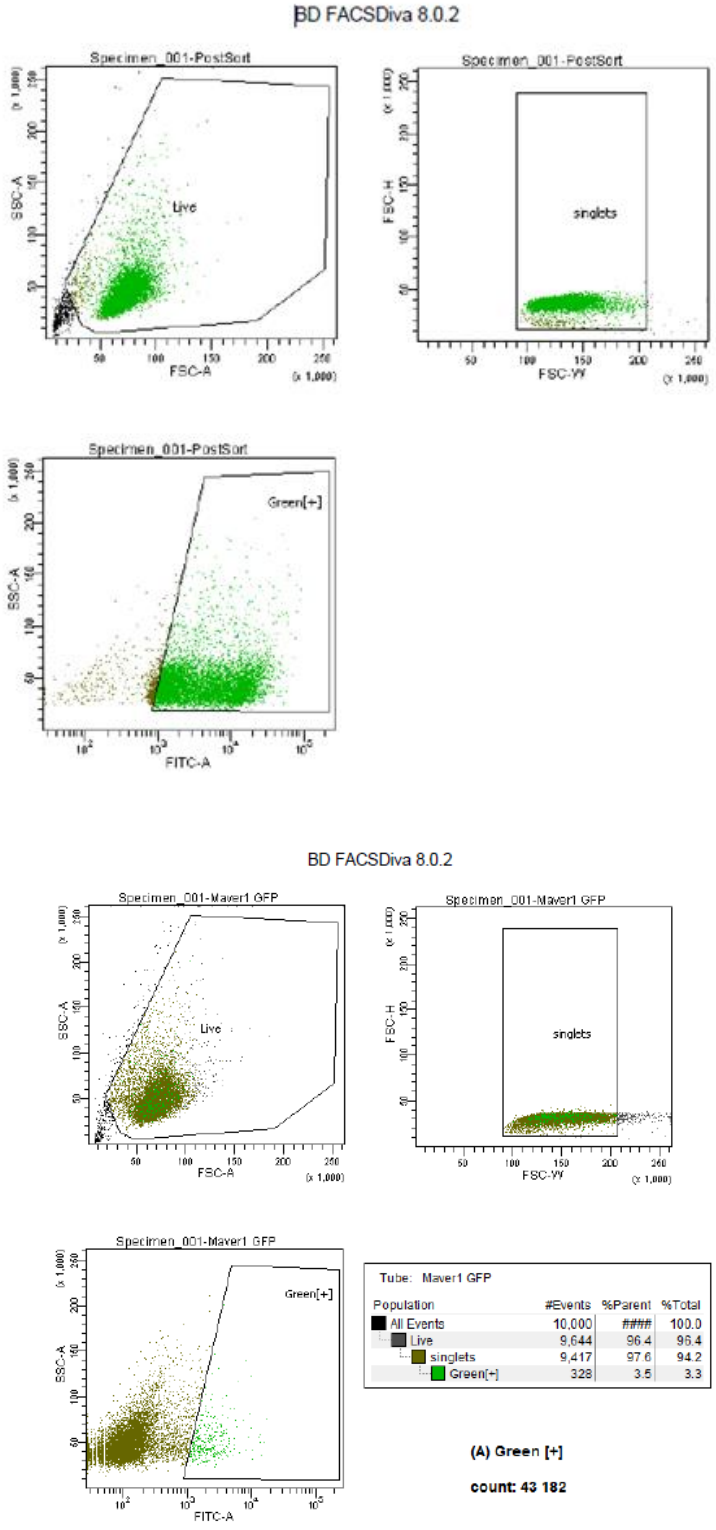

A5: Snapshot of MAVER-1 cells sorting using FACS Aria II. A) MAVER-1 cells sorted for ARPC5 overexpression accompanied with GFP. B) MAVER-1 cells sorted for ARPC5L overexpression accompanied with GFP.

Bibliography

1. Vieira, P. and A. Cumano, *Differentiation of B Lymphocytes From Hematopoietic Stem Cells*, in *B Cell Protocols*, H. Gu and K. Rajewsky, Editors. 2004, Humana Press: Totowa, NJ. p. 67-76.
2. Orkin, S.H. and L.I. Zon, *Hematopoiesis: an evolving paradigm for stem cell biology.* Cell, 2008. **132**(4): p. 631-644.
3. Benlagha, K., et al., *Modifications of Igα and Igβ Expression as a Function of B Lineage Differentiation.* Journal of Biological Chemistry, 1999. **274**(27): p. 19389-19396.
4. Schroeder, H.W. and L. Cavacini, *Structure and function of immunoglobulins.* The Journal of allergy and clinical immunology, 2010. **125**(2 Suppl 2): p. S41-52.
5. Melchers, F., *The pre-B-cell receptor: selector of fitting immunoglobulin heavy chains for the B-cell repertoire.* Nature Reviews Immunology, 2005. **5**(7): p. 578-584.
6. Wu, Y.-C., D. Kipling, and D. Dunn-Walters, *Assessment of B Cell Repertoire in Humans*, in *Immunosenescence: Methods and Protocols*, A.C. Shaw, Editor. 2015, Springer New York: New York, NY. p. 199-218.
7. Nemazee, D., *Mechanisms of central tolerance for B cells.* Nature reviews. Immunology, 2017. **17**(5): p. 281-294.
8. Sandel, P.C. and J.G. Monroe, *Negative Selection of Immature B Cells by Receptor Editing or Deletion Is Determined by Site of Antigen Encounter.* Immunity, 1999. **10**(3): p. 289-299.
9. Nossal, G.J. and B.L. Pike, *Clonal anergy: persistence in tolerant mice of antigen-binding B lymphocytes incapable of responding to antigen or mitogen.* Proceedings of the National Academy of Sciences of the United States of America, 1980. **77**(3): p. 1602-1606.
10. Cariappa, A., et al., *Naive recirculating B cells mature simultaneously in the spleen and bone marrow.* Blood, 2006. **109**(6): p. 2339-2345.
11. Martin, V.G., et al., *Transitional B Cells in Early Human B Cell Development - Time to Revisit the Paradigm?* Frontiers in immunology, 2016. **7**: p. 546-546.
12. Rothstein, T.L., et al., *Human B-1 cells take the stage.* Annals of the New York Academy of Sciences, 2013. **1285**: p. 97-114.
13. Cambier, J.C., et al., *B-cell anergy: from transgenic models to naturally occurring anergic B cells?* Nature reviews. Immunology, 2007. **7**(8): p. 633-643.
14. Zenz, T., et al., *From pathogenesis to treatment of chronic lymphocytic leukaemia.* Nature Reviews Cancer, 2010. **10**(1): p. 37-50.
15. Liu, Y.-J. and J. Banchereau, *Regulation of B-cell commitment to plasma cells or to memory B cells.* Seminars in Immunology, 1997. **9**(4): p. 235-240.
16. Fulcher, D. and A. Basten, *B cell life span: A review.* Immunology & Cell Biology, 1997. **75**(5): p. 446-455.
17. *Chapter 5 - B Cell Development, Activation and Effector Functions*, in *Primer to the Immune Response (Second Edition)*, T.W. Mak, M.E. Saunders, and B.D. Jett, Editors. 2014, Academic Cell: Boston. p. 111-142.
18. Corcos, D., M.J. Osborn, and L.S. Matheson, *B-cell receptors and heavy chain diseases: guilty by association?* Blood, 2011. **117**(26): p. 6991-6998.
19. Taher, T.E., et al., *Intracellular B Lymphocyte Signalling and the Regulation of Humoral Immunity and Autoimmunity.* Clinical reviews in allergy & immunology, 2017. **53**(2): p. 237-264.

20. Seda, V. and M. Mraz, *B-cell receptor signalling and its crosstalk with other pathways in normal and malignant cells.* European Journal of Haematology, 2015. **94**(3): p. 193-205.
21. Zhang, J., et al., *Phosphorylation of Syk Activation Loop Tyrosines Is Essential for Syk Function: AN IN VIVO STUDY USING A SPECIFIC ANTI-Syk ACTIVATION LOOP PHOSPHOTYROSINE ANTIBODY.* Journal of Biological Chemistry, 2000. **275**(45): p. 35442-35447.
22. Katagiri, T., et al., *Selective Regulation of Lyn Tyrosine Kinase by CD45 in Immature B Cells (*).* Journal of Biological Chemistry, 1995. **270**(47): p. 27987-27990.
23. Puente, X.S., et al., *Non-coding recurrent mutations in chronic lymphocytic leukaemia.* Nature, 2015. **526**(7574): p. 519-524.
24. Barua, D., W.S. Hlavacek, and T. Lipniacki, *A computational model for early events in B cell antigen receptor signaling: analysis of the roles of Lyn and Fyn.* Journal of immunology (Baltimore, Md. : 1950), 2012. **189**(2): p. 646-658.
25. Woyach, J.A., A.J. Johnson, and J.C. Byrd, *The B-cell receptor signaling pathway as a therapeutic target in CLL.* Blood, 2012. **120**(6): p. 1175-1184.
26. Ishiura, N., et al., *Differential phosphorylation of functional tyrosines in CD19 modulates B-lymphocyte activation.* European Journal of Immunology, 2010. **40**(4): p. 1192-1204.
27. Deane, J.A. and D.A. Fruman, *Phosphoinositide 3-Kinase: Diverse Roles in Immune Cell Activation.* Annual Review of Immunology, 2004. **22**(1): p. 563-598.
28. Verkoczy, L., et al., *Basal B Cell Receptor-Directed Phosphatidylinositol 3-Kinase Signaling Turns Off RAGs and Promotes B Cell-Positive Selection.* The Journal of Immunology, 2007. **178**(10): p. 6332-6341.
29. Chiu, C.W., et al., *BLNK: molecular scaffolding through 'cis'-mediated organization of signaling proteins.* The EMBO journal, 2002. **21**(23): p. 6461-6472.
30. Hong, J.J., et al., *Regulation of Signaling in B Cells through the Phosphorylation of Syk on Linker Region Tyrosines: A MECHANISM FOR NEGATIVE SIGNALING BY THE Lyn TYROSINE KINASE.* Journal of Biological Chemistry, 2002. **277**(35): p. 31703-31714.
31. Kim, Y.J., et al., *Mechanism of B-cell receptor-induced phosphorylation and activation of phospholipase C-gamma2.* Molecular and cellular biology, 2004. **24**(22): p. 9986-9999.
32. Smrcka, A.V., *Regulation of phosphatidylinositol-specific phospholipase C at the nuclear envelope in cardiac myocytes.* Journal of cardiovascular pharmacology, 2015. **65**(3): p. 203-210.
33. Spitaler, M. and D.A. Cantrell, *Protein kinase C and beyond.* Nature Immunology, 2004. **5**(8): p. 785-790.
34. Teixeira, C., et al., *Integration of DAG signaling systems mediated by PKC-dependent phosphorylation of RasGRP3.* Blood, 2003. **102**(4): p. 1414-1420.
35. Aiba, Y., et al., *Activation of RasGRP3 by phosphorylation of Thr-133 is required for B cell receptor-mediated Ras activation.* Proceedings of the National Academy of Sciences of the United States of America, 2004. **101**(47): p. 16612-16617.
36. McCormick, F., *How receptors turn Ras on.* Nature, 1993. **363**(6424): p. 15-16.
37. Richards, J.D., et al., *Inhibition of the MEK/ERK Signaling Pathway Blocks a Subset of B Cell Responses to Antigen.* The Journal of Immunology, 2001. **166**(6): p. 3855-3864.

38. McCubrey, J.A., et al., *Differential abilities of activated Raf oncoproteins to abrogate cytokine dependency, prevent apoptosis and induce autocrine growth factor synthesis in human hematopoietic cells.* Leukemia, 1998. **12**(12): p. 1903-1929.
39. Weinstein-Oppenheimer, C.R., et al., *The Raf signal transduction cascade as a target for chemotherapeutic intervention in growth factor-responsive tumors.* Pharmacology & Therapeutics, 2000. **88**(3): p. 229-279.
40. Fruman, D. and J. Limon, *Akt and mTOR in B Cell Activation and Differentiation.* Frontiers in Immunology, 2012. **3**(228).
41. Limon, J.J. and D.A. Fruman, *Akt and mTOR in B Cell Activation and Differentiation.* Frontiers in immunology, 2012. **3**: p. 228-228.
42. Oppezzo, P. and G. Dighiero, *"Role of the B-cell receptor and the microenvironment in chronic lymphocytic leukemia''.* Blood Cancer Journal, 2013. **3**(9): p. e149-e149.
43. Wurzer, H., et al., *Actin Cytoskeleton Straddling the Immunological Synapse between Cytotoxic Lymphocytes and Cancer Cells.* Cells, 2019. **8**(5): p. 463.
44. Tse, K.W.K., et al., *B cell receptor-induced phosphorylation of Pyk2 and focal adhesion kinase involves integrins and the Rap GTPases and is required for B cell spreading.* The Journal of biological chemistry, 2009. **284**(34): p. 22865-22877.
45. Hou, P., et al., *B cell antigen receptor signaling and internalization are mutually exclusive events.* PLoS biology, 2006. **4**(7): p. e200-e200.
46. Jang, C., S. Machtaler, and L. Matsuuchi, *The role of Ig-α/β in B cell antigen receptor internalization.* Immunology Letters, 2010. **134**(1): p. 75-82.
47. Avalos, A.M. and H.L. Ploegh, *Early BCR Events and Antigen Capture, Processing, and Loading on MHC Class II on B Cells.* Frontiers in immunology, 2014. **5**: p. 92-92.
48. Stoddart, A., A.P. Jackson, and F.M. Brodsky, *Plasticity of B Cell Receptor Internalization upon Conditional Depletion of Clathrin.* Molecular Biology of the Cell, 2005. **16**(5): p. 2339-2348.
49. Roper, S.I., et al., *B cells extract antigens at Arp2/3-generated actin foci interspersed with linear filaments.* eLife, 2019. **8**: p. e48093.
50. Malhotra, S., et al., *B cell antigen receptor endocytosis and antigen presentation to T cells require Vav and dynamin.* The Journal of biological chemistry, 2009. **284**(36): p. 24088-24097.
51. Gardell, J.L. and D.C. Parker, *CD40L is transferred to antigen-presenting B cells during delivery of T-cell help.* European journal of immunology, 2017. **47**(1): p. 41-50.
52. Fletcher, D.A. and R.D. Mullins, *Cell mechanics and the cytoskeleton.* Nature, 2010. **463**(7280): p. 485-492.
53. Shekhar, S., J. Pernier, and M.-F. Carlier, *Regulators of actin filament barbed ends at a glance.* Journal of Cell Science, 2016. **129**(6): p. 1085-1091.
54. Narita, A., T. Oda, and Y. Maéda, *Structural basis for the slow dynamics of the actin filament pointed end.* The EMBO journal, 2011. **30**(7): p. 1230-1237.
55. Lee, S.H. and R. Dominguez, *Regulation of actin cytoskeleton dynamics in cells.* Molecules and cells, 2010. **29**(4): p. 311-325.
56. Goode, B.L. and M.J. Eck, *Mechanism and Function of Formins in the Control of Actin Assembly.* Annual Review of Biochemistry, 2007. **76**(1): p. 593-627.
57. Sharma, S., G. Orlowski, and W. Song, *Btk Regulates B Cell Receptor-Mediated Antigen Processing and Presentation by Controlling Actin Cytoskeleton Dynamics in B Cells.* The Journal of Immunology, 2009. **182**(1): p. 329-339.

58. Li, J., et al., *The Coordination Between B Cell Receptor Signaling and the Actin Cytoskeleton During B Cell Activation.* Frontiers in Immunology, 2019. **9**(3096).
59. Baeker, T.R., E.R. Simons, and T.L. Rothstein, *Cytochalasin induces an increase in cytosolic free calcium in murine B lymphocytes.* The Journal of Immunology, 1987. **138**(8): p. 2691-2697.
60. Hao, S. and A. August, *Actin depolymerization transduces the strength of B-cell receptor stimulation.* Molecular biology of the cell, 2005. **16**(5): p. 2275-2284.
61. Neisch, A.L. and R.G. Fehon, *Ezrin, Radixin and Moesin: key regulators of membrane-cortex interactions and signaling.* Current opinion in cell biology, 2011. **23**(4): p. 377-382.
62. Itoh, K., et al., *Cutting Edge: Negative Regulation of Immune Synapse Formation by Anchoring Lipid Raft to Cytoskeleton Through Cbp-EBP50-ERM Assembly.* The Journal of Immunology, 2002. **168**(2): p. 541-544.
63. Treanor, B., et al., *The membrane skeleton controls diffusion dynamics and signaling through the B cell receptor.* Immunity, 2010. **32**(2): p. 187-199.
64. Treanor, B., et al., *Dynamic cortical actin remodeling by ERM proteins controls BCR microcluster organization and integrity.* The Journal of experimental medicine, 2011. **208**(5): p. 1055-1068.
65. Yasuda, S., et al., *A model integrating tonic and antigen-triggered BCR signals to predict the survival of primary B cells.* Scientific Reports, 2017. **7**(1): p. 14888.
66. Gupta, N., et al., *Quantitative proteomic analysis of B cell lipid rafts reveals that ezrin regulates antigen receptor–mediated lipid raft dynamics.* Nature Immunology, 2006. **7**(6): p. 625-633.
67. Harwood, N.E. and F.D. Batista, *Early Events in B Cell Activation.* Annual Review of Immunology, 2010. **28**(1): p. 185-210.
68. Freeman, S.A., et al., *Cofilin-Mediated F-Actin Severing Is Regulated by the Rap GTPase and Controls the Cytoskeletal Dynamics That Drive Lymphocyte Spreading and BCR Microcluster Formation.* The Journal of Immunology, 2011. **187**(11): p. 5887-5900.
69. Fleire, S.J., et al., *B Cell Ligand Discrimination Through a Spreading and Contraction Response.* Science, 2006. **312**(5774): p. 738-741.
70. Liu, C., et al., *Actin reorganization is required for the formation of polarized B cell receptor signalosomes in response to both soluble and membrane-associated antigens.* Journal of immunology (Baltimore, Md. : 1950), 2012. **188**(7): p. 3237-3246.
71. Song, W., C. Liu, and A. Upadhyaya, *The pivotal position of the actin cytoskeleton in the initiation and regulation of B cell receptor activation.* Biochimica et Biophysica Acta (BBA) - Biomembranes, 2014. **1838**(2): p. 569-578.
72. Freeman, S.A., et al., *Toll-like receptor ligands sensitize B-cell receptor signalling by reducing actin-dependent spatial confinement of the receptor.* Nature Communications, 2015. **6**(1): p. 6168.
73. Dyche Mullins, R. and T.D. Pollard, *Structure and function of the Arp2/3 complex.* Current Opinion in Structural Biology, 1999. **9**(2): p. 244-249.
74. Welch, M.D., et al., *The human Arp2/3 complex is composed of evolutionarily conserved subunits and is localized to cellular regions of dynamic actin filament assembly.* The Journal of cell biology, 1997. **138**(2): p. 375-384.
75. Cifrová, P., et al., *Division of Labor Between Two Actin Nucleators—the Formin FH1 and the ARP2/3 Complex—in Arabidopsis Epidermal Cell Morphogenesis.* Frontiers in Plant Science, 2020. **11**(148).

76. Blanchoin, L., et al., *Direct observation of dendritic actin filament networks nucleated by Arp2/3 complex and WASP/Scar proteins.* Nature, 2000. **404**(6781): p. 1007-1011.
77. Goley, E.D., et al., *Critical Conformational Changes in the Arp2/3 Complex Are Induced by Nucleotide and Nucleation Promoting Factor.* Molecular Cell, 2004. **16**(2): p. 269-279.
78. Park, H., D. Ishihara, and D. Cox, *Regulation of tyrosine phosphorylation in macrophage phagocytosis and chemotaxis.* Archives of biochemistry and biophysics, 2011. **510**(2): p. 101-111.
79. Abe, K., et al., *Vav2 Is an Activator of Cdc42, Rac1, and RhoA.* Journal of Biological Chemistry, 2000. **275**(14): p. 10141-10149.
80. Guinamard, R., et al., *Tyrosine phosphorylation of the Wiskott-Aldrich Syndrome protein by Lyn and Btk is regulated by CDC42.* FEBS Letters, 1998. **434**(3): p. 431-436.
81. Kelly, A.E., et al., *Actin binding to the central domain of WASP/Scar proteins plays a critical role in the activation of the Arp2/3 complex.* The Journal of biological chemistry, 2006. **281**(15): p. 10589-10597.
82. Bolger-Munro, M., et al., *Arp2/3 complex-driven spatial patterning of the BCR enhances immune synapse formation, BCR signaling and B cell activation.* eLife, 2019. **8**: p. e44574.
83. Smith, B.A., et al., *Pathway of actin filament branch formation by Arp2/3 complex revealed by single-molecule imaging.* Proceedings of the National Academy of Sciences, 2013. **110**(4): p. 1285-1290.
84. Pollard, T.D., *Regulation of Actin Filament Assembly by Arp2/3 Complex and Formins.* Annual Review of Biophysics and Biomolecular Structure, 2007. **36**(1): p. 451-477.
85. Tolar, P., *Cytoskeletal control of B cell responses to antigens.* Nature Reviews Immunology, 2017. **17**(10): p. 621-634.
86. Jain, N. and T. Thanabalu, *Molecular difference between WASP and N-WASP critical for chemotaxis of T-cells towards SDF-1α.* Scientific Reports, 2015. **5**(1): p. 15031.
87. Sharma, S., G. Orlowski, and W. Song, *Btk regulates B cell receptor-mediated antigen processing and presentation by controlling actin cytoskeleton dynamics in B cells.* Journal of immunology (Baltimore, Md. : 1950), 2009. **182**(1): p. 329-339.
88. Padrick, S.B. and M.K. Rosen, *Physical Mechanisms of Signal Integration by WASP Family Proteins.* Annual Review of Biochemistry, 2010. **79**(1): p. 707-735.
89. Benesch, S., et al., *Phosphatidylinositol 4,5-Biphosphate (PIP2)-induced Vesicle Movement Depends on N-WASP and Involves Nck, WIP, and Grb2.* Journal of Biological Chemistry, 2002. **277**(40): p. 37771-37776.
90. Park, H., M.M. Chan, and B.M. Iritani, *Hem-1: Putting the "WAVE" into actin polymerization during an immune response.* FEBS Letters, 2010. **584**(24): p. 4923-4932.
91. Uruno, T., et al., *Activation of Arp2/3 complex-mediated actin polymerization by cortactin.* Nature Cell Biology, 2001. **3**(3): p. 259-266.
92. Wu, H. and J.T. Parsons, *Cortactin, an 80/85-kilodalton pp60src substrate, is a filamentous actin-binding protein enriched in the cell cortex.* The Journal of cell biology, 1993. **120**(6): p. 1417-1426.
93. Kirkbride, K.C., et al., *Cortactin: a multifunctional regulator of cellular invasiveness.* Cell adhesion & migration, 2011. **5**(2): p. 187-198.

94. Helgeson, L.A. and B.J. Nolen, *Mechanism of synergistic activation of Arp2/3 complex by cortactin and N-WASP.* eLife, 2013. **2**: p. e00884-e00884.
95. Weaver, A.M., et al., *Cortactin promotes and stabilizes Arp2/3-induced actin filament network formation.* Curr Biol, 2001. **11**(5): p. 370-4.
96. Cai, L., et al., *Coronin 1B Antagonizes Cortactin and Remodels Arp2/3-Containing Actin Branches in Lamellipodia.* Cell, 2008. **134**(5): p. 828-842.
97. Abella, J.V.G., et al., *Isoform diversity in the Arp2/3 complex determines actin filament dynamics.* Nature Cell Biology, 2016. **18**(1): p. 76-86.
98. Goley, E.D. and M.D. Welch, *The ARP2/3 complex: an actin nucleator comes of age.* Nature Reviews Molecular Cell Biology, 2006. **7**(10): p. 713-726.
99. Liu, C., et al., *N-wasp is essential for the negative regulation of B cell receptor signaling.* PLoS biology, 2013. **11**(11): p. e1001704-e1001704.
100. Castellanos-Martínez, R., K.E. Jiménez-Camacho, and M. Schnoor, *Cortactin Expression in Hematopoietic Cells: Implications for Hematological Malignancies.* The American Journal of Pathology, 2020. **190**(5): p. 958-967.
101. Padrick, S.B., et al., *Arp2/3 complex is bound and activated by two WASP proteins.* Proceedings of the National Academy of Sciences, 2011. **108**(33): p. E472-E479.
102. Cavnar, P.J., et al., *The actin regulatory protein HS1 interacts with Arp2/3 and mediates efficient neutrophil chemotaxis.* The Journal of biological chemistry, 2012. **287**(30): p. 25466-25477.
103. Frezzato, F., et al., *HS1, a Lyn kinase substrate, is abnormally expressed in B-chronic lymphocytic leukemia and correlates with response to fludarabine-based regimen.* PloS one, 2012. **7**(6): p. e39902-e39902.
104. Uruno, T., et al., *Haematopoietic lineage cell-specific protein 1 (HS1) promotes actin-related protein (Arp) 2/3 complex-mediated actin polymerization.* The Biochemical journal, 2003. **371**(Pt 2): p. 485-493.
105. Du, Y., et al., *Identification of a novel cortactin SH3 domain-binding protein and its localization to growth cones of cultured neurons.* Molecular and cellular biology, 1998. **18**(10): p. 5838-5851.
106. Hao, J.-J., et al., *The Coiled-coil Domain Is Required for HS1 to Bind to F-actin and Activate Arp2/3 Complex.* Journal of Biological Chemistry, 2005. **280**(45): p. 37988-37994.
107. Helgeson, L.A., et al., *Interactions with Actin Monomers, Actin Filaments, and Arp2/3 Complex Define the Roles of WASP Family Proteins and Cortactin in Coordinately Regulating Branched Actin Networks *.* Journal of Biological Chemistry, 2014. **289**(42): p. 28856-28869.
108. Bouma, G., S.O. Burns, and A.J. Thrasher, *Wiskott-Aldrich Syndrome: Immunodeficiency resulting from defective cell migration and impaired immunostimulatory activation.* Immunobiology, 2009. **214**(9-10): p. 778-790.
109. Dayel, M.J., E.A. Holleran, and R.D. Mullins, *Arp2/3 complex requires hydrolyzable ATP for nucleation of new actin filaments.* Proceedings of the National Academy of Sciences of the United States of America, 2001. **98**(26): p. 14871-14876.
110. Rodal, A.A., et al., *Conformational changes in the Arp2/3 complex leading to actin nucleation.* Nature Structural & Molecular Biology, 2005. **12**(1): p. 26-31.
111. Mullins, R.D., W.F. Stafford, and T.D. Pollard, *Structure, Subunit Topology, and Actin-binding Activity of the Arp2/3 Complex from Acanthamoeba.* Journal of Cell Biology, 1997. **136**(2): p. 331-343.

112. Robinson, R.C., et al., *Crystal Structure of Arp2/3 Complex.* Science, 2001. **294**(5547): p. 1679-1684.
113. Rouiller, I., et al., *The structural basis of actin filament branching by the Arp2/3 complex.* The Journal of cell biology, 2008. **180**(5): p. 887-895.
114. Randzavola, L.O., et al., *Loss of ARPC1B impairs cytotoxic T lymphocyte maintenance and cytolytic activity.* The Journal of Clinical Investigation, 2019. **129**(12): p. 5600-5614.
115. Gournier, H., et al., *Reconstitution of Human Arp2/3 Complex Reveals Critical Roles of Individual Subunits in Complex Structure and Activity.* Molecular Cell, 2001. **8**(5): p. 1041-1052.
116. Millard, T.H., et al., *Identification and characterisation of a novel human isoform of Arp2/3 complex subunit p16-ARC/ARPC5.* Cell Motility, 2003. **54**(1): p. 81-90.
117. Hoeller, S., et al., *Composite mantle cell lymphoma and chronic lymphocytic leukemia/small lymphocytic lymphoma: a clinicopathologic and molecular study.* Human pathology, 2013. **44**(1): p. 110-121.
118. Puente, X.S., P. Jares, and E. Campo, *Chronic lymphocytic leukemia and mantle cell lymphoma: crossroads of genetic and microenvironment interactions.* Blood, 2018. **131**(21): p. 2283-2296.
119. Seifert, M., et al., *Cellular origin and pathophysiology of chronic lymphocytic leukemia.* The Journal of experimental medicine, 2012. **209**(12): p. 2183-2198.
120. Damle, R.N., et al., *Ig V Gene Mutation Status and CD38 Expression As Novel Prognostic Indicators in Chronic Lymphocytic Leukemia: Presented in part at the 40th Annual Meeting of The American Society of Hematology, held in Miami Beach, FL, December 4-8, 1998.* Blood, 1999. **94**(6): p. 1840-1847.
121. Slotta-Huspenina, J., et al., *The impact of cyclin D1 mRNA isoforms, morphology and p53 in mantle cell lymphoma: p53 alterations and blastoid morphology are strong predictors of a high proliferation index.* Haematologica, 2012. **97**(9): p. 1422-1430.
122. Aubrey, B.J., et al., *How does p53 induce apoptosis and how does this relate to p53-mediated tumour suppression?* Cell Death & Differentiation, 2018. **25**(1): p. 104-113.
123. Fu, K., et al., *Cyclin D1-negative mantle cell lymphoma: a clinicopathologic study based on gene expression profiling.* Blood, 2005. **106**(13): p. 4315-4321.
124. Mozos, A., et al., *SOX11 expression is highly specific for mantle cell lymphoma and identifies the cyclin D1-negative subtype.* Haematologica, 2009. **94**(11): p. 1555-1562.
125. Hsiao, S.-C., et al., *SOX11 is useful in differentiating cyclin D1-positive diffuse large B-cell lymphoma from mantle cell lymphoma.* Histopathology, 2012. **61**(4): p. 685-693.
126. Vegliante, M.C., et al., *SOX11 regulates PAX5 expression and blocks terminal B-cell differentiation in aggressive mantle cell lymphoma.* Blood, 2013. **121**(12): p. 2175-2185.
127. Tellier, J., et al., *Blimp-1 controls plasma cell function through the regulation of immunoglobulin secretion and the unfolded protein response.* Nature immunology, 2016. **17**(3): p. 323-330.
128. Shapiro-Shelef, M. and K. Calame, *Regulation of plasma-cell development.* Nature Reviews Immunology, 2005. **5**(3): p. 230-242.
129. Puiggros, A., G. Blanco, and B. Espinet, *Genetic abnormalities in chronic lymphocytic leukemia: where we are and where we go.* BioMed research international, 2014. **2014**: p. 435983-435983.

130. Pekarsky, Y. and C.M. Croce, *Role of miR-15/16 in CLL.* Cell death and differentiation, 2015. **22**(1): p. 6-11.
131. Palamarchuk, A., et al., *13q14 deletions in CLL involve cooperating tumor suppressors.* Blood, 2010. **115**(19): p. 3916-3922.
132. Yu, G., et al., *APRIL and TALL-1 and receptors BCMA and TACI: system for regulating humoral immunity.* Nature Immunology, 2000. **1**(3): p. 252-256.
133. Burger, J.A. and J.G. Gribben, *The microenvironment in chronic lymphocytic leukemia (CLL) and other B cell malignancies: Insight into disease biology and new targeted therapies.* Seminars in Cancer Biology, 2014. **24**: p. 71-81.
134. Wang, C. and X. Wang, *The role of TP53 network in the pathogenesis of chronic lymphocytic leukemia.* International journal of clinical and experimental pathology, 2013. **6**(7): p. 1223-1229.
135. Mittal, A.K., et al., *Chronic lymphocytic leukemia cells in a lymph node microenvironment depict molecular signature associated with an aggressive disease.* Molecular medicine (Cambridge, Mass.), 2014. **20**(1): p. 290-301.
136. van Attekum, M.H.A., et al., *CD40 signaling instructs chronic lymphocytic leukemia cells to attract monocytes via the CCR2 axis.* Haematologica, 2017. **102**(12): p. 2069-2076.
137. van Attekum, M.H., E. Eldering, and A.P. Kater, *Chronic lymphocytic leukemia cells are active participants in microenvironmental cross-talk.* Haematologica, 2017. **102**(9): p. 1469-1476.
138. Buggins, A.G.S., et al., *Evidence for a macromolecular complex in poor prognosis CLL that contains CD38, CD49d, CD44 and MMP-9.* British Journal of Haematology, 2011. **154**(2): p. 216-222.
139. Packham, G. and F. Stevenson, *The role of the B-cell receptor in the pathogenesis of chronic lymphocytic leukaemia.* Seminars in Cancer Biology, 2010. **20**(6): p. 391-399.
140. Till, K.J., A.R. Pettitt, and J.R. Slupsky, *Expression of functional sphingosine-1 phosphate receptor-1 is reduced by B cell receptor signaling and increased by inhibition of PI3 kinase δ but not SYK or BTK in chronic lymphocytic leukemia cells.* Journal of immunology (Baltimore, Md. : 1950), 2015. **194**(5): p. 2439-2446.
141. Herishanu, Y., et al., *Biology of chronic lymphocytic leukemia in different microenvironments: clinical and therapeutic implications.* Hematology/oncology clinics of North America, 2013. **27**(2): p. 173-206.
142. Geissmann, F., et al., *Homing Receptor α4β7 Integrin Expression Predicts Digestive Tract Involvement in Mantle Cell Lymphoma.* The American Journal of Pathology, 1998. **153**(6): p. 1701-1705.
143. Buchner, M. and M. Müschen, *Targeting the B-cell receptor signaling pathway in B lymphoid malignancies.* Current opinion in hematology, 2014. **21**(4): p. 341-349.
144. Burger, J.A. and A. Wiestner, *Targeting B cell receptor signalling in cancer: preclinical and clinical advances.* Nature Reviews Cancer, 2018. **18**(3): p. 148-167.
145. Hadzidimitriou, A., et al., *Is there a role for antigen selection in mantle cell lymphoma? Immunogenetic support from a series of 807 cases.* Blood, 2011. **118**(11): p. 3088-3095.
146. Agathangelidis, A., et al., *Stereotyped B-cell receptors in one-third of chronic lymphocytic leukemia: a molecular classification with implications for targeted therapies.* Blood, 2012. **119**(19): p. 4467-4475.

147. Minden, M.D.-v., et al., *Chronic lymphocytic leukaemia is driven by antigen-independent cell-autonomous signalling.* Nature, 2012. **489**(7415): p. 309-312.
148. Minici, C., et al., *Distinct homotypic B-cell receptor interactions shape the outcome of chronic lymphocytic leukaemia.* Nature Communications, 2017. **8**(1): p. 15746.
149. Niemann, C.U. and A. Wiestner, *B-cell receptor signaling as a driver of lymphoma development and evolution.* Seminars in cancer biology, 2013. **23**(6): p. 410-421.
150. Camacho, F.I., et al., *Molecular heterogeneity in MCL defined by the use of specificVH genes and the frequency of somatic mutations.* Blood, 2003. **101**(10): p. 4042-4046.
151. Bernard, S., et al., *Inhibitors of BCR signalling interrupt the survival signal mediated by the micro-environment in mantle cell lymphoma.* International Journal of Cancer, 2015. **136**(12): p. 2761-2774.
152. Bürkle, A., et al., *Overexpression of the CXCR5 chemokine receptor, and its ligand, CXCL13 in B-cell chronic lymphocytic leukemia.* Blood, 2007. **110**(9): p. 3316-3325.
153. Cristina, G., et al., *Cortactin, another player in the Lyn signaling pathway, is over-expressed and alternatively spliced in leukemic cells from patients with B-cell chronic lymphocytic leukemia.* Haematologica, 2014. **99**(6): p. 1069-1077.
154. Woyach, J.A., et al., *Prolonged lymphocytosis during ibrutinib therapy is associated with distinct molecular characteristics and does not indicate a suboptimal response to therapy.* Blood, 2014. **123**(12): p. 1810-1817.
155. Fiorcari, S., et al., *The PI3-Kinase Delta Inhibitor Idelalisib (GS-1101) Targets Integrin-Mediated Adhesion of Chronic Lymphocytic Leukemia (CLL) Cell to Endothelial and Marrow Stromal Cells.* PLOS ONE, 2013. **8**(12): p. e83830.
156. de Rooij, M.F.M., et al., *Ibrutinib and idelalisib synergistically target BCR-controlled adhesion in MCL and CLL: a rationale for combination therapy.* Blood, 2015. **125**(14): p. 2306-2309.
157. Wiestner, A., *BCR pathway inhibition as therapy for chronic lymphocytic leukemia and lymphoplasmacytic lymphoma.* Hematology, 2014. **2014**(1): p. 125-134.
158. Ghielmini, M. and E. Zucca, *How I treat mantle cell lymphoma.* Blood, 2009. **114**(8): p. 1469-1476.
159. Huhn, D., et al., *Rituximab therapy of patients with B-cell chronic lymphocytic leukemia.* Blood, 2001. **98**(5): p. 1326-1331.
160. Weiner, G.J., *Rituximab: Mechanism of Action.* Seminars in Hematology, 2010. **47**(2): p. 115-123.
161. Zlotnik, A., A.M. Burkhardt, and B. Homey, *Homeostatic chemokine receptors and organ-specific metastasis.* Nature Reviews Immunology, 2011. **11**(9): p. 597-606.
162. Singh, A.K., et al., *Chemokine receptor trio: CXCR3, CXCR4 and CXCR7 crosstalk via CXCL11 and CXCL12.* Cytokine & growth factor reviews, 2013. **24**(1): p. 41-49.
163. Julio, D., et al., *Chronic lymphocytic leukemia: from molecular pathogenesis to novel therapeutic strategies.* Haematologica, 2020. **105**(9): p. 2205-2217.
164. Zhang, C., et al., *Actin cytoskeleton regulator Arp2/3 complex is required for DLL1 activating Notch1 signaling to maintain the stem cell phenotype of glioma initiating cells.* Oncotarget, 2017. **8**(20): p. 33353-33364.
165. Casamayor-Pallejà, M., et al., *BCR ligation reprograms B cells for migration to the T zone and B-cell follicle sequentially.* Blood, 2002. **99**(6): p. 1913-1921.

166. Kinoshita, T., et al., *Actin-related protein 2/3 complex subunit 5 (ARPC5) contributes to cell migration and invasion and is directly regulated by tumor-suppressive microRNA-133a in head and neck squamous cell carcinoma.* International journal of oncology, 2012. **40**(6): p. 1770-1778.
167. Xiong, T. and Z. Luo, *The Expression of Actin-Related Protein 2/3 Complex Subunit 5 (ARPC5) Expression in Multiple Myeloma and its Prognostic Significance.* Medical science monitor : international medical journal of experimental and clinical research, 2018. **24**: p. 6340-6348.
168. Barretina, J., et al., *The Cancer Cell Line Encyclopedia enables predictive modelling of anticancer drug sensitivity.* Nature, 2012. **483**(7391): p. 603-607.
169. *<KARATASAKI,S,Phosphoproteomic profiling of BCR signalling,2018, 10.1763803035009.pdf>.*
170. Gnad, F., et al., *PHOSIDA (phosphorylation site database): management, structural and evolutionary investigation, and prediction of phosphosites.* Genome Biology, 2007. **8**(11): p. R250.
171. Hornbeck, P.V., et al., *PhosphoSite: A bioinformatics resource dedicated to physiological protein phosphorylation.* PROTEOMICS, 2004. **4**(6): p. 1551-1561.
172. Nakade, S., et al., *Biased genome editing using the local accumulation of DSB repair molecules system.* Nature Communications, 2018. **9**(1): p. 3270.
173. Renkawitz, J., et al., *Chpater 5 - Micro-engineered "pillar forests" to study cell migration in complex but controlled 3D environments*, in *Methods in Cell Biology*, M. Piel, D. Fletcher, and J. Doh, Editors. 2018, Academic Press. p. 79-91.
174. van Panhuys, N., *TCR Signal Strength Alters T–DC Activation and Interaction Times and Directs the Outcome of Differentiation.* Frontiers in Immunology, 2016. **7**(6).
175. Volkmann, C., et al., *Molecular requirements of the B-cell antigen receptor for sensing monovalent antigens.* The EMBO journal, 2016. **35**(21): p. 2371-2381.
176. Hoellenriegel, J., et al., *Selective, novel spleen tyrosine kinase (Syk) inhibitors suppress chronic lymphocytic leukemia B-cell activation and migration.* Leukemia, 2012. **26**(7): p. 1576-1583.
177. Gold, M.R., et al., *The B Cell Antigen Receptor Activates the Akt (Protein Kinase B)/Glycogen Synthase Kinase-3 Signaling Pathway Via Phosphatidylinositol 3-Kinase.* The Journal of Immunology, 1999. **163**(4): p. 1894.
178. Agathangelidis, A., et al., *Establishment and Characterization of PCL12, a Novel CD5+ Chronic Lymphocytic Leukaemia Cell Line.* PloS one, 2015. **10**(6): p. e0130195-e0130195.
179. Song, W., et al., *Actin-mediated feedback loops in B-cell receptor signaling.* Immunological reviews, 2013. **256**(1): p. 177-189.
180. Duckworth, A.D., et al., *Multiplexed profiling of RNA and protein expression signatures in individual cells using flow or mass cytometry.* Nature Protocols, 2019. **14**(3): p. 901-920.
181. Spaargaren, M., et al., *The B cell antigen receptor controls integrin activity through Btk and PLCgamma2.* The Journal of experimental medicine, 2003. **198**(10): p. 1539-1550.
182. Gutjahr, J.C., R. Greil, and T.N. Hartmann, *The Role of CD44 in the Pathophysiology of Chronic Lymphocytic Leukemia.* Frontiers in immunology, 2015. **6**: p. 177-177.
183. Cuesta-Mateos, C., et al., *Of Lymph Nodes and CLL Cells: Deciphering the Role of CCR7 in the Pathogenesis of CLL and Understanding Its Potential as Therapeutic Target.* Frontiers in immunology, 2021. **12**: p. 662866-662866.

184. Mattila, P.K., F.D. Batista, and B. Treanor, *Dynamics of the actin cytoskeleton mediates receptor cross talk: An emerging concept in tuning receptor signaling.* Journal of Cell Biology, 2016. **212**(3): p. 267-280.
185. Liu, J., et al., *Internalization of B Cell Receptors in Human EU12 μHC⁺ Immature B Cells Specifically Alters Downstream Signaling Events.* BioMed Research International, 2013. **2013**: p. 807240.
186. Dustin, M.L., *Cell adhesion molecules and actin cytoskeleton at immune synapses and kinapses.* Current opinion in cell biology, 2007. **19**(5): p. 529-533.
187. Jacobsen, K., et al., *Adhesion Receptors on Bone Marrow Stromal Cells: In Vivo Expression of Vascular Cell Adhesion Molecule-1 by Reticular Cells and Sinusoidal Endothelium in Normal and γ-Irradiated Mice.* Blood, 1996. **87**(1): p. 73-82.
188. Oostendorp, R.A.J. and P. Dörmer, *VLA-4-Mediated Interactions Between Normal Human Hematopoietic Progenitors and Stromal Cells.* Leukemia & Lymphoma, 1997. **24**(5-6): p. 423-435.
189. Guinamard, R., et al., *B cell antigen receptor engagement inhibits stromal cell-derived factor (SDF)-1alpha chemotaxis and promotes protein kinase C (PKC)-induced internalization of CXCR4.* The Journal of experimental medicine, 1999. **189**(9): p. 1461-1466.
190. Reversat, A., et al., *Cellular locomotion using environmental topography.* Nature, 2020. **582**(7813): p. 582-585.
191. Li, J., et al., *The Coordination Between B Cell Receptor Signaling and the Actin Cytoskeleton During B Cell Activation.* Frontiers in immunology, 2019. **9**: p. 3096-3096.
192. Zhang, Y., et al., *Arp2/3 complex controls T cell homeostasis by maintaining surface TCR levels via regulating TCR+ endosome trafficking.* Scientific Reports, 2017. **7**(1): p. 8952.
193. Maus, M., et al., *B cell receptor-induced Ca2+ mobilization mediates F-actin rearrangements and is indispensable for adhesion and spreading of B lymphocytes.* Journal of Leukocyte Biology, 2013. **93**(4): p. 537-547.
194. Ichikawa, D., et al., *GRAIL (gene related to anergy in lymphocytes) regulates cytoskeletal reorganization through ubiquitination and degradation of Arp2/3 subunit 5 and coronin 1A.* The Journal of biological chemistry, 2011. **286**(50): p. 43465-43474.
195. Scielzo, C., et al., *HS1 protein is differentially expressed in chronic lymphocytic leukemia patient subsets with good or poor prognoses.* The Journal of clinical investigation, 2005. **115**(6): p. 1644-1650.
196. Martini, V., et al., *Cortactin, a Lyn substrate, is a checkpoint molecule at the intersection of BCR and CXCR4 signalling pathway in chronic lymphocytic leukaemia cells.* British Journal of Haematology, 2017. **178**(1): p. 81-93.
197. Ten Hacken, E., et al., *The importance of B cell receptor isotypes and stereotypes in chronic lymphocytic leukemia.* Leukemia, 2019. **33**(2): p. 287-298.
198. Merolle, M.I., et al., *The B cell receptor signaling pathway in mantle cell lymphoma.* Oncotarget, 2018. **9**(38): p. 25332-25341.
199. Mullins, R.D., J.A. Heuser, and T.D. Pollard, *The interaction of Arp2/3 complex with actin: Nucleation, high affinity pointed end capping, and formation of branching networks of filaments.* Proceedings of the National Academy of Sciences, 1998. **95**(11): p. 6181-6186.
200. Balcer, H.I., K. Daugherty-Clarke, and B.L. Goode, *The p40/ARPC1 subunit of Arp2/3 complex performs multiple essential roles in WASp-regulated actin nucleation.* The Journal of biological chemistry, 2010. **285**(11): p. 8481-8491.

201. Zheng, Y., et al., *Decreased deformability of lymphocytes in chronic lymphocytic leukemia.* Scientific Reports, 2015. **5**(1): p. 7613.